NTNU
Norwegian University of
Science and Technology

Entrainment potential of rock avalanches in Norway.

Parameter test and case study at the unstable rock slope Børa (Romsdal Valley, western Norway)

Martine Lund Andresen

Geotechnology
Submission date: April 2017
Supervisor: Reginald Hermanns, IGP
Co-supervisor: Thierry Oppikofer, NGU

Norwegian University of Science and Technology
Department of Geoscience and Petroleum

NTNU
Det skapende universitet

MASTERKONTRAKT
- uttak av masteroppgave

1. Studentens personalia

Etternavn, fornavn	Fødselsdato
Andresen, Martine Lund	**04. des 1990**
E-post	Telefon
martinelandresen@gmail.com	**98496918**

2. Studieopplysninger

Fakultet	
Fakultet for ingeniørvitenskap og teknologi	
Institutt	
Institutt for geologi og bergteknikk	
Studieprogram	Studieretning
Tekniske geofag	**Ingeniørgeologi og bergmekanikk**

3. Masteroppgave

Oppstartsdato	Innleveringsfrist
15. jan 2016	**10. jun 2016**
Oppgavens (foreløpige) tittel **Evaluating the debris entrainment potential of rock avalanches using numerical run out modelling in combination with field observations at Børa (Romsdal Valley, western Norway)**	
Oppgavetekst/Problembeskrivelse Rock avalanches are frequently reported to entrain significant volumes of loose material on their travel path, which can increase the total volume and the rock avalanche mobility. However, little is known about the debris entrainment potential in Norway. This master thesis focuses on evaluating the debris entrainment potential of rock avalanches using numerical run-out modelling in combination wiht field observations. The study area is the unstable rock slope Børa in Romsdal Valley (western Norway).Field work is carried out on the scree slopes under the unstable area. The results from field work and laboratory work is presented in a project, which forms the base for this thesis. The aim of the study is to better understand the processes involved in debris entrainment. The tasks comprise: - to assess the thickness of scree deposits at Børa. - to determine input parameters for numerical run-out modelling in DAN3D (using results from field work). - numerical run-out modelling in DAN3D The master thesis will be carried out in collaboration with NGU and is part of the method development for the analysis of consequences of rock avalanches.	
Hovedveileder ved institutt **Professor II Reginald Hermanns**	Medveileder(e) ved institutt
Ekstern bedrift/institusjon **NGU**	Ekstern veileder ved bedrift/instutisjon **Thierry Oppikofer**
Merknader **1 uke ekstra p.g.a påske.**	

4. Underskrift

Student: Jeg erklærer herved at jeg har satt meg inn i gjeldende bestemmelser for mastergradsstudiet og at jeg oppfyller kravene for adgang til å påbegynne oppgaven, herunder eventuelle praksiskrav.

Partene er gjort kjent med avtalens vilkår, samt kapitlene i studiehåndboken om generelle regler og aktuell studieplan for masterstudiet.

Trondheim, 12.01.2016
Sted og dato

Martine Lunde Andersen
Student

Hovedveileder

*This is the original master contract. The submission date is therefore 10.06.2016. The submission of the thesis was delayed due to the birth of my son, Birk in April 2016 and the following10 months of maternity leave. The new submission date is 08.04.2017.

Abstract

Rock avalanches are frequently reported to entrain significant volumes of debris on their travel path. However, little is known about the debris entrainment potential in Norway. This thesis aims to evaluate and better understand the debris entrainment potential of Norwegian rock avalanches and to study how the run-out is affected by entrainment of debris. Numerical run-out modelling of the unstable rock slope Børa, Romsdal Valley, western Norway is performed to evaluate the mentioned topics.

A sensitivity analysis is carried out in order to determine reasonable input parameters for numerical run-out modelling in DAN3D and to assess the run-outs sensitivity to the different input parameters. The analyses are carried out on three scenarios of different volumes; Børa C (76 000 m^3), Børa C Large (476 000 m^3) and Børa B (2 400 000 m^3). The Voellmy rheology with friction coefficient $\mu = 0.15$ and turbulence coefficient $\xi = 500$ m/s^2 are considered appropriate parameters for the scenarios at Børa, and are applied as a reference. The run-out is sensitive to the friction coefficient μ and the friction angle φ_b (frictional model), showing decreasing run-outs for increasing values. In addition, the run-out of the larger volumes are slightly sensitive to changes in the turbulence coefficient ξ. None of the remaining input parameters in DAN3D are found to affect modelled run-out distance.

Scenario Børa C is used for the purpose of assessing the entrainment potential. Entrainment of unsaturated material decreases the run-out distance. However, entrainment of completely unsaturated material is not considered realistic at Børa. The opposite is observed for saturated material, showing increasing run-out for increasing pore pressure. In addition, the run-out is highly sensitive to the input friction angle φ_b, indicating that the properties of the debris are of great importance when parameters are determined. Further analyses shows that entrainment of material (with pore pressure) from lower parts of the slope provides longer run-outs and larger final volumes compared to entrainment from the upper part.

Entrainment in DAN3D is controlled by a user defined entrainment rate, *E*. The parameter is difficult to assess. Mainly because the expected final volume is required as input. This is extremely difficult to assess, especially in a forward analysis. At Børa, the modelled final volume does not equal the expected final volume. The results indicate that the input final volume should be increased by a factor of one to obtain expected final volumes when modelling, but further analyses are required to state this. Based on the results of this thesis, it is suggested that perhaps DAN3D will not constitute the best tool when a forward analysis of an entrainment event is to be carried out.

Sammendrag

Det er ofte observert at fjellskred medriver store mengder løsmasser i skredbanen. Det eksisterer likevel liten kunnskap om potensialet for medriving av løsmasser i Norge. Hovedmålet med denne oppgaven er å bedre forståelsen for potensialet for medriving av løsmasser i norske fjellskred samt studere hvordan skredets utløp påvirkes av dette. Analysene er utført ved numerisk modellering av det ustabile fjellpartiet Børa i Romsdalen.

Det er utført en sensitivitetsanalyse for å bestemme fornuftige input parametere for numerisk utløpsmodellering i DAN3D samt for å studere utløpslengdens sensitivitet til de ulike parameterne. Analysene er utført på tre scenarier av ulik størrelse: Børa C (76 000 m^3), Børa C Large (476 000 m^3) og Børa B (2 400 000 m^3). Voellmy reologi med friksjonskoeffisient μ = 0.15 og turbulenskoeffisient ξ = 500 m/s^2 er funnet å være fornuftige input for scenariene på Børa, og er derfor benyttet som referanseverdier. Utløpsdistansen er sensitiv til friksjonskoeffisienten μ og friksjonsvinkelen φ_b (friksjonsreologi), med synkende utløpslengder for økende verdier av disse parameterne. I tillegg er utløpet fra de større volumene noe sensitiv til endringer i turbulenskoeffisienten ξ. Resultatene indikerer at ingen av de resterende input parameterne i DAN3D påvirker utløpsdistansen i nevneverdig grad.

Scenario Børa C er benyttet for å studere medrivingspotensialet. Medriving av umettet materiale minsker utløpsdistansen. Medriving av helt umettede masser er ikke ansett som et realistisk tilfelle på Børa på grunn av mektigheten av avsetningene og klimatiske forhold. Det omvendte er imidlertid observert for mettede masser, med økende utløpsdistanser for økende poretrykk. I tillegg viser utløpsdistansen høy grad av sensitivitet til friksjonsvinkelen, φ_b for medrivingsmaterialet. Videre analyser viser at medriving av masser (med poretrykk) fra nedre del av skråningen, gir lengre utløp enn medriving fra øvre del. Sluttvolumet er også større ved medriving av masser fra nedre del.

I DAN3D kontrollers medriving av en bruker-definert medrivingsrate, *E*. Denne parameteren er vanskelig å bestemme, hovedsakelig fordi forventet sluttvolum er nødvendig input. Dette er ekstremt vanskelig å bestemme, spesielt i en før-analyse slik som her. Modellering av scenario Børa C viser at det modellerte sluttvolumet ikke samsvarer med det forventede sluttvolumet. Resultatene indikerer at input sluttvolum må økes med en faktor på en for at forventet sluttvolum skal oppnås, men videre analyser er nødvendig for at dette skal kunne stadfestes. Basert på resultater fra denne oppgaven, antydes det at DAN3D ikke er det optimale verktøyet ved en før-analyse av en hendelse som antas å medrive store mengder løsmasser.

Acknowledgements

This thesis is the final work of my master degree in engineering geology and rock mechanics at the Department of Geoscience and Petroleum at the Norwegian University of Science and Technology (NTNU). The thesis is written in collaboration with the Geological Survey of Norway (NGU). My supervisors have been Reginald Hermanns (head of the Geohazard and Earth Observation team NGU and professor at NTNU) and Thierry Oppikofer (NGU). The work with this thesis was divided in two periods, spring 2016 and spring 2017, due to the birth of my son, Birk.

First I would like to thank my supervisors Reginald Hermanns and Thierry Oppikofer for all help, reviewing, discussions and guidance with this thesis. It has been essential! Secondly I would like to thank Ivanna Penna (NGU), who gave me an introduction to the software used for the analyses. Thanks also to Oldrich Hungr and Scott McDougall for helping me with software problems.

I would also like to thank Kaja Krogh, fellow student at NTNU, for contribution during the fieldwork that was carried out in the project work leading up to this thesis. Your help and good company was of great importance!

A huge thanks goes to my sister Maren and cohabitant Fredrik, who has reviewed the thesis. Your comments and support have been extremely helpful. Last, I will say thanks to my son, Birk who has made the work with this thesis both more and less effective.

Trondheim, March 2017

Martine Lund Andresen

Contents

1 Introduction

1.1 Background

Large rock-slope failures frequently appear in mountain regions all over the world. In Norway, heavy erosion by the ice have caused steep mountainsides and deep valleys. The over-steepened terrain found in Norwegian fjords and valleys provides a relief prone to large rock-slope failures, meaning rock avalanches, rock-ice avalanches, rockslides and rock falls (Hermanns and Longva, 2012, Saintot et al., 2012, Lied, 2014).

Rock avalanches are among the most severe hazard scenarios in Norway (DSB, 2013). A rock avalanche may lead to catastrophic damages. Damming of river valleys and landslide-triggered displacement waves are the most important secondary effects (Braathen et al., 2004, Hermanns and Longva, 2012). The prediction of the run-out parameters, including maximum distance and impact area, are important information for territorial planning to decrease the potential of consequences.

In order to deal with the hazard, the Geological Survey of Norway (NGU) has carried out systematic mapping of unstable rock-slopes since 2005 (Oppikofer et al., 2013). A systematic mapping approach for unstable rock-slopes for hazard- and risk classification was developed at NGU, aiming to detect all unstable rock-slopes in Norway (Hermanns et al., 2014). The system does not include details on evaluating possible consequences of rock avalanches, therefore a project highlighting on this specific subject was started in 2013 (Oppikofer et al., 2016a) This thesis is a part of the project called “method development for the analysis of consequences of rock avalanches”. The unstable rock slopes detected are registered in the unstable rock slope database, developed and maintained by NGU (Oppikofer et al., 2015).

Rock avalanches are frequently reported to entrain significant volumes of loose material on their travel path. Entrainment of debris material will increase the total volume and change the rock avalanche mobility. This may enhance the run-out distance (Hungr and Evans, 2004). Knowledge about the effect of entrainment on the run-out distance may thus provide better estimates of maximum run-out distance.

Limited knowledge exists about the debris entrainment potential in Norway. The Norwegian Quaternary geology is dominated by poorly consolidated glacial deposits and landslide deposits. Rock avalanches have had a major effect on the formation of the Quaternary landscape in Norway, including valleys and fjords. Scree deposits are often the most recent infill in valleys, and cover valley sides and floors. The volume of material available for entrainment is

therefore significant in many Norwegian rock-avalanche prone areas. How the deposits will behave during the rapid loading of a rock avalanche and how the mobility of Norwegian rock avalanches will be affected, is not understood. Understanding the processes and effects of entrainment in Norwegian conditions are therefore of interest for future run-out distance estimates.

1.2 Problem statement and thesis structure

The super eminent aim of the study is to better understand the debris entrainment potential and how debris entrainment influence the run-out distance of rock avalanches in Norway. The thesis focuses on evaluating entrainment potential using the numerical run-out model DAN3D, in combination with field observations. The study area is the unstable rock slope Børa, in Romsdal Valley, western Norway.

Field work and laboratory work were carried out and presented in a project that forms the base for this thesis (Andresen, 2015). The field observations provide valuable data to set up the model. A geomorphologic map was produced in this student project to estimate the volume of the scree deposits at Børa, that will be further used in this thesis. In addition, results from granulometry analyses from that student project will attempted to be implemented in the input parameters in DAN3D.

The main objectives of this study are:

- To assess the thickness and the volume of the scree deposits at Børa using the Sloping Local Base Level (SLBL) method.
- To determine reasonable input parameters for numerical run-out modelling in DAN3D by sensitivity analysis.
- Assess the sensitivity of the run-out distance to the input parameters in DAN3D.
- To include results from fieldwork and laboratory work in the input parameters.
- To carry out numerical run-out modelling in DAN3D and study the effect of entrainment on the run-out distance.
- To study what factors influence the entrainment potential.

A brief presentation of the geographical and geological setting of the study area is given in chapter two. The unstable rock slope, including results from the project work, is presented in chapter three. Chapter four involves theory relevant for the work of the thesis, before the applied methodology is described in chapter five. The results of the analyses are presented in chapter six. Further, discussion of the applied methods and results are given in chapter seven. Chapter eight involves the conclusion of the study while suggestions for further analyses are presented in chapter nine.

2 Geographical and geological setting

Børa is located in Romsdal Valley in the western part of Norway (Figure 2.1). The slope is located in Møre & Romsdal county and Rauma municipality.

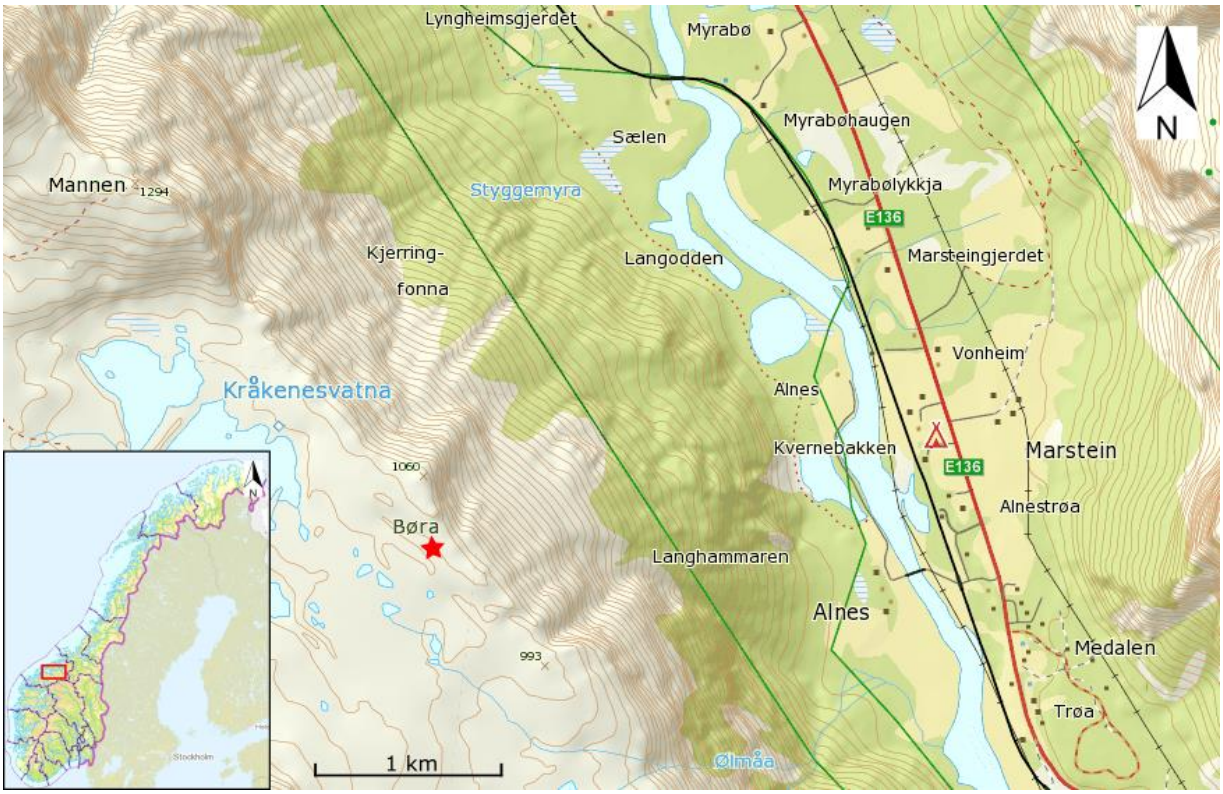

Figure 2.1: Location map. The geographic location of Børa, above Romsdal Valley is marked with a red star. The geographic setting of the study area in Norway is marked with a red rectangle on the map in the inset.

2.1 Bedrock geology

Romsdal Valley is a part of the Western Gneiss Region of Norway. The bedrock in the region is of Precambrian age, and mainly consists of gneiss (1850-1500 M years) and granite (1000-950 M years) (Nordgulen and Andresen, 2006). Romsdal Valley cuts into the crystalline basement of these Precambric bedrocks (Tveten et al., 1998). The geological structures in the gneiss-region are mostly a result of the Caledonian Orogeny, caused by the collision of Laurentia and Baltica (Nordgulen and Andresen, 2006).

The bedrock map of Romsdal Valley exists in 1:250 000 scale (Tveten et al., 1998). The resolution is therefore not high enough to give other information than an overview of the bedrock geology in the area. Gneiss is the main rock in the area. The gneiss is dioritic to granitic, migmatittic in some areas (Tveten et al., 1998). These geological features are observed in the area of Børa as well (Saintot et al., 2012, Braathen et al., 2004). A steep to vertical foliation shapes parts of the cliff at the edge of the plateau. The foliation is characteristic for other unstable rock slopes in the area, and several instabilities have developed along back cracks parallel to the foliation, causing frequent rockfalls (Saintot et al., 2012).

2.2 Quaternary geology

The Quaternary deposits in Romsdal Valley and at the study area Børa can be divided into three main categories; the steep slopes, the plateaus including the topmost part of the mountains and the valley bottoms. The steep slopes are dominated by deposits from rock falls, rock avalanches, snow avalanches and debris slides (pink polygons in Figure 2.2). In the plateaus and topmost part of the mountains, the bedrock is fully exposed, or covered by a thin layer of loose material (light pink). The valley bottom is dominated by fluvial material (yellow). Moraine (green) can be seen at some of the more elevated plateaus (NGU, 2015a, Sollid and Kristiansen, 1984).

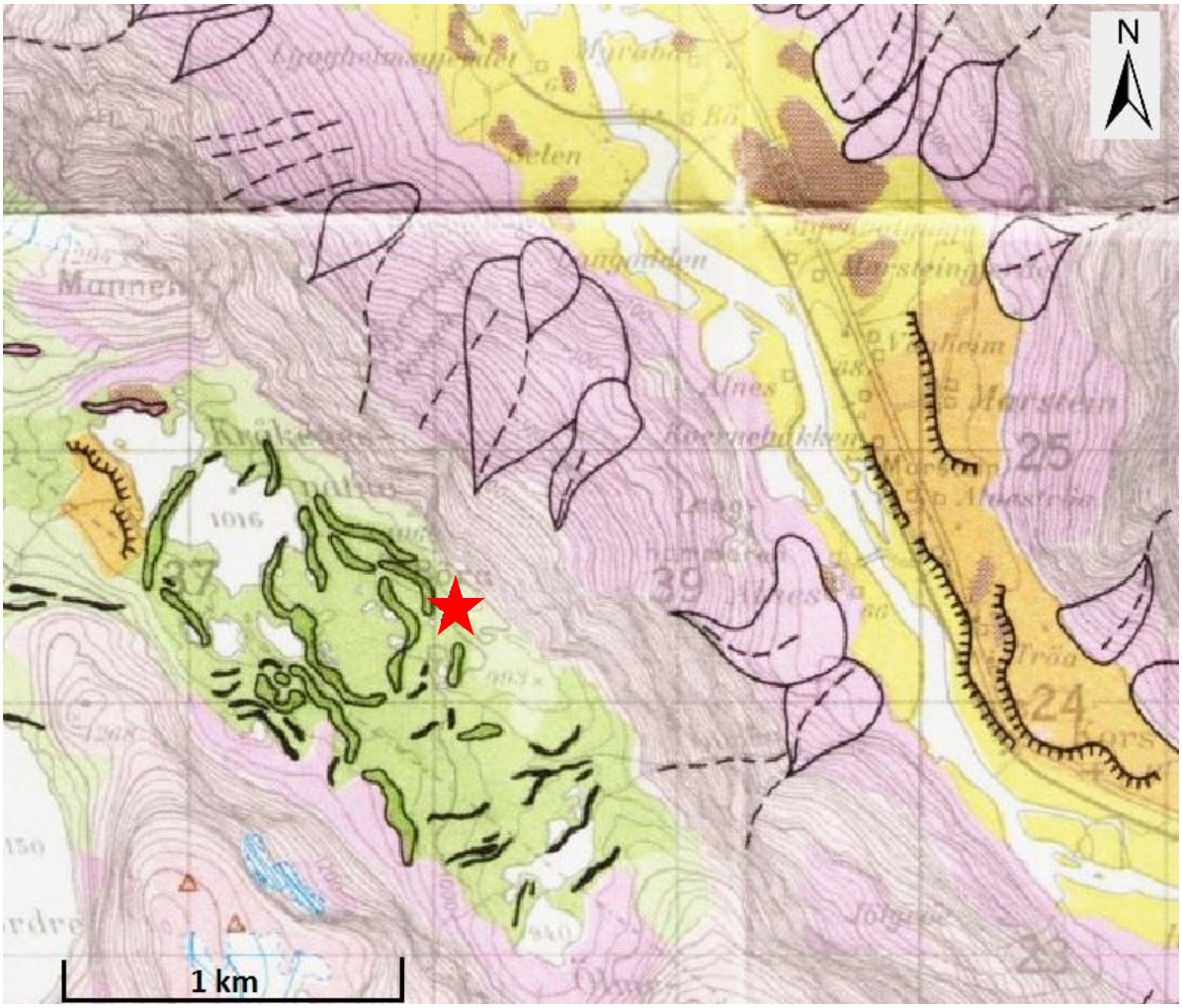

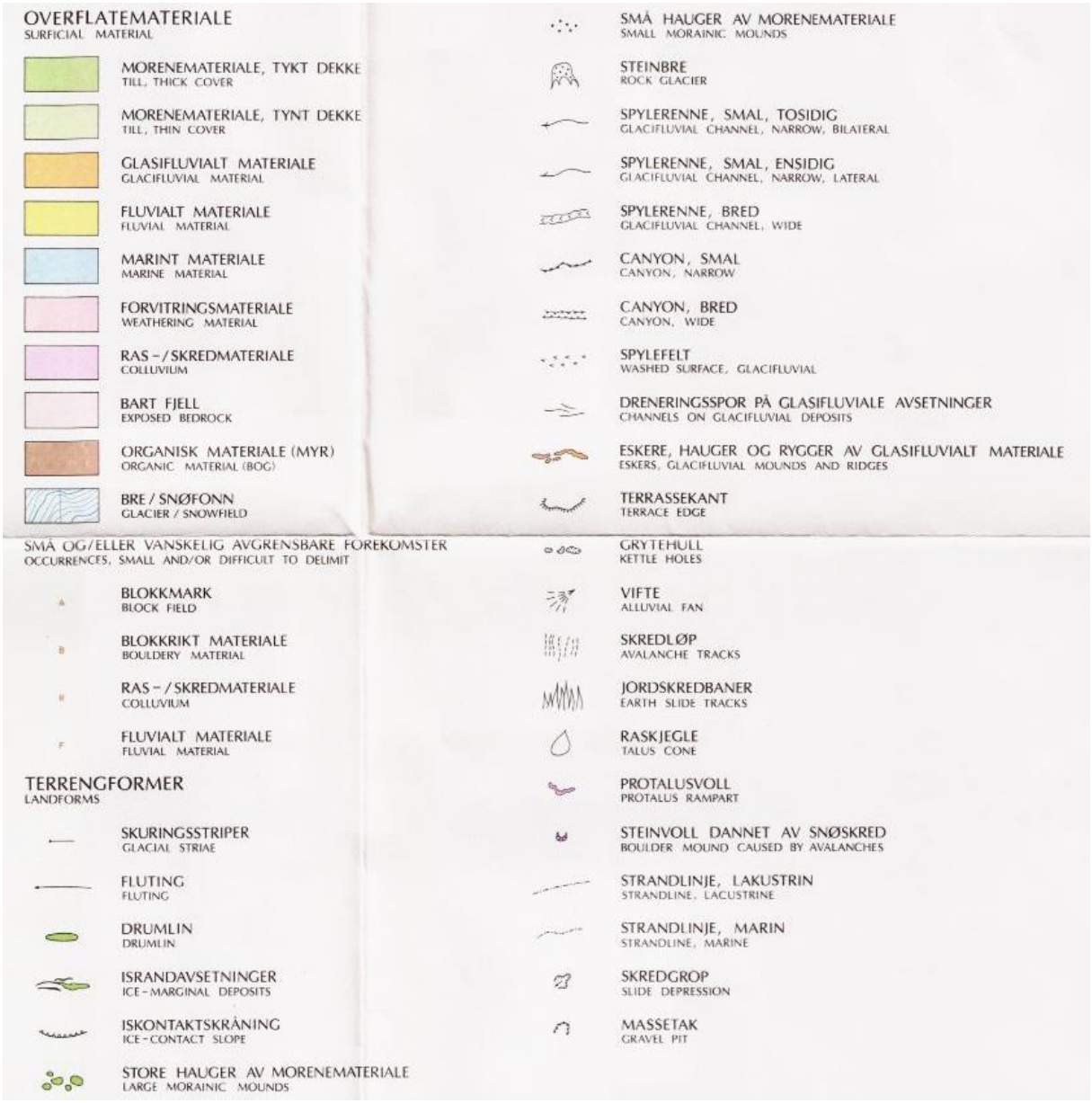

Figure 2.2: Map of the Quaternary deposits in Romsdal Valley. Børa is marked with a red star. (Sollid and Kristiansen, 1984)

3 The unstable rock slope Børa

Romsdal Valley is characterized by high spatial density of past rock slope failures in Norway, with approximately 10 large failures originating from the steep mountainsides along the 30 km long valley (Saintot et al., 2012, Oppikofer et al., 2013). Børa is one of the slopes prone to failure along the valley.

Large rock avalanches and their deposits have played a major role in forming the Quaternary landscape in Romsdal Valley. Landslide deposits counts for the most recent infill of sediments in the valley bottom, and are the most dominating feature of the deposits in the valley (Figure 3.1). The scree slopes at Børa shows attests of recent activity. The last known event of importance was a small rock avalanche in 2007. The size of the event is estimated to be in the order of 10 000 m^3 (Dahle et al., 2008).

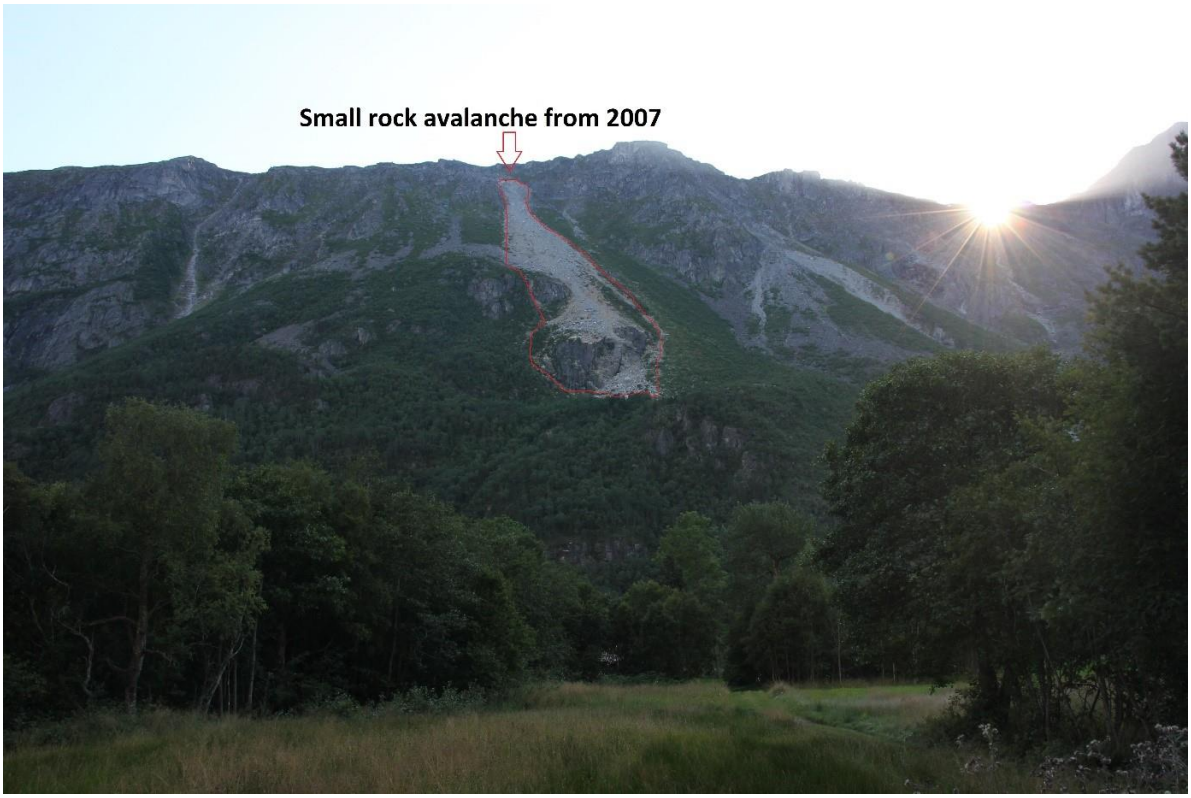

Figure 3.1: Overview of the scree slopes at Børa. The event from 2007 is marked in the middle of the photo.

In the following sections a presentation of previous work carried out at Børa, including the project work done by the author during summer and autumn 2015, will be given. A description of the unstable slope with the possible scenarios and hazards will be presented as well.

3.1 Available data

In addition to results from previous work done at Børa, the available data listed below have been essential for the analysis carried out in this thesis (Table 3.1).

Table 3.1: Available data.

Available data	Source
Existing papers and reports on Børa	(Blikra et al., 1999, Dalsegg and Tønnesen, 2004, Braathen et al., 2004, Saintot et al., 2012, Oppikofer et al., 2013)
Project assessments on Børa	(Farsund, 2010, Andresen, 2015)
LiDAR (1 m resolution)	NGU
Aerial photos	Norwegian mapping authority (Statens Kartverk)
Bedrock map (1:250 000)	NGU
Quaternary map (1:250 000)	NGU
Quaternary map (1 :80 000)	University of Oslo,

Results from the project work carried out by the author summer and autumn 2015 are presented in a separate subsection (Section 3.2.1). The results from the project are based on fieldwork performed by the author and Kaja Krogh both from the Norwegian University of Science and Technology (NTNU) and laboratory tests carried out at the geological engineering laboratory at the Department of Geoscience and Petroleum, NTNU.

3.2 Previous work

The Geological Survey of Norway (NGU) has since 2005 carried out systematic mapping of unstable rock slopes in Møre & Romsdal county (Oppikofer et al., 2013). Børa is a part of this project. The unstable slope Børa has been studied in the field since the 1990s and has been periodically monitored since 2003 by differential Global Navigation Satellite System (dGNSS) and Terrestrial Laser Scanning (TLS). The velocity is measured to up to 13.8 mm/year at some freestanding blocks near the scarp. However, two points in the central part of the unstable area shows a horizontal movement of approximately 1 mm/year, which is considered more representative for the unstable slope (Oppikofer et al., 2013). In addition to mapping, NGU has done geophysical measurements at Børa, aiming to detect the lower limit of the unstable rock slope. The methods used were 2D resistivity and refraction seismic (Dalsegg and Tønnesen, 2004). A previous student project is also carried out at Børa, focusing on the relationship between geology, structures and slope instabilities. A detailed structural geological landslide map and a rock avalanche inventory map of Romsdal Valley were produced (Farsund, 2010).

3.2.1 Project by the author

The author of the thesis carried out a project during summer and autumn 2015 focusing on the scree deposits at Børa (Andresen, 2015). The study included the following tasks:

- Map the geomorphology at Børa, including the extent of the scree deposits and the rock outcrops.
- Determine block sizes and forms of the scree deposits.
- Determine grain size distribution of the slope material.

The work comprised fieldwork and laboratory work in addition to analyses and literature study. During fieldwork, the extent of the geomorphologic features in the area were mapped. In addition, measurements of block size, block form and roundness were carried out. 100 blocks were measured at 24 stations spread out on the slope, and six samples for laboratory tests were taken. The methods used at the laboratory in order to assess the grain size distribution were sieving and Coulter Laser. The total grain size distribution of the slope material was found by connecting results from the two laboratory methods and fieldwork.

The project resulted in:

- A geomorphologic map, which is improved for the aim of this study (Figure 5.1).
- Granulometric description of the scree deposits at Børa.
- Grain size distribution curves covering the entire range of slope material.
- Description of the rock-avalanche deposits at the foot of the slope at Børa.

Summary of results relevant for this study:

Geomorphologic map: The map is used for the purpose of volume estimation of the scree deposits (Figure 5.1). See Section 5.1.1 and Figure 5.1 for further information. Four distinct rock-avalanche deposits were interpreted based on field mapping and studies of the DEM at the office.

Granulometric description of the scree deposits: Scree deposits are distributed all over the slope at Børa. The deposits reach from the rock-cliffs at the top to the bouldery rock-avalanche deposits at the foot of the slope. A belt of rock outcrops is dominant in the middle part of the slope. Gullies eroded by previous landslides show that the thickness of the scree deposits is in the 10 meter-scale at some locations. No differences in granulometry can be seen between the NW, central and SE part of the study area.

The block size of the deposits varies, but a trend can be seen. The mean block size is larger at the lower part of the slope (Figure 3.2). Measurements of block size taken in the eroded gullies show a smaller mean than the mean from measurement stations at the same elevation but on the surface of the deposit. This indicates an inverse grading of the material.

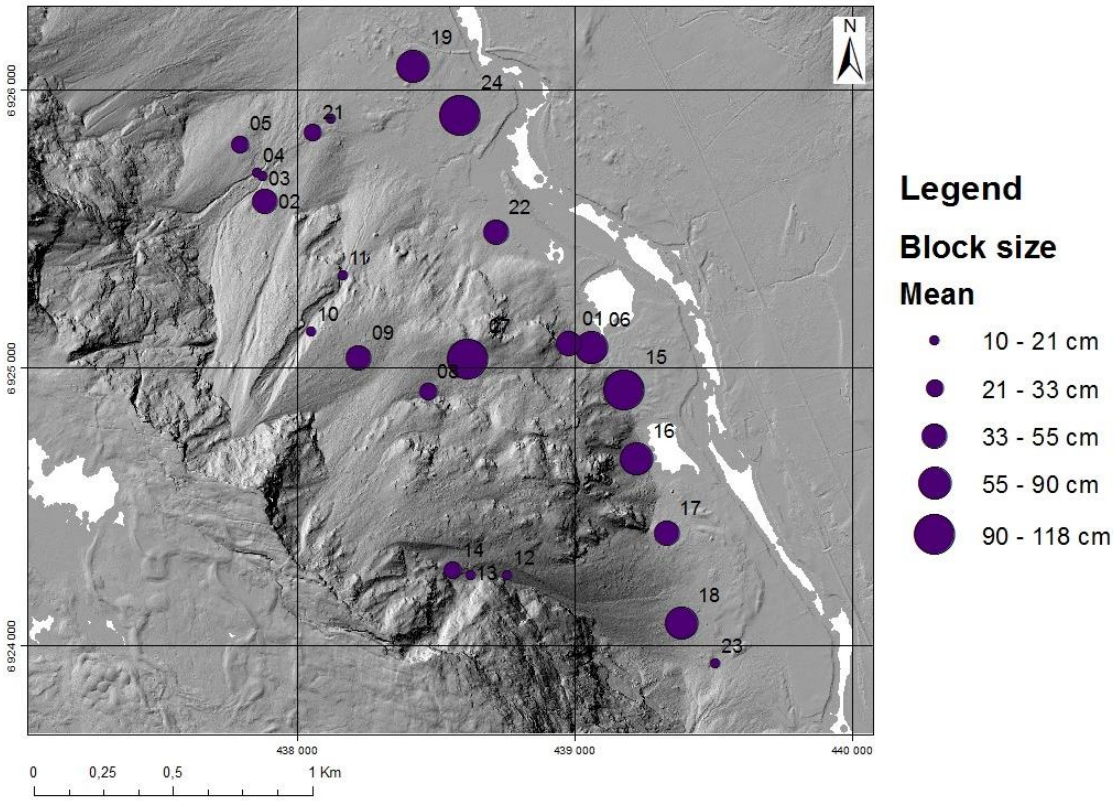

Figure 3.2: Mean block size at each measurement location. The circles are graduated after the size of the mean. The numbers on the map indicate the location number. (Andresen, 2015)

The block form is described by the terms elongated and cubic. The dominating block form at Børa is elongated, meaning that the sphericity of the blocks is low. Roundness is described by the terms introduced by Powers (1953). The scale ranges from very-angular to well-rounded and includes six classes. The roundness of the blocks at Børa are generally angular to sub-angular. This correlates well with the short, gravitational-driven transportation process that the rock boulders have been exposed to (Schleier et al., 2015, Brattli, 2015). Some of the locations at lower elevations show a more sub-angular to sub-rounded trend. At these locations, the block size is generally larger and the material is characterized as rock-avalanche deposits. The block form and roundness will affect the materials friction and resistance to movement. The properties of the material regarding these factors thus need to be implemented when evaluating entrainments effect on run-out distance.

Grain size distribution curves: The total grain size distribution curves clearly show that the amount of finer material is small (Figure 3.3). The study shows that material with a grain size < 100 mm only contributes for maximum 7 wt. %. There are some errors and limitations in the method used, and the exact number should not be given too much attention. However, the fact that the amount of finer material is small is reasonable. This should be taken into consideration when entrainment and erosion are included in the run-out distance modelling, and input parameters are given to the material available for entrainment.

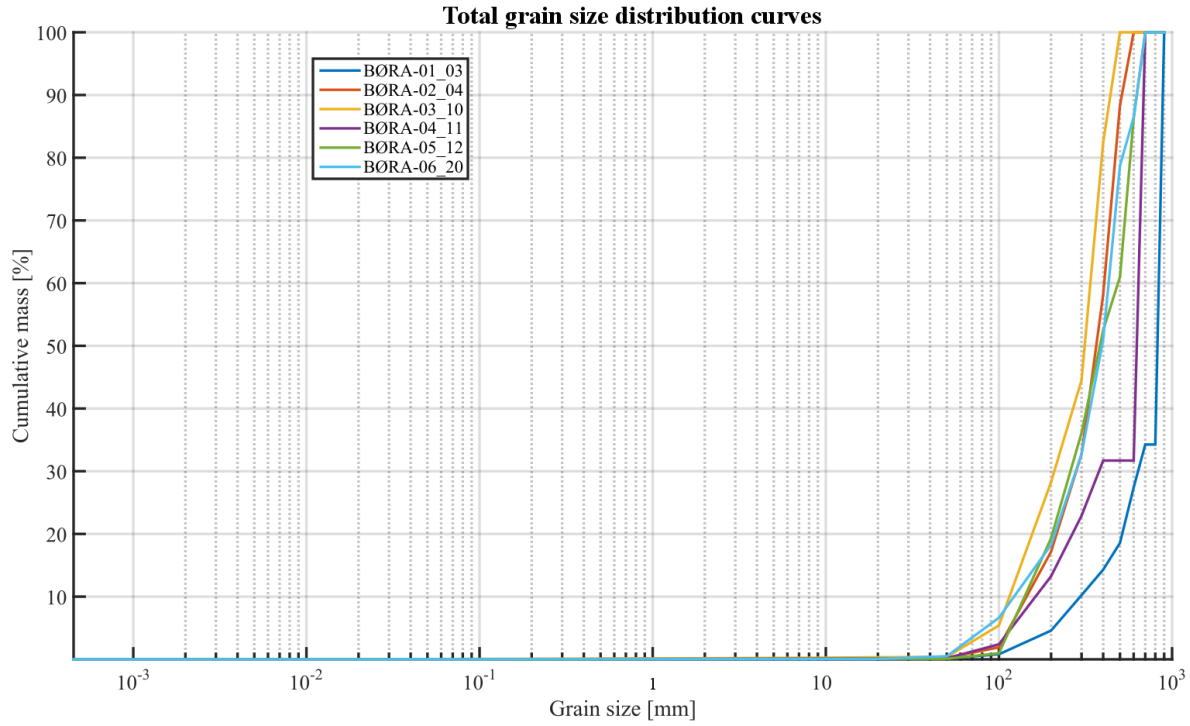

Figure 3.3 Grain size distribution curves of the slope material at Børa. Combined results from laboratory tests and field work (Andresen, 2015).

3.3 Description of the unstable slope

The unstable rock slope Børa is categorized as a complex field and consists of a more than 2 km long plateau located approximately 900 m above the valley bottom (Braathen et al., 2004). The slope is northeast facing. Børa has been studied in the field for almost 25 years and the most likely failure scenarios and dominating structures are identified.

The entire rock slope at Børa shows signs of movement, but a collapse of the entire slope with indication of instability (a total volume of 400 million m^3), is not considered as realistic (NGU, 2015b). Thus, five smaller scenarios that are reasonable to fail were identified (Figure 3.4). The volume estimations of the scenarios at Børa are done by the Sloping Local Base Level method (Oppikofer, 2016b).

- Scenario A, with an approximate volume of 4.7 million m^3, is located at the highest point of the mountain Børa. A back-scarp that consists of several joints and depressions restricts the scenario in the rear part. The lateral and lower limits are not precisely defined.
- Scenario B consists of a volume of about 2.4 million m^3 and is located on the southeastern end of the unstable rock slope. A back scarp with an opening of up to 20 m can be seen in relation to this scenario.
- Scenario C and D: The volumes of scenario C and D are approximately 135 000 m^3 and 24 000 m^3 respectively. The scenarios consist of two loose blocks, separated from the rest of the unstable area.
- Scenario E is an area of heavily fractured rock with an approximate volume of less than 250 000 m^3. The area could be the source of a potential rock fall hazard (NGU, 2015b).

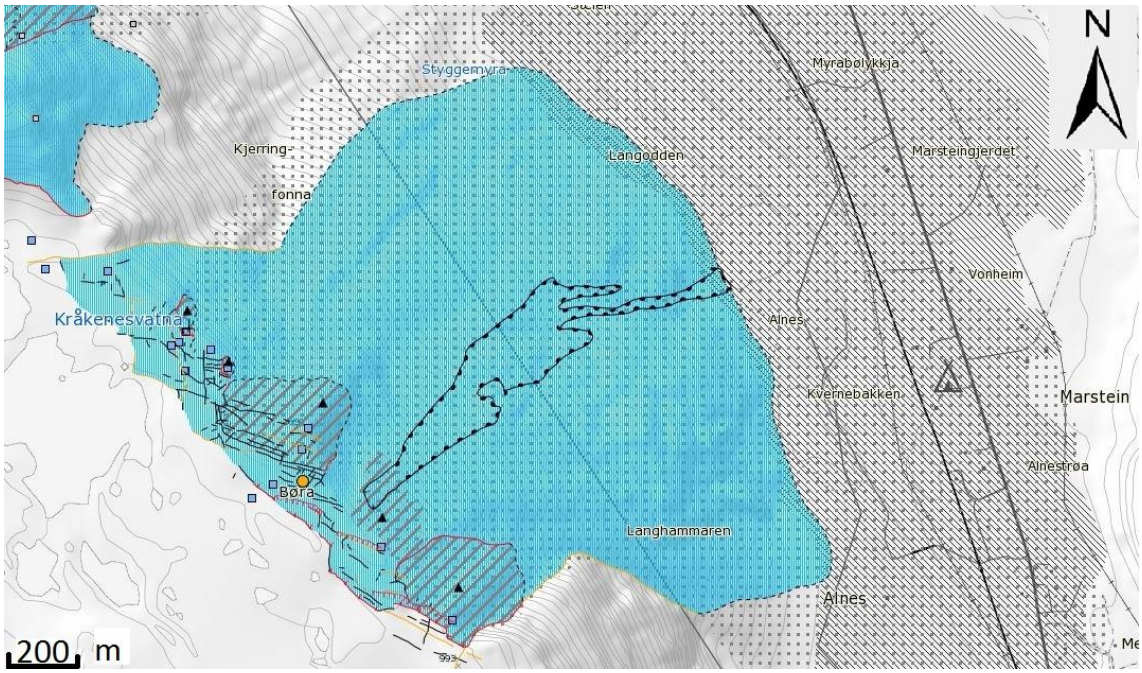

Figure 3.4: Map of Børa. The blue area is the main area of the unstable rock slope, and the grey dots are the run-out zone. The blue area in the left corner is the unstable rock slope Mannen. Modified from (NGU, 2015a).

The hazard classification of the scenarios at Børa are from medium to high. Considering the possible consequences of an event, this is resulting in a medium to high risk classification of the unstable slope (NGU, 2015b). Possible secondary effects of a rock avalanche depend on the scenario that fails. Damming of the river Rauma causing an upstream flood, a possible dam break and downstream flood are, similar to the Mannen site, the most severe consequences (NVE, 2009, Hermanns et al., 2013).

4 Theory

The theory chapter will provide the reader with theoretical knowledge relevant for this thesis. First, a presentation of different methods for volume estimation of debris is given. The chapter includes an introduction to the method used in this thesis, the Sloping Local Base Level (SLBL) technique and its applications. The mobility of rock avalanches and associated phenomena meaning fragmentation of rock masses and entrainment of debris material are of importance to this thesis and are therefore presented. Last, the reader is introduced to run-out prediction by numerical modelling tools in general and DAN3D, the model used in the analysis of the scenario at Børa, in specific.

4.1 Estimation of debris thickness and volume

Landslide investigation requires knowledge about volume and failure surface geometry. This is important in order to assess the run-out distance, impact area and to calculate the factor of safety. However, only a few methods are available for the purpose of volume estimation and assessment of failure surface geometry. Most methods are based on morphometric characterization, displacement observations and interpolation techniques (Jaboyedoff et al., 2015). No systematic and automatic methods are available yet, and approaches need to be developed.

Simple geometrical methods can be used to assess landslide volumes by the failure surface. A volume defined by the mean thickness multiplied by the surface area or the use of a semi-ellipsoid (Figure 4.1) are two possible approaches (Cruden and Varnes, 1996).

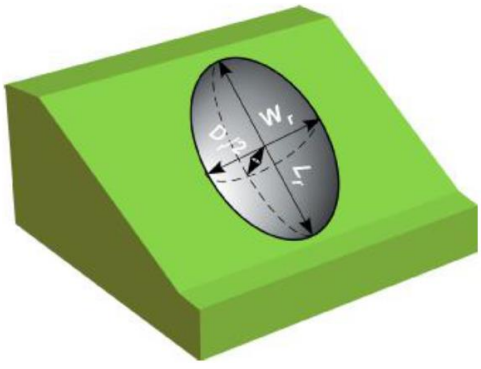

Figure 4.1: Illustration of the semi-ellipsoid used to define volumes of landslides by the failure surface. D_r is the half thickness of the ellipsoid (landslide), W_r is the width and L_r is the length of the ellipsoid. (Jaboyedoff et al., 2015)

The landslide volume defined by the semi-ellipsoid is given by variables given in Figure 4.1 (Equation 4.1):

$$V_r = \frac{1}{6}\pi \times D_r \times W_r \times L_r \quad (4.1)$$

The relationship between the landslide volume V_r and the volume of the displaced mass or of the deposit, V_d, is given by Equation 4.2 (Cruden and Varnes, 1996):

$$V_d = \frac{4}{3}V_r \quad (4.2)$$

Observations of the scarp and/or the total surface displacement can provide profiles of failure surfaces and thus the thickness of the landslide (Jaboyedoff et al., 2015). The observations required depends on whether it is a rotational or a translational slide. For a rotational slide, measurements of the height of the scarp Δh and the angle of rotation α lead to assessment of the radius R of the sliding surface (Equation 4.3).

$$R = \frac{\Delta h}{2 \times \sin(\alpha/2)} \quad (4.3)$$

Thus, the sliding surface may be drawn by locating the center of the circle using the scarp or estimates of the initial failure surface (Jaboyedoff et al., 2009). Translational slides require analyses of a topographic profile and the movement along the sliding surface to estimate the thickness of the slide (Hutchinson, 1983).

The method is called balanced cross-section, and is based on the assumption that the void area A_1 created near the head scarp by the translational motion should exit the system, leaving surface A_2 (Figure 4.2). The displacement L is measured and the thickness D can be deduced assuming that $A_2 = L \times D$. The thickness D is given below (Equation 4.4):

$$D = \frac{1}{f}\frac{A_1}{L} \quad (4.4)$$

Where f is an expansion coefficient added to address the volumetric expansion of the sliding rock masses.

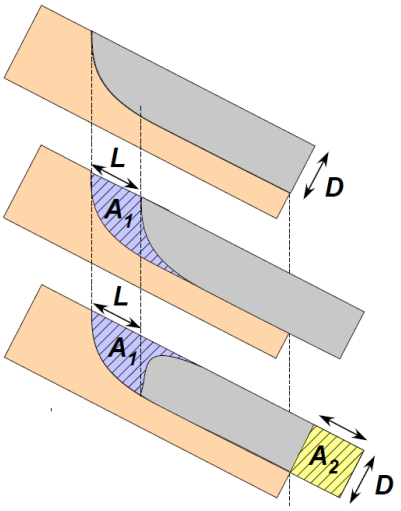

Figure 4.2: Illustration of the principle of balanced cross-section. The void area A1 at the scarp can be used to deduce the thickness D (Jaboyedoff et al., 2015).

Use of a digital elevation model (DEM) gives several possibilities regarding modelling of 3D surfaces and volume estimations. By combining morphometric features providing the limits of the unstable area or the deposits and DEM analyses, various interpolation techniques can be used. Examples are 3D splines, surface fitting and iterative procedures (Jaboyedoff et al., 2015). The Sloping Local Base Level (SLBL) technique is among these methods and will be presented thoroughly in the coming section (Section 4.1.1).

4.1.1 Sloping Local Base Level (SLBL)

The Sloping Local Base Level method (SLBL) allows the user to calculate the potential geometry of the landslide failure surface. A 3D surface geometry can be produced from geomorphic data provided by a digital elevation model (DEM). The product of the analysis is the definition of the total potential unstable volume (Travelletti et al., 2010).

The concept of Sloping Local Base Level (SLBL) was proposed by Jaboyedoff et al. (2004). The SLBL technique is based on the principle of base level, which is a geomorphological concept. The base level is defined as the lowest level of which erosion can occur (Allaby, 2013). At a regional scale, sea level provides a base level, while hillslopes, lakes or the junction between a tributary and the main river provide base levels at local scale. The base level concept itself is not very useful for landslide characterization, because all erosional processes are included and the period of time is beyond the short-term concept of landslide processing. The result of applying a base level concept is a peneplain, which is also unfavorable applied to slopes. However, when assuming that a local, short-term, sloping base level can be defined, the

concept may be used for the purpose of landslide characterization. The sloping local base level (SLBL) is the level of which erosion by landsliding can affect a limited vertical thickness of a slope (Jaboyedoff et al., 2004). The SLBL defines the possible sliding surface, which means that the volume above the SLBL may be affected by gravitational movement, and may slide on the SLBL surface (Jaboyedoff et al., 2004, Derron et al., 2005).

The SLBL method is an iterative process that progressively lowers the topography, as by erosion, down to a limiting curvature (Derron et al., 2005, Pedrazzini et al., 2013). This is, in short terms, done by replacing the altitude of a DEM cell by the average altitude of neighboring cells. This is repeated in numerous iterations (Figure 4.3). When the difference between subsequent iterations is near to zero, the computation is stopped (Pedrazzini et al., 2012).

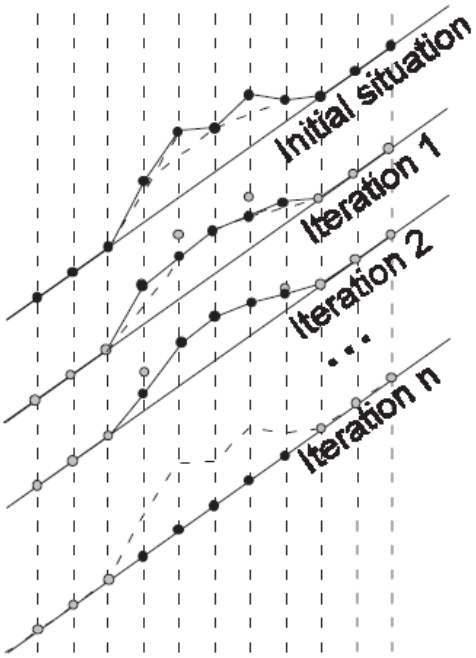

Figure 4.3: Illustration of some steps of the computation of the SLBL for a 2D-infinite slope containing a spur. The black dots represent the result for a given step and the grey dots represent the previous step(s). The procedure flattens and lowers spurs in the terrain. Several intermediate steps are missing. (Jaboyedoff et al., 2004)

The result of the procedure is a straight line between fixed points. The fixed points are manually defined by the user. Examples of such fixed points are rivers, geomorphic features and rockslide limits (Jaboyedoff et al., 2004, Derron et al., 2005). In order to create a second degree curve

representing a curved surface, a tolerance value or curvature, *Δz*, is introduced (Jaboyedoff et al., 2004). The process now flattens and lowers the spurs in the terrain between the fixed zero points and leaves a more or less curved surface, depending on the size of the chosen curvature. Depending on the sign of the tolerance value, *Δz*, the procedure leaves a concave (positive curvature) or convex (negative curvature) curved surface. The curvature may be calculated (Equation 4.5) by using the maximum horizontal length, *L*, of the profile, the assumed maximum thickness of the deposits or unstable area, h_{max}, and the cell size, *Δx*, of the DEM (Oppikofer et al., 2012).

$$\Delta z = \frac{4h^2 max \Delta x}{L^2} \tag{4.5}$$

The residual of the SLBL process is the difference in altitude between the topography and the SLBL surface. This gives the thickness of the potential unstable volume or, as in the case of this study, the scree deposits on the slope (Travelletti et al., 2010). If this result from the SLBL analysis is multiplied by the area of the given feature, the total volume may be estimated.

The Sloping Local Base Level (SLBL) technique allows, as mentioned above, the user to identify the total unstable volume of a slope. This is successfully carried out in several studies, which will be briefly presented in this section. The SLBL algorithm can be used for other purposes as well, by adjusting the tolerance value, *Δz* or invert the computation procedure. The four main purposes are (Oppikofer et al., 2012):

- Defining the possible sliding surface of an unstable slope.
- Reconstruction of the pre-event topography.
- Estimate the thickness of deposits in a main valley, including or not including rockslide scars.
- Estimate the thickness of secondary rockslide deposits on the main rock avalanche deposits.

Overview of some previous studies.

The potential sliding surface of the unstable rock slope Oppstadhornet, Norway was defined by Derron et al. (2005) using the SLBL method. Definition of such a potential sliding surface makes volume estimation of the total unstable volume possible. The difference between the SLBL surface and the topography from the DEM provides the volume of the landslide, which is estimated to 10 million m^3 at Oppstadhornet. This is in agreement with volume estimations

based on field work carried out by Blikra et al. (2001), which suggested that the volume of a potential landslide from Oppstadhornet is 10-20 million m^3.

Jaboyedoff et al. (2009) and Pedrazzini et al. (2012) have carried out analysis on the unstable rock slope at Turtle Mountain in Alberta, Canada by using the SLBL method. Jaboyedoff et al. (2009) defined the possible sliding surface and estimated the total potential unstable volume. In a real case, only 60% of the total unstable volume defined by the SLBL surface are likely to be involved in a single event. Pedrazzini et al. (2012) estimated the volumes of different potential unstable blocks in the area, which are more likely to fail than the entire volume. The SLBL method was found suitable for analysis of the potential sliding volume in this area. Thus, the study proves that the method is suitable for analyses of smaller areas within large unstable slopes, which often are more prone to failure than the entire slope.

The study by Travelletti et al. (2010) proposes a new method to develop the spatial information and quickly estimate the magnitude and intensity of a landslide. This is done by upscaling local information and failure surfaces derived from geophysical data. The study area is a large-scale landslide situated in a former glacial valley along the Rhône within the Western European Alps. The SLBL was included in the method in order to complement the seismic interpretations. Irregular surface topography and a study area that is difficult to reach, restricts the seismic profiles to a limited number. Thus, a method that complements the results was necessary. The main findings of the study regarding the SLBL was that to obtain optimal results and to find a SLBL surface, seismic data needed to be included in the SLBL calculations. This, to ensure that the SLBL-surface correlates well with the failure surface found from the seismic interpretations. There are two main failure surfaces of the landslide, the upper failure surface is well reproduced by the SLBL, but the depth of the lower surface is too low compared to the seismic data. The geomorphic limits of the landslide were included in the SLBL routine in order to improve the results. The authors conclude that the SLBL technique in combination with seismic profiling can produce 3D geometry of a landslide by including basic geomorphic criteria. The SLBL can be efficient for preliminary assessment of volume estimations to assess the magnitude and intensity of a gravitational event.

Pedrazzini et al. (2013) used the SLBL routine to reconstruct the pre-failure topography and estimate the volume of the Sierre landslide, located in the Swiss Alps. This is done by reversing the SLBL calculation. Volume estimation is also done manually in order to verify the SLBL results. The estimated volumes are in the same magnitude, between 1.4 and 1.65 km^3 for the SLBL results and between 1.6 and 2.0 km^3 for the manual estimation. The results from the

manual estimation are considered more conservative as the thickness is assumed constant. Thus, the complex shape of the failure surface is not considered. The SLBL calculation that corresponds best with the geologic and geomorphic observations in the field, gives a volume of 1.6 km^3. Construction of pre-event topography in order to compute the volume of a rock avalanche is done in several studies. One example is the Punt Cola rock avalanche in Patagonia, Southern Chile (Oppikofer et al., 2012).

Jaboyedoff and Derron (2005) used the SLBL method to estimate the infilling of alluvial sediments of glacial valleys. Volume estimations of sediments are normally based on time consuming and expensive methods such as interpolation of seismic profiles, drill holes or geometrical methods, as interpolation of gravimetric profiles. Applying the SLBL method, the depth to the bedrock surface in sediment-filled glacial valleys can be found in an effective way, and thus the volume of sediments. The researchers estimated the sediment filling in the Rhone Valley, located in the western part of the Swiss Alps. The volume of the sediments in the valley is already estimated by interpretations of seismic sections and gravimetric data, which makes it easy to verify the results from the SLBL routine. The results from the SLBL analysis are in agreement with the two other interpretation techniques. The volume estimate from the SLBL method is 118 km^3, while the estimations based on seismic results are 80-100 km^3 and 106 km^3. As observed, the results from the two methods are in the same order of magnitude. However, the authors propose that some errors can be noticed. This applies to the geometry of the valley shape. The valley shape produced by the SLBL method is quite symmetrical and in most cases U-shaped. Without other knowledge of the area than what the DEM gives, this may lead to rapid assumptions with errors. In the example from the Rhone Valley, the seismic and gravimetric interpretations are more V-shaped and irregular. However, the SLBL method provides results that gives reasonable volume estimates of valley sediments.

The SLBL technique is also widely applied on rock-slopes in Norway. The Geological Survey of Norway (NGU) use the SLBL as standard tool for volume assessment of unstable rock slopes. The SLBL is used to detect the potential rupture surface, giving the base for assessing the volume. The tool is a part of the workflow for consequence assessment, which is the result of the project this thesis is a part of. Volume assessment using the SLBL is the first of five levels in the standard procedure (Oppikofer et al., 2016a). In this thesis, the SLBL is used for assessment of the volume of scree deposits at Børa. A similar study was carried out by Oppikofer in his PhD-thesis. The volume of scree deposits at three sites in Tafjord, western

Norway were assessed (Oppikofer, 2008). There are local differences in the thickness of scree deposits in the area (Figure 4.4).

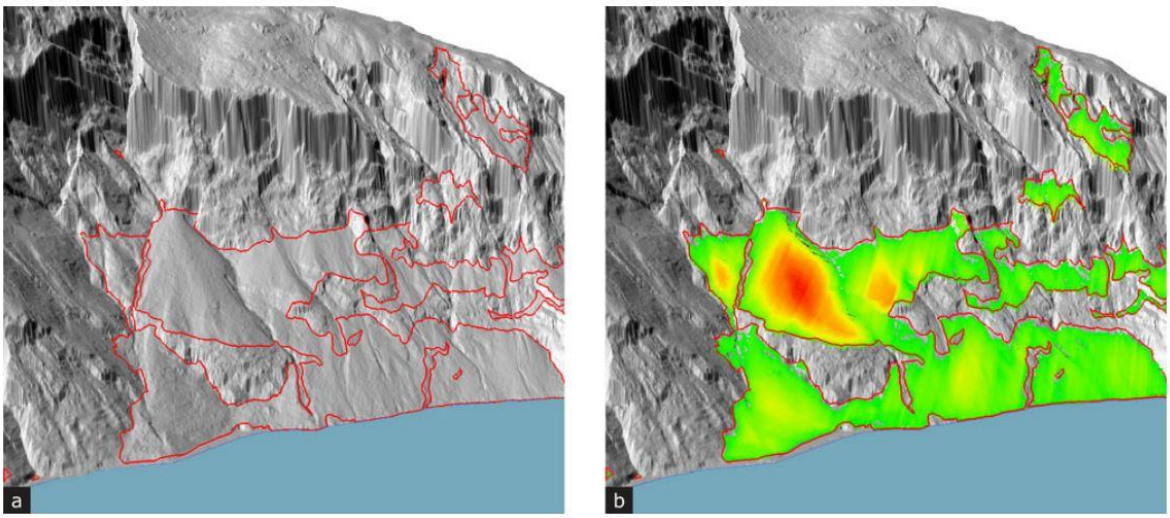

Figure 4.4: Scree slopes beneath the unstable rock-slope Hegguraksla, Tafjord, wastern Norway. a) hillshade showing the extent of the scree deposits and scree-filled gullies. b) SLBL model of thickness of the scree deposits. Thickness is represented by colour scale. (green = 0 m, red = 53.7 m) (Oppikofer, 2008).

4.2 Rock avalanche run-out

4.2.1 Mobility of rock avalanches

Rock avalanches are by Hungr et al. (2014) classified as "Extremely rapid, massive, flow-like motion of fragmented rock from a large rock slide or rock fall". They appear when a coherent mass of rock releases from its original location, disintegrates, and fragments into a granular flow. The bulk of the rock avalanche mass is dry during motion. This is due to the rapid motion, which makes it impossible to fill the new created pore-space with water. However, many rock avalanches are reported to travel on a basal, saturated layer, consisting of saturated material entrained from the travel path. The path material liquefies due to the rapid undrained loading from the rock masses and creates a basal saturated layer as it is entrained. The processes of entrainment are described in a forthcoming section (Section 4.3).

The mobility of rock avalanches is reported to be high, causing surprisingly long run-outs (Evans et al., 2006, Hungr et al., 2014). It is found that the mobility increases with the volume of the event, meaning that large volumes give longer run-out. The degree of mobility exceeds what is expected for such a dry and frictional flow (Hungr et al., 2014). Deposits from large rock avalanches are observed to extend much farther from the source than deposits from smaller

events, considering the proportion of elevation loss (Davies and McSaveney, 2012). The phenomenon of extremely long run-out distances was first discovered in the nineteenth century in Switzerland (Heim, 1932).

The phenomenon is described by the ratio *H/L* (Equation 4.6), called "Fahrböschung" (Heim, 1932) or angle of reach (Corominas, 1996).

$$\frac{H}{L} = \tan \alpha \qquad 4.6$$

Where *H* is the difference in elevation between the top of the source area and the distal tip of the deposit and *L* is the horizontal distance between the same points (Figure 4.5). Fahrböschung, α is the angle between the top of the source area and the distal part of the deposits. The travel angle, α' is one of the output values of the numerical model (DAN3D) used in this thesis. It is the angle between the centre of gravity of the source area and the centre of the deposits (Figure 4.5). It can be difficult to determine the points accurately in the field, thus, the travel angle is used less frequently than the Fahrböschung (Bowman et al., 2012).

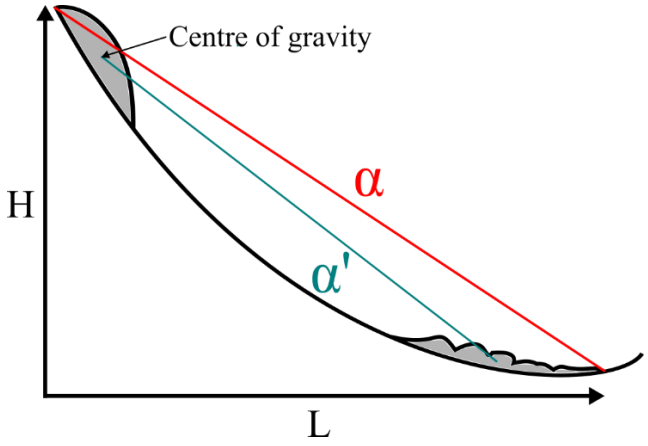

Figure 4.5: Illustration of Fahrböschung, α and the travel angle, α'. H is the difference in elevation between the top of the source area ant the distal tip of the deposit. L is the horizontal distance between the same points. The travel angle, α' is the angle between the centre of gravity of the source area and the centre of the deposits.

The ratio *H/L* was assumed to equal the internal friction coefficient of the rock material, μ, but studies have shown that the friction seems to be reduced for larger events. For smaller events $H/L = \tan\alpha \sim 0.6$, where α is usually approximately 30-35°. For larger events, *H/L* values of down to 0.05 have been observed (Davies and McSaveney, 2012). The decrease in *H/L*, and thus the friction, for events of larger volumes is called the "size effect", first proposed by Scheidegger (1973). Analyzing 33 rock avalanches, Scheidegger (1973) found a relationship between landslide volume, *V* and the ratio *H/L*, leading to a best-fit curve (Figure 4.6). This

allows an empirical estimation of run-out distance if the volume of the unstable rock-slope is known (Equation 4.7). The curve and the volume provides the user the angle of reach *α*, which equals the ratio *H/L*. By using the fall height *H*, the run-out distance, *L*, may be estimated. Corominas (1996) proposed that for smaller events (V < 250 000 m^3), a fixed angle of 31° should be used when estimating the run-out distance with this method.

$$\frac{H}{L} = \tan\alpha = 10^{0.62419} \times V^{-0.15666} \qquad 4.7$$

The method is a conservative estimate for Norwegian cases (Figure 4.6). 90% of the analyzed events in Norway have a shorter run-out distance than predicted by the Scheidegger relationship (Blikra et al., 2001, Oppikofer et al., 2016b). A common range of *H/L* in Norway is 0.2 - 0.7, with decreasing values for increasing volumes. The largest events are found to have values down to 0.1. The geological conditions in Norway, meaning hard rock and coarse material, increases the friction in the moving mass and decrease the run-out (Domaas and Grimstad, 2014).

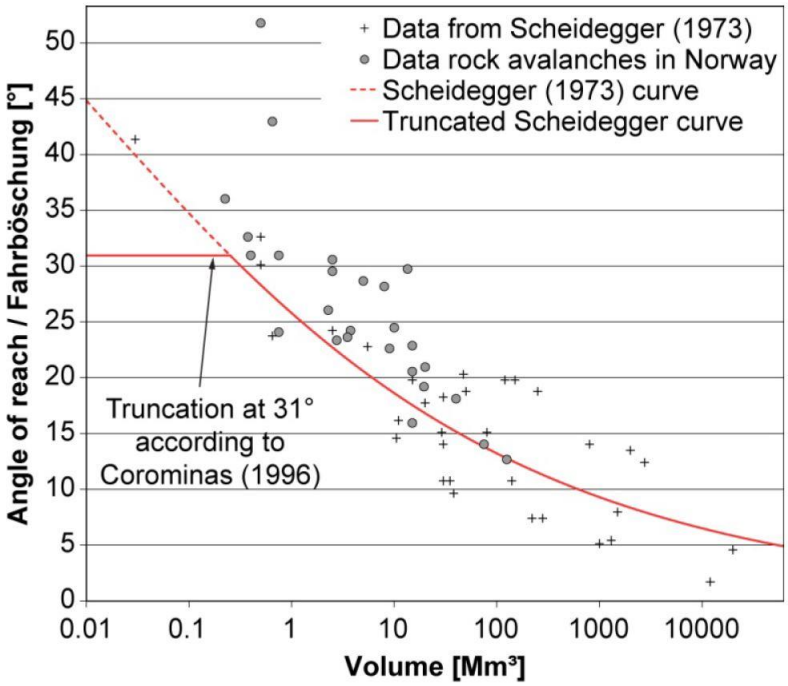

Figure 4.6: Correlation between landslide volume and angle of reach based on Scheidegger (1973). Norwegian events (from Blikra et al. (2001)) having a shorter run-out than what the curve indicates. Figure from (Oppikofer et al., 2016b).

Several alternative ways of describing the relationship between *H* and *L* have been proposed in order to emphasize the "size effect". Hsü (1975) explained the high mobility by the "excess travel distance", L_e (Equation 4.8). The distance equals the "horizontal displacement of the tip of the rock avalanche beyond what is expected from a frictional slide down an incline with a normal coefficient of friction of *tan32°* (0.62)".

$$L_e = L - \frac{H}{tan32°} \qquad 4.8$$

Nicoletti and Sorriso-Valvo (1991) proposed a system to distinguish in what ways the local morphology controls the shape and mobility of a rock avalanche. The total energy involved in a landslide process is constant, but the initial mechanical energy is transformed into other, more degraded forms as the masses move. The rate at which the energy is dissipated varies. The rate is controlled, among other factors, by the local morphology. After studying 40 rock avalanches, the researchers were able to distinguish in which ways the local morphology controls the shape and mobility of a rock avalanche (Table 4.1, Figure 4.7). The features of the three categories are the shape of the landslide including a description of the debris mass and the degree of mobility decided by the rate of dissipation of the total mechanical energy (Table 4.1).

Table 4.1: Description of the three categories of rock avalanches from the study by Nicoletti and Sorriso-Valvo (1991). For sketches see Figure 4.7.

	Shape	Description of debris mass	Mobility	Energy-dissipative control
A	Elongated Hourglass	Channeling	High	Low
B	Nearly Oval, Lengthened Trapezium or Tongue	Unobstructed spreading	Intermediate	Moderate
C	Deformed T	Right-angle impact against opposite slope.	Low	High

Several measurements of morphologic features resulted in the categories explained in the table above (Table 4.1). The ones marked on Figure 4.7 are:

- L – the overall run-out (travel distance) of the rock avalanche.
- D – the length of the rock avalanche, measured horizontally. Equals L in case A and B.
- W_m – the width of the rock avalanche measured at $D/2$.
- W_a – the maximum width of the deposit zone.

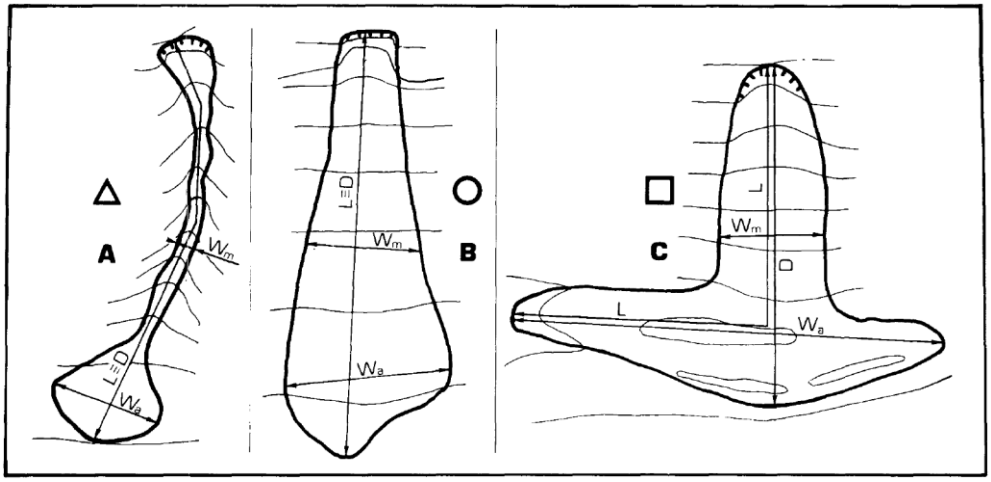

Figure 4.7: The three configurations that a rock avalanche can assume as a result of geomorphic control. A: High-mobility rock avalanche. B: Intermediate-mobility rock avalanche. C: Low-mobility rock avalanche (Nicoletti and Sorriso-Valvo, 1991). See Table 4.1for further descriptions.

Davies and McSaveney (2012) quantified the run-out in relation to volume. A rock avalanche is defined as an event with a volume, $V > 10^6$ m^3. The horizontal run-out of a small event (10^{-4} m^3 < V < 10^6 m^3) is given by Davies and McSaveney (2012) as:

$$R_h/h^* \leq 4 \tag{4.9}$$

Where R_h is the run-out on a horizontal plane and $h^* = (volume)^{1/3}$.

Large rock avalanches are, as mentioned, observed to have a longer run-out, given by:

$$6 \leq R_h/h^* \leq 10 \tag{4.10}$$

The interested reader is referred to Davies and McSaveney (2012) for more information about other explanations.

The high mobility and extremely long run-outs of large rock avalanches have led to discussions. Several hypotheses and explanations of the phenomenon exists, but researchers have not agreed upon a universal theory (Hungr et al., 2014). Some of the main hypotheses are listed below, as described in Hungr and Evans (2004):

- Mobilization by an air cushion, overridden and trapped beneath the mass of the rock avalanche (Shreve, 1968).
- Fluidization by similarly trapped air or by steam generated by vaporization of groundwater (Goguel and Pachoud, 1972).
- Fluidization by dust dispersion (Hsü, 1975).
- Rock melting or dissociation by the heat of friction (Erismann, 1979).
- "Mechanical fluidization" understood as a process of spontaneous reduction of friction angle at high rates of shearing (Scheidegger, 1975, Campbell, 1989).
- Acoustic fluidization – reduction of the friction angle resulting from acoustic-frequency vibrations at the base of the flowing mass (Melosh, 1979).
- Increase in areal dispersion of debris as a result of fragmentation (Davies and McSaveney, 1999).
- Lubrication by liquefied saturated soil entrained from the slide path (Buss and Heim, 1881, Abele, 1974, Abele, 1997, Sassa, 1985) .

Increased volume may enhance the mobility of the rock avalanche and thus the run-out distance. Both grain fragmentation and entrainment of path material are proposed to be the explanation of the excess run-outs of large rock avalanches (Hungr and Evans, 2004, Davies and McSaveney, 2012). However, the researchers, as mentioned, do not agree upon one theory. Entrainment is one of the main subjects of this thesis, a description of the phenomenon is given in a forthcoming section (Section 4.3). Fragmentation is explained in the next subsection.

4.2.2 Fragmentation of rock avalanche masses

The rock mass suffers from severe fragmentation during sliding. Fragmentation is a complex process caused by changes in the stresses in the translating mass of rock. A clast in a moving rock mass is exposed to both direct stress and rotational stress. The direct stress from the overburden material and the rotational stress from the shear motion it is a part of. Local stress concentrations that exceed the strength of the rock may occur, causing the rock clast to explode. The explosion and following formation of fragments, releases elastic strain energy as kinetic

energy of moving clast fragments. There is a small energy loss due to creation of new surfaces (Davies and McSaveney, 2002). The result of several fragmentation events is an increased longitudinal pressure within the moving mass. The fragmentation leads to spreading of the material and thus an increased run-out of the distal part of the masses and in addition, a reduced travel distance of the proximal masses (Davies et al., 1999). Due to the relatively high stresses that are required, fragmentation is mostly a subsurface phenomenon. For the local stress concentrations in the rock clasts to exceed the strength of the rock, the stresses it suffers from need to be of a certain size. Thus, the overburden must be large enough. Observations of an inverse grading in rock avalanche deposits, with a finely fragmented interior and a blocky surface, supports this (Dunning and Armitage, 2011).

Fragmentation is proposed to be one of the reasons for the excess run-out of large rock avalanches (Davies et al., 1999, Davies and McSaveney, 2002, Davies and McSaveney, 2012). Fragmentation induces an additional spreading of the masses. It is proven that the excess run-out of large rock avalanches can occur without decrease in friction coefficients if pressures higher than normal internal pressure are present. This is the case when grain fragmentation occurs. Numerical modelling of the Falling Mountain rock avalanche in Arthur's Pass National Park, New Zealand, showed that by increasing the earth pressure coefficients, it was possible to reconstruct the long run-out without decreasing the friction to unrealistic low values. However, the researchers did not succeed in recreating all observed features of the avalanche (Davies and McSaveney, 2002).

However, the theory of long run-outs explained by grain fragmentation has not yet been intensively tested under laboratory conditions. Even though it is one of the sufficient explanations of long run-outs by now, new mechanisms will be proposed in the future (Davies and McSaveney, 2012).

4.3 Entrainment

Volume increase of landslide masses happens by two processes: fragmentation of the masses and entrainment of material along the travel path. The processes of entrainment will be the focus of both this section and the thesis. Fragmentation is briefly explained in Section 4.2.2.

The mechanism of material entrainment is complex and poorly understood (McDougall and Hungr, 2005). Entrainment is assumed to cause volume and rheology changes of rapid landslides along the path. Landslide paths are often covered by deposits of various thickness. Rapid loading, as from a landslide, may cause failure of the deposits due to the rapid stress changes induced. The failed deposits will increase the initial volume of the landslide. The deposits may have different properties than the source material, especially when it comes to water content and granulometry (McDougall and Hungr, 2005).

The two physical processes that constitutes entrainment are direct basal entrainment and frontal plowing (Hungr and McDougall, 2009). Entrainment thus occur at the front and beneath the body of moving mass (Figure 4.8).

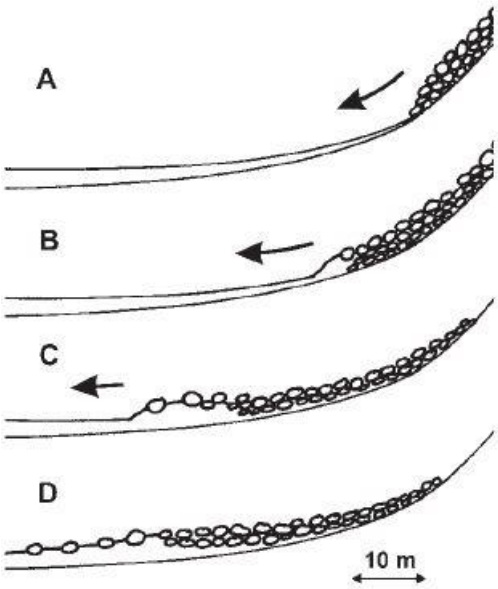

Figure 4.8: Hypothetical mechanism of entrainment of substrate material. (B) and (C) shows how the moving masses impact the substrate by plowing and loading, and how the loading causes liquefaction. (Hungr and Evans, 2004).

Entrainment of debris material from the slope can affect a landslide in different ways. A rock fall or rock avalanche entraining material from the slope will increase its total volume. Water can also be added to the rock masses by entrainment of saturated soil in the path. This is the only process that makes significant water blend in with the rock masses, because the water content in most rock masses is negligible. Entrainment of saturated soil by the rapid undrained loading that a moving rock avalanche will cause (Figure 4.8), may lead the saturated substrate material to liquefy (Sassa, 1985). This will change the character of the basal parts of the moving mass. Volume increase and increase of water content in the rock avalanche masses, as described above, may enhance the mobility of the moving masses (Hungr and Evans, 2004). This will affect the rock avalanche run out distance. The Huascarán events in 1962 and 1970 were originated as rock/ice falls and transformed into debris flows by entrainment of path material. The high-velocity mass movements were reported to have extremely long run-outs, approximately 180 km (Evans et al., 2009). This emphasizes the effect of entrainment to the mobility of a landslide.

The entrainment ratio, *ER*, is defined as the ratio between entrained volume and the initial landslide volume (Equation 4.11). The ratio quantifies the entrainment process and addresses its impact and importance on the particular landslide.

$$ER = \frac{V_{Entrained}}{V_{Fragmented}} = \frac{V_E}{V_R(1 + F_F)} \tag{4.11}$$

Where V_E is the volume of entrained material, V_R is the volume of the initial rockslide and F_F is the fractional amount of volume expansion due to fragmentation (Hungr and Evans, 2004).

A few estimates of the volume increase exists. According to Hungr and Evans (2004) the volume increase due to fragmentation F_F is assumed ~ 25 % for deposits at rest. A high entrainment ratio implies that volume increase is an important factor of the particular landslide. Hungr and Evans (2004) proposed a term for rock fall and rock avalanche events in which the entrainment ratio, *ER*, exceeds 0.25 in order to emphasize the important influence of entrainment. The term is “rock slide-debris avalanche”, which describes the increase in mobility and extensive damage such events can cause. Entrainment of path material may transform the initial landslide to a completely different form, as seen in the Huascarán-events (Evans et al., 2009).

4.3.1 Norwegian case studies

There are examples of Norwegian rock-slope failures entraining significant volumes of debris material (Table 4.2). Loen in western Norway suffered from disastrous events in 1905 and 1936. The Loen-events in 1905 are both reported to have mobilized the talus slopes, leading to a dramatically increase in volume. The debris impacted Loenvatnet lake and triggered tsunamis that caused 61 fatalities. The event January 15, 1905 was initiated by a 50 000 m^3 block that fell approximately 500 m and entrained 300 000 m^3 debris. The event in September, 1905 started with the collapse of a part of Ramnefjell, approximately 15 000 m^3, entraining about 50 000 m^3 on the travel path (Grimstad and Nesdal, 1990, Hermanns et al., 2006). However, the methods for volume estimations in 1905 are not known, and the volume estimates should accordingly be carefully considered.

In Tafjord, western Norway, an unstable part of a rock-slope collapsed 730 m.a.s.l in April 1934. The scree slopes beneath was mobilized, leading to a tsunami that killed 40 persons. The initial volume of rock is estimated to 1.5 million m^3. The rock mass mobilized material of approximately the same volume, meaning that 3 million m^3 hit the water (Furseth, 1995).

Table 4.2: Overview of some entrainment events in Norway. Data from (Grimstad and Nesdal, 1990) and (Furseth, 1995).

Location	Date	Height of outfall [m.a.s.l.]	Initial volume [m^3]	Volume entrained [m^3]
Loen	15.01.1905	500	50 000	300 000
Loen	20.09.1905	400	15 000	50 000
Tafjord	07.04.1934	730	1 500 000	1 500 000

Mapping of pre-historic rock avalanche deposits has revealed the impact of entrainment. The rock avalanche at Venge in Romsdal Valley, western Norway is one example. The event is dated to 1500 years and the estimated volume is 0.5-1 million m^3 (Anda and Blikra, 1998). Deposits from the landslide at Venge crosses the entire valley. Debris flow deposits are found at the front of the rock avalanche deposits and are reported to cover the distal part of the rock avalanche deposits (Figure 4.9). The run-out distance of the rock avalanche is 1000 m, but debris material are found at a distance of another 700 m, giving a horizontal run-out of 1700 m in total (Dahle et al., 2008). The sediment cover and debris deposits are interpreted to be formed

by secondary debris flows initiated by the rock avalanche, meaning that debris material was entrained by the rock masses (Blikra et al., 1999, Blikra et al., 2002, Dahle et al., 2008).

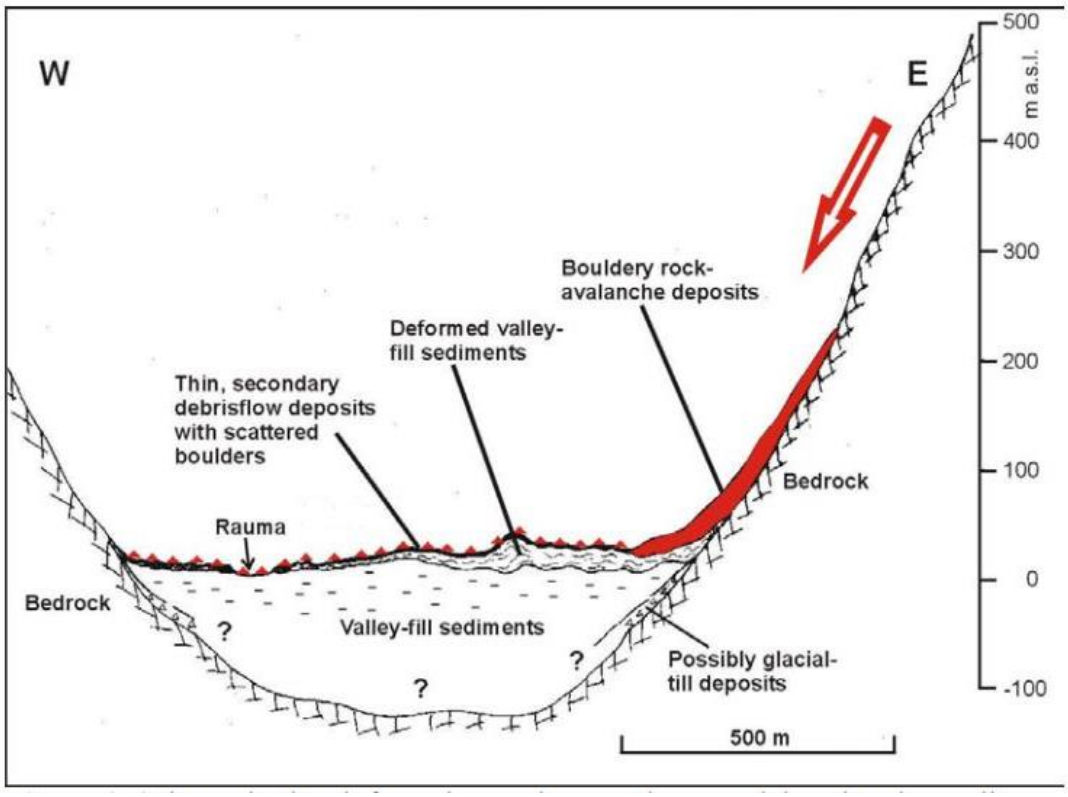

Figure 4.9: Sketch showing the Venge event, Romsdal valley and its impact on the valley-fill sediments. Modified from.(Blikra et al., 2002).

4.4 Numerical run-out modelling

Rapid landslides are among the most dangerous and damaging of all landslide phenomena. Prediction of run-out parameters including maximum distance reached, flow velocity and thickness and distribution of deposits are essential to decrease their potential for destruction (Hungr, 1995). Landslide run-out prediction can be done by empirical and/or analytical methods. The empirical methods use observational data correlations to predict the run-out zone of a landslide. Analytical methods aim to predict the motion of a landslide from source area to final deposit by including lumped mass and continuum mechanical models (McDougall and Hungr, 2004). Numerical modelling is a suitable tool for the purpose of run-out prediction, and should be included in a rock avalanche prediction study. However, it is important that results from numerical modelling do not overrule practical and critical thinking and judgement. Thus, empirical and numerical analysis used in combination are of advantage (Eberhardt, 2006).

According to McDougall et al. (2012) most modern numerical models are able to simulate the main characteristics of a real landslide. There are difficulties in modelling a heterogeneous moving mass with a complex behavior during propagation (Pirulli and Mangeney, 2008). Even though the models rely on simplified assumptions, the most important features are possible to reconstruct. The main challenge is to assess and determine the input parameters needed to run the model. Due to lack of information and reliable techniques, the value of the parameters must be obtained by back-calculation or by trial-and-error, depending on the situation (McDougall et al., 2012). Studies have shown that modelled results are highly affected by the set input parameters. Chosen rheology and values of parameters both influence the modelled results significantly (Hungr and McDougall, 2009).

The most commonly used approach for numerical run-out modelling is based on the continuum mechanics. Continuum mechanics applies the principles of conservation of mass, momentum and energy for sliding and rheological properties for flowing. The approach is a deformable body-approach, which allows simulations of the deformation of the moving mass along the flow path. The program used in this study, DAN3D, applies these concepts (Hungr, 1995). Even though models based on continuum mechanics are usually preferred for landslide run-out prediction, different approaches exist as well (Crosta et al., 2003).

A number of different numerical models exists today. Some of the existing models are listed in the table below (Table 4.3). For further information about model descriptions, see McDougall et al. (2012).

Table 4.3: Overview of some existing numerical models. Modified after (McDougall et al., 2012).

Model denotation	Type	Model description
Wang	2D, continuum	Wang (2008)
DAN	2D, continuum	Hungr (1995)
DAN3D	3D, continuum	McDougall (2006)
FLATModel	3D, continuum	Medina et al. (2008)
FLO-2D	3D, continuum	FLO-2D Software Inc. (2007)
MADFLOW	3D, continuum	Chen and Lee (2000)
Pastor	3D, continuum	Pastor et al. (2009)
PFC	3D, discontinuum	Poisel and Preh (2008)
RAMMS	3D, continuum	Christen et al. (2010)
RASH3D	3D, continuum	Pirulli (2005)
Sassa-Wang	3D, continuum	Wang and Sassa (2002)
SHALTOP-2D	3D, continuum	Mangeney-Castelnau et al. (2003)
TITAN2D	3D, continuum	Pitman et al. (2003)
TOCHNOG	3D, continuum	Roddeman (2002)
3dDMM	3D, continuum	Kwan and Sun (2007)

4.5 DAN3D

The two-dimensional code DAN was developed especially to model propagation of rapid landslides of the flow type, such as rock avalanches (Hungr, 1995). DAN3D (Dynamic Analysis in Three Dimensions) is a more advanced model, based on a depth-averaged, two-dimensional form of the DAN code. DAN3D was developed by Scott McDougall as a part of his PhD thesis (McDougall, 2006). DAN3D allows modelling of landslide propagation over a complex three-dimensional terrain (McDougall and Hungr, 2004, Hungr and McDougall, 2009) and has the ability to entrain material along the path (McDougall and Hungr, 2005). The model is verified and validated by analyzing well documented events and by laboratory experiments, where granular materials are tested on both straight and curved paths (McDougall and Hungr, 2004).

4.5.1 Model theory

DAN3D applies the concept of equivalent fluid (Figure 4.10), which is a simplified semi-empirical approach defined by Hungr (1995). Landslide material is complex and heterogeneous by nature. The concept of equivalent fluid models the landslide material as a hypothetical material governed by simple rheological relationships, where the internal and basal rheologies may be different from each other (Figure 4.10). The model rheology expresses the resistance force inside the flow.

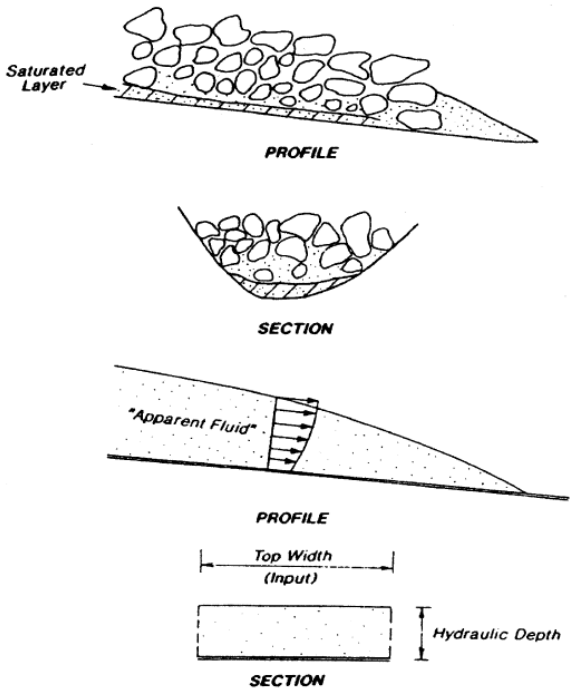

Figure 4.10: Schematic illustration of equivalent fluid approach applied to a rock avalanche. The complex landslide material is modelled as a hypothetical homogenous material. The material is governed by simple internal and basal rheologies. (Hungr, 1995, Hungr and McDougall, 2009)

The concept treats the mass as a number of blocks. The net driving force, F, acting on each block with height H_i and width B_i, consists of three components (Equation 4.12, Figure 4.11). The tangential component of weight, the basal resisting force, T, and the tangential internal pressure resultant, P (Hungr, 1995).

$$F = \gamma H_i B_i \, ds \sin\alpha + P - T \qquad 4.12$$

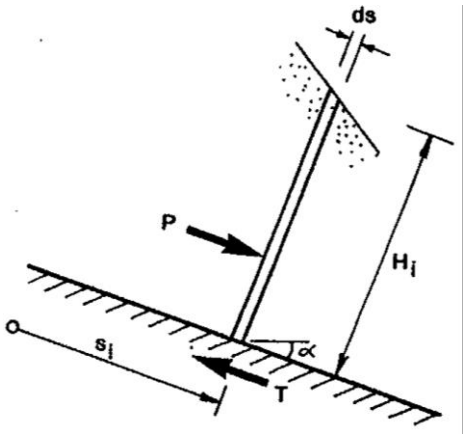

Figure 4.11: Illustration of the net driving forces acting on each block (Hungr, 1995).

By separating the internal and basal rheology, the basal friction term may be different from the internal. This is consistent with the situation existing in many natural landslides, where a rigid mass of material flows on top of a more mobile basal layer. The differences between the basal layer and the rest of the landslide masses are mostly due to the degree of water saturation and pore pressure. Granulometry and porosity are also important factors causing differences between the internal and basal layer in a landslide. Entrainment and liquefaction of saturated material from the path of the flow are the main processes causing differences in these factors (Hungr and McDougall, 2009).

4.5.2 Input parameters

A list with short descriptions of the input parameters in DAN3D is given in order to introduce the parameters and make the reader familiar with terms used later in the thesis. There are both material and program related parameters. Some parameters are required to run the model, while others are optional. There are defaulted values for some of the parameters. Only the parameters included or mentioned as a part of the analyses carried out in this thesis are listed. For further information, the reader is referred to the DAN3D user manual (Hungr, 2010), papers by Hungr and McDougall (Hungr, 1995, McDougall and Hungr, 2004, McDougall and Hungr, 2005) and Scott McDougall's PhD. thesis (McDougall, 2006).

Control parameters

- *Number of materials*: Number of materials or rheologies used in the problem.
- *Number of particles*: Number of smooth particles used. See Section 4.5.4.
- *Erosion rate*: Explained in Section 4.5.5. DAN3D is containing a build-in calculator, which allows the user to calculate the erosion rate based on simple input data.
- *Maximum simulation time*: Time at which the simulation should stop. The stopping criteria of the model.

General parameters

- *Smoothing length constant*: Determines the radius of influence of each particle. Defaulted to 4.
- *Velocity smoothing coefficient*: Coefficient used to determine how potent the velocity smoothing algorithm is. Defaulted to 0.01.
- *Stiffness coefficient*: Used in the calculation of the stress coefficients. Defaulted to 200.
- *Slide margin cutoff thickness*: Related to the graphical presentation of the simulation in DAN3D. Determines the minimum cutoff value below which particles or grid nodes will not be drawn on the screen during the simulation. The nodes are not eliminated in the output files.

Material properties

It is possible to run the model with several materials. Each material is given a number, which must coincide with the numbers used in the erosion grid input file. The materials can be given different properties, where some are associated with the chosen rheology.

- *Rheology*: There are five rheology types for the user to choose. Frictional, plastic, Newtonian, Bingham and Voellmy. The frictional and Voellmy rheology are most suitable for rock avalanches and thus the most relevant in this thesis. See Section 4.5.3.
- *Unit weight, [kN/m^3]*: Unit weight of the material.
- *Friction angle, φ [deg]*: Friction angle of the material. See Section 4.5.3.
- *Pore-pressure coefficient, R_u*: Ratio of pore pressure to the total normal stress at the base of the sliding mass.
- *Friction coefficient, μ*: Coefficient used in the Voellmy rheology. Defines the frictional term of the basal flow resistance equation. See Section 4.5.3.
- *Turbulence coefficient, ξ [m/s^2]*: Coefficient used in the Voellmy rheology. Defines the turbulent term of the basal flow resistance equation. See Section 4.5.3.

- *Internal friction angle*: Defines the amount of internal friction in a material. DAN3D assumes that all internal deformation is frictional (Section 4.5.3). The defaulted value is 35°, which is appropriate for dry, fragmented rock. The user is encouraged to experiment with other values.
- *Maximum erosion depth, [m]*: Depth to which the material is eroded after the whole slide mass passes over (Section 4.5.5).

4.5.3 Rheological relationships

In DAN3D, the internal rheology is assumed to always be frictional, while the basal friction is defined by various rheological relationships, where the rheology is of the user's choice. This gives the user the opportunity to reproduce the external behavior of real-life events if estimates from field observations are available. However, the possibility to choose the rheology of the model, and change it along the path or within the slide mass makes it easier to fit the model to the actual case by calibration or back-calculation. The two rheology models most common for rock-avalanche run-out are the frictional and the Voellmy rheology (McDougall, 2006, McKinnon et al., 2008). They will be briefly presented in this section. The interested reader is referred to (McDougall, 2006, Hungr, 1995) for more information about the other rheologies available in DAN3D.

The basal rheology gives the basal shear resistance,τ_{zx}, which opposes motion. The equations for the shear resistance (Equation 4.13 - 4.15) are derived from uniform flow equations and are depending on the rheology. The derivation of the equations can be found in (McDougall, 2006).

Frictional rheology

$$\tau_{zx} = -\sigma_z(1 - r_u)tan\varphi \tag{4.13}$$

Where φ is the dynamic basal friction angle and σ_z is the total stress. r_u is the pore pressure ratio, $r_u = u/\sigma_z$, where u is the pore fluid pressure at the base.

Equation 4.13 can be simplified to include only one single variable, the bulk basal friction angle φ_b.

$$\tau_{zx} = -\sigma_z tan\varphi_b \tag{4.14}$$

Where $\varphi_b = (1 - r_u)tan\varphi$. This implies use of a constant pore-pressure ratio, and assumes a loading response between purely drained and undrained (Hungr and McDougall, 2009).

The frictional rheology assumes the resisting shear force, τ_{zx}, only to depend on the effective normal stress (Sosio et al., 2008).

Voellmy rheology

Voellmy rheology combines frictional and turbulent behavior.

$$\tau_{zx} = -(\sigma_z \mu + \frac{\rho g v_x^2}{\xi}) \tag{4.15}$$

Where μ is the friction coefficient and ξ is the turbulence coefficient. The coefficients are rheology-specific input parameters required when running the model with a Voellmy rheology. σ_z is the total stress, ρ is the constant material density, g is the gravitational acceleration and v_x is the depth averaged flow velocity (Hungr and McDougall, 2009).

The total resistance of the flowing mass is in the Voellmy rheology described as the sum of a frictional and a turbulent term. The frictional term takes into account the frictional components of flow resistance and relates the shear stress to the normal stress through the friction coefficient, μ. The turbulent term accounts for all velocity-dependent factors of flow resistance, and is represented by the turbulence coefficient, ξ, which scales with the velocity squared and the density of the debris (Sosio et al., 2008, Hungr and McDougall, 2009). The idea of separating the resistance in two terms was introduced by Voellmy (1955) for the propagation of snow avalanches. The turbulent term was originally introduced to account for air drag on snow avalanches.

According to Hungr and McDougall (2009) the modelled results are strongly dependent on the chosen rheology. A frictional model will calculate high velocities and predict forward-tapering deposits. A model run with Voellmy rheology will result in lower velocities and a forward bulging deposit (McDougall, 2006).

4.5.4 Numerical solution

The numerical solution scheme in DAN3D is based on the concept of Smoothed Particle Hydrodynamics (SPH). The concept is a variation of the Langrange procedure. By applying this numerical method, the discretization of the total volume of the slide results in a number of reference columns where the equations are applied to the center of the column (McDougall and Hungr, 2004, Sosio et al., 2008).

The solution is meshless, and the reference columns indicate the position of the particles (Figure 4.12). The particles are assumed smooth particles, which have a finite volume and together represent the total slide mass. The volume of the particles can increase due to material entrainment. The depth and depth gradient of each particle at a given time can be estimated based on the reference column's location. For each time step, the flow velocities are updated and the columns advance to new positions (Nigussie, 2013).

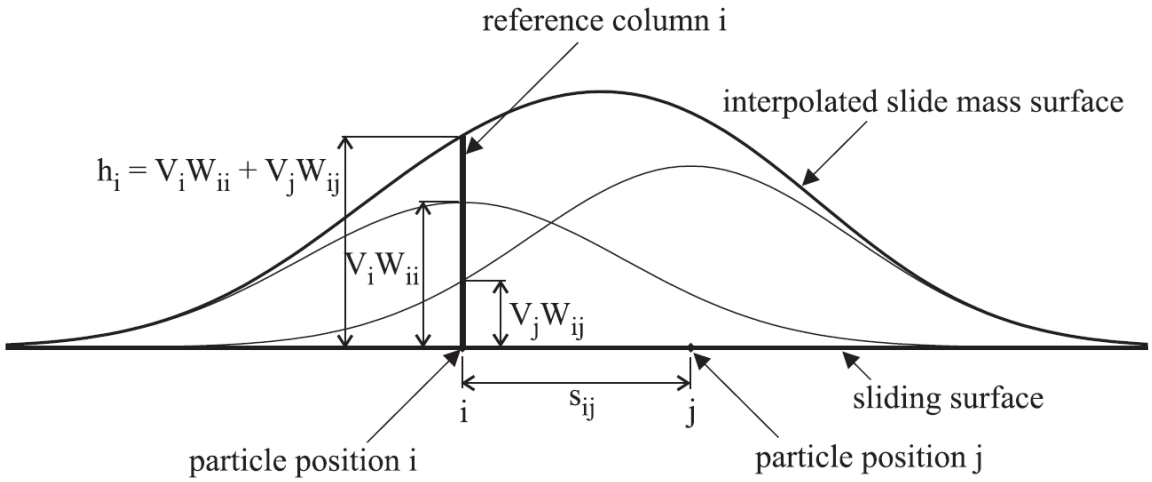

Figure 4.12: A physical interpretation of Smoothed Particle Hydrodynamics (SPH). The reference column represents the particle position at a given time (McDougall and Hungr, 2004). V is the volume of each particle, W is the interpolating kernel and h is the flow depth.

4.5.5 Entrainment in DAN3D

DAN3D allows for material entrainment along the path. Entrainment is an important feature of many rapid landslides, as it increases the volume and changes the mobility (McDougall and Hungr, 2005). It is challenging to estimate the volume of material available for entrainment and the rate at which it is entrained by the landslide. A simple entrainment algorithm, based on natural exponential growth of material, and a user-defined erosion rate, *E*, controls entrainment in DAN3D (Equation 4.16). The entrainment rate *E* controls the growth of material, while an erosion depth, which is also specified by the user, limits the available material. The maximum predicted erosion depth is reached only after the entire landslide passes. The entrainment rate represents the increase in local flow volume per meter travelled, without considering the flow velocity.

The erosion rate, *E*, is given by:

$$\frac{\partial b}{\partial t} = Ehv \tag{4.16}$$

Where *v* is the flow velocity, *h* is the flow height and $\frac{\partial b}{\partial t}$ is the erosion velocity (McDougall and Hungr, 2005).

When a particle is centered within a fixed grid cell containing erodible material, entrainment occurs. The areas containing material available for erosion and entrainment are given by the erosion input file. It is possible to give the materials different rheologies and properties by separating the material of the source area and the material in an erosion zone. This allows the user to simulate the effect of reduction in basal shear strength caused by undrained loading or changes in water content or strength of path material.

The simple algorithm applied in DAN3D account for both volume and rheology changes. According to McDougall and Hungr (2005) the main limitation of the simple entrainment approach is the use of the user-specified entrainment rate. The parameter must be added by trial-and-error to obtain a reasonable distribution of entrained material in the study area. However, a preliminary estimate of the entrainment rate can be found (Equation 4.17). The average growth rate $\bar{E}$ for a specific entrainment zone of approximate length $\bar{S}$ can be defined as:

$$\bar{E} = \frac{\ln(\frac{V_f}{V_0})}{\bar{S}} \tag{4.17}$$

Where V_0 is the estimated total volume entering the zone and V_f is the estimated total volume exiting the zone. The build-in calculator in DAN3D, which allows the user to calculate the erosion rate, is based on this equation. The required input parameters are the approximate length of the entrainment zone and the total volumes entering and exiting the zone.

The entrainment rate is a difficult parameter to assess. According to McDougall and Hungr (2004) it may depend on the basal shear stress, the flow velocity, bed material strength and the amount of material available for entrainment. The rate of debris entrainment will also depend on material properties, such as density, gradation and degree of saturation. The slope angle and the current mass of the avalanche will also affect the entrainment rate (Hungr and Evans, 2004).

McDougall and Hungr (2005) did a back-calculation of the Nomash River landslide in British Columbia, Canada in order to calibrate the model parameters regarding entrainment in DAN3D. Their results were compared to field observations and modelling in DAN carried out by Hungr and Evans (2004). An erosion rate $E = 0.00019\ m^{-1}$ was computed based on knowledge of initial slide volume, final volume and length of entrainment zone. The simulated maximum erosion depth corresponds with the field estimate, being 8.1 and 8 m respectively.

5 Methodology

5.1 Estimation of debris thickness and volume

The volume estimation of the scree deposits at Børa is carried out by the Sloping Local Base Level (SLBL) technique, presented in chapter 4.1.1. The procedure is implemented in the CONEFALL software. This section gives an overview of the procedure of this method.

5.1.1 Preparation: Creating input files

A geomorphologic map of the area is necessary to identify the different geomorphic features (Figure 5.1). Geomorphologic mapping was carried out as a part of the project thesis, which forms the base for this thesis (Andresen, 2015). Fixed points are defined based on the mapped geomorphology presented as polygons on the geomorphological map (Figure 5.1). Scree deposits are given the value -1, while the other geomorphological features mapped are given the value 1. This, to identify the fixed points and the areas where the computation will be run. Rock outcrops are defined as fixed points in this study.

Six profile lines were drawn on the geomorphological map (Figure 5.1). Many SLBL-models with different curvature were made. The profile lines were analyzed in order to choose the most plausible SLBL-models. The digital elevation model (DEM) available has a resolution of 1 m. To decrease the time of simulation, the resolution of the DEM used for this purpose was changed to 5 m.

The raster data from the previous steps are converted to ASCII files, as the CONEFALL software requires input files in ASCII format. The required input in CONEFALL are files with the defined fixed points (Figure 5.2), the DEM and the chosen curvature, Δz.

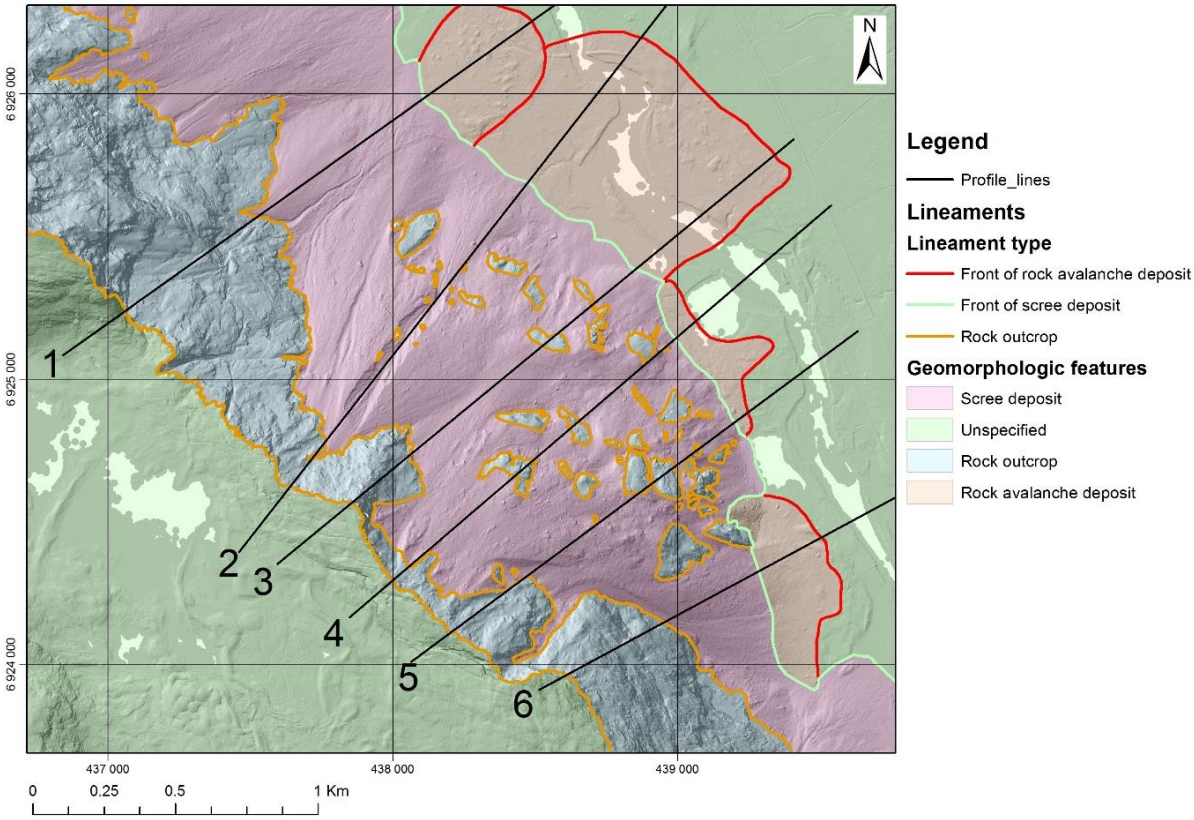

Figure 5.1: Geomorphological map of the study area and the profile lines used for the analysis.

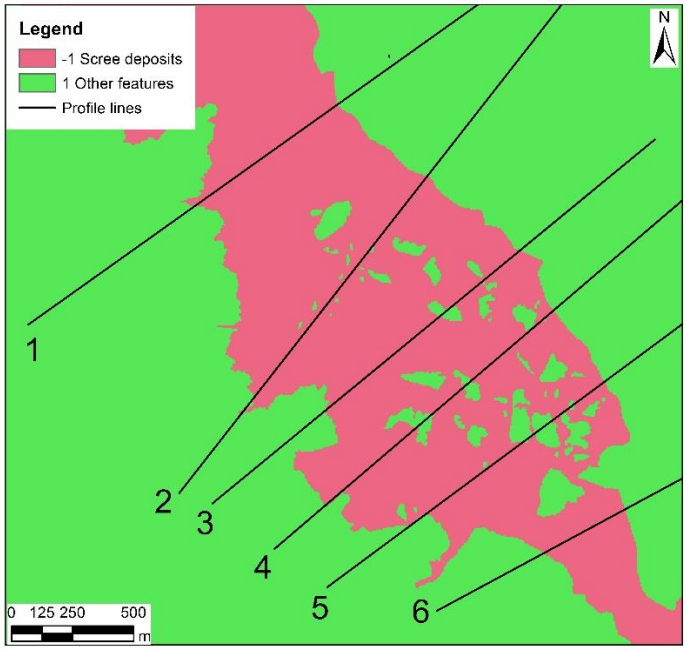

Figure 5.2: Polygons with profile lines used for SLBL analyses.

5.1.2 Assessing curvature, *Δz*

The most suitable tolerance value needs to be estimated for each scree deposit zone along each profile line. The number of scree deposit zones vary from one to three per profile line. Estimating the most suitable tolerance value is done by studying the profiles derived from the analyses in CONEFALL, and choosing the tolerance value, *Δz*, that provides the most reasonable curvature in each case. All profiles may be seen in Appendix I.

The first estimate of curvature, *Δz*, tested was calculated by using Equation 4.5 on profile 1. This gave *Δz* = -0.1 as an initial input for the first computation. Next computation was done with *Δz* = -0.01 in order to assess the range of the tolerance value. Several computations were done to find the best-fit curvature for each scree deposit zone (Figure 5.3,

Table 6.1). A maximum, mean and minimum value of curvature were defined for each zone (Appendix II).

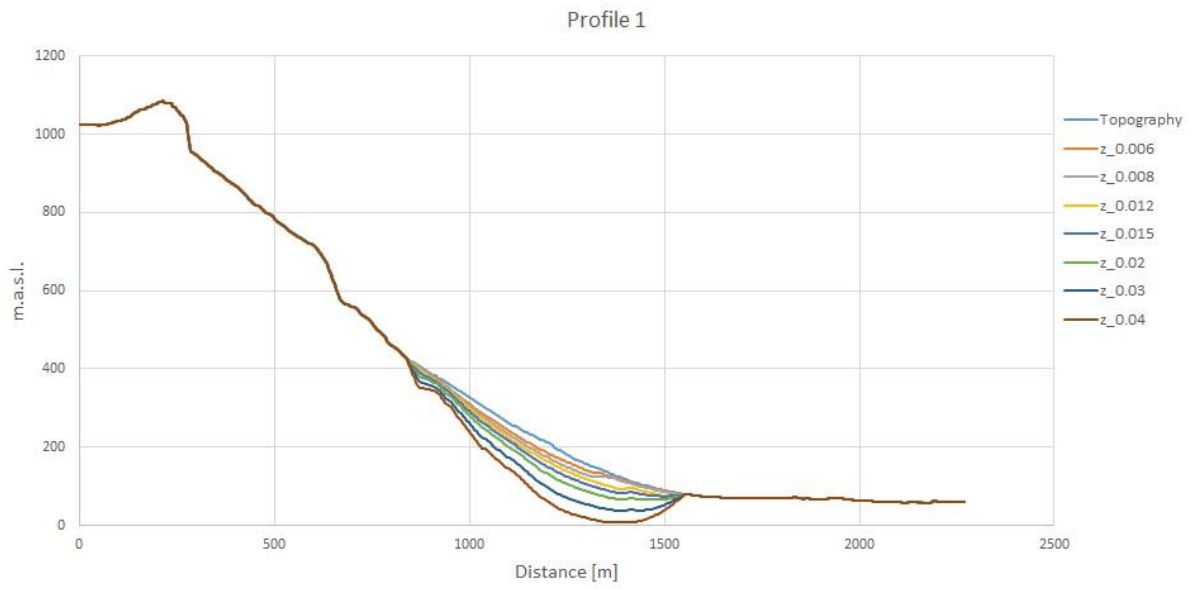

Figure 5.3: Profile lines showing computation of curvature for Profile 1. The upper, blue line represents the topography. The most suitable and realistic curvature was chosen, in this case Δz = 0.012 (yellow line). The same procedure is repeated for all six profile lines, results are given in (Table 6.1). All values tested are included in the figure, meaning that profile lines that are too deep or too shallow are drawn. It is not realistic with a curvature providing profiles deeper than the valley floor.

5.1.3 Volume computation

Polygons of areas with similar curvature are created based on the previous step. The mean value was chosen and used in the next steps of the procedure. The result of the SLBL model is the estimated thickness of deposits for each pixel of the raster grid. The estimations of debris thickness are carried out using the zonal statistics to table tool in ArcGIS. The tool summarizes the values of a raster within the zones of another dataset and reports the result to a table (ArcGIS Resource Center, 2016). The inputs required are raster files with polygons and estimated curvatures, Δz for each polygon.

The output of the ArcGIS analysis in this step is the residuals, i.e. the height difference between the input rasters. Thus, the thickness calculated is the altitude difference between the DEM and the SLBL surfaces. The SLBL surfaces represents the computed lower limits of the scree deposits. The volumes, V, of the polygons are calculated by multiplying the sum of the height difference, Σx, from the zonal output table with the DEM cell size (Equation 5.1) (Oppikofer, 2016a).

$$V = \Sigma x \times 5m \times 5m \qquad 5.1$$

5.2 Analysis of run-out distance

Analyses of run-out distance of a potential landslide from Børa are carried out by numerical run-out modelling. The numerical run-out model used is DAN3D (see chapter 4.5). This section gives an overview of the methodology of the run-out analyses and the chosen values of the input parameters.

5.2.1 Model set-up

DAN3D requires topographic input files in the form of ASCII elevation grid files (grd.). The files are prepared by using the program Surfer 8 (Golden Software, Inc.). One of the files represents the path topography, and thus the sliding surface. A second file represents the source topography, which defines the vertical depth topography of the sliding mass before the collapse, or at the initial time *t=0*. This is the distance between the original ground surface and the rupture surface, measured in a vertical direction. The grid of the files must be of the same size. When erosion and entrainment are to be included in the model, a third file in the same format is required. The erosion map file defines the distribution of different materials throughout the path topography by associating each grid node to a material number (Hungr, 2010). The different materials will be given different properties, which makes it possible to define the areas of material available for entrainment on the travel path, and thus the areas that will be eroded.

The material input parameters required depend on the chosen rheology. Voellmy is the preferred material rheology of this study, on the background of the paper by Schleier et al. (2015) and experience from studies carried out by the team for Geohazards and Earth Observation at the Geological Survey of Norway (NGU). Thus, the model requires the friction coefficient, μ, and the turbulence coefficient, ξ, in addition to the standard material parameters unit weight of the material and the internal friction angle. There are a number of program parameters, related to the model or the algorithm used. They are set to defaulted values if nothing else is specified. The parameters relevant for this study are presented in the sensitivity analysis section (Section 5.2.2). The maximum simulation time is the stopping criteria in DAN3D and is specified by the user. The simulation is stopped by the user when the particles in the deposit area does not move anymore. Illustrating the simulation by a particle velocity plot, one can observe when the particles in the deposit area have come to rest (Figure 5.4).

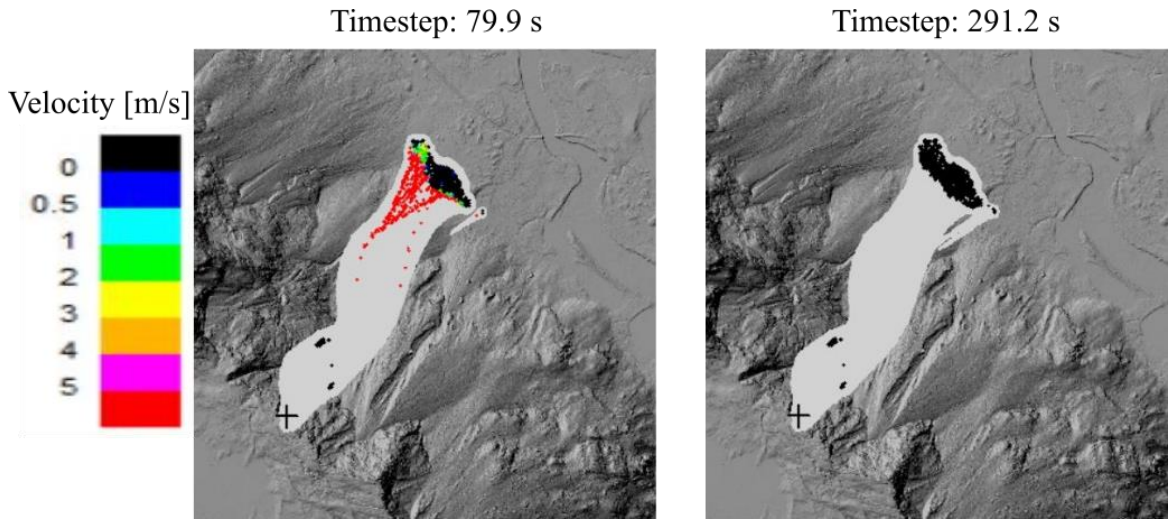

Figure 5.4: Illustration of a simulation. The simulations are stopped when the particles in the area of deposits have come to rest (are black).

5.2.2 Sensitivity analysis

In order to investigate the influence of the input parameters on the modelled run-out distance, a sensitivity analysis is carried out. The aim of the study is to obtain simulation results of sufficient representation by quantifying the variation on the model run-out distance due to variations in the input parameters. The input parameters are briefly explained in the theory chapter (Section 4.5.2).

Parameter test.

Performing a sensitivity analysis based on the input parameters in DAN3D is helpful to establish the influence they have in the final modelled results. Analyses are performed on both material parameters and program parameters. The main rheology used for this purpose is the Voellmy rheology, but the frictional rheology is tested in order to investigate its deviation from the Voellmy rheology. The choice of rheology is discussed further on in this section. The modelled run-out distances sensitivity to the input parameters are given most attention, but the parameters influence on the modelled maximum velocity is also analyzed. Both are analyzed, but the parameters' sensitivity to the modelled run-out distance are paid more attention than the parameters' influence on the modelled maximum velocity. In addition, Fahrböschung is calculated based on measurements in ArcMap and compared to the travel angle, which is one of the output-values from DAN3D (Section 4.2.1, Figure 4.5).

The sensitivity analysis is carried out for scenario C, one of the scenarios that is located above the large scree deposit at Børa. The scenario is approximately 76 000 m^3, and is located at the northwestern end of the slope (Figure 3.4). As one can see from Section 3.3, the estimated volume of this scenario (135 000 m^3) is much larger than used for this purpose. This is due to more precise volume computations that were done in connection with preparing the input-files for this analysis (Oppikofer, 2016b).

The sensitivity analysis of the input parameters is done without entrainment and erosion. This is done with the intention of testing the different parameters' influence on the run-out distance. The initial input parameters used (Table 5.1) are the parameters suggested by Schleier et al. (2015) in the study of rock avalanches in Innerdalen, Western Norway. The material parameters of the source rock in this area are assumed similar at Børa. This is considered the reference simulation, and all results are compared to this simulation in order to assess sensitivity and deviation of the results.

Table 5.1: Initial input parameters for numerical run-out modelling in DAN3D. Used in the parameter test.(Schleier et al., 2015)

Parameter	Value
Rheology	Voellmy
Unit weight [kNm^{-3}]	28
Friction coefficient, μ	0.15
Turbulence coefficient, ξ [ms^{-2}]	500
Internal friction angle [deg]	35

One parameter is changed, while the others are kept constant and equal to the the initial input values (Table 5.1). Sosio et al. (2008) proposes that both frictional and Voellmy rheology are suitable for run-out modelling of rock avalanches. In this study the Voellmy rheology is preferred on the background of the paper by Schleier et al. (2015) and experience from studies carried out by Geohazard and Earth Observation team at the Geological Survey of Norway (NGU). Their experience is that when running the model with a frictional rheology, the run-out distance is too short (Penna, 2016). The aim of this sensitivity analysis is to test the input parameters influence on the run-out distance, and running the model with too short run-out

distances is not favorable for obtaining optimal results. However, the frictional rheology is tested in order to compare the run-out distance it provides with the run-out distance given by the Voellmy rheology.

The range of parameters tested are given in the following tables. The Voellmy coefficients tested (Table 5.2) are as defined in Sosio et al. (2008).

Table 5.2: Values of Voellmy coefficients tested in the sensitivity analysis.(Sosio et al., 2008)

Parameter	Values
Friction coefficient, μ	0.1, 0.15, 0.17, 0.20, 0.25
Turbulence coefficient, ξ [ms^{-2}]	450, 500, 600, 800, 1000

The influence of other material parameters not related to the rheology are tested as well. The values of the internal friction angle and the unit weight tested are given in the table below (Table 5.3). The range of the unit weight of gneiss is determined according to a publication by SINTEF (2015) and results from numerous test at the rock mechanics laboratory at the Norwegian University of Science and Technology (NTNU) and SINTEF (Myrvang, 2001). The range of the internal friction angle are chosen based on the initial value from Schleier et al. (2015). Program parameters and other control parameters related to the algorithm are tested as well, in order to investigate their influence on the results. No suggestions are given regarding the range of number of particles, the smoothing length constant or the velocity smoothing coefficient, but a range is chosen based on the defaulted values (Hungr, 2010).

Table 5.3: Values of the input parameters tested in the sensitivity analysis. The rheology is Voellmy.

Parameter	Values
Material properties	
Internal friction angle [deg]	30, 35, 38, 40, 45, 50
Unit weight [kNm^{-3}]	26, 28, 30
Program parameters	
Number of particles	1000, 2000, 4000
Smoothing length constant	1, 3, 4, 5, 7
Velocity smoothing coefficient	0, 0.01, 0.05, 0.1

The stiffness coefficient and the slide margin cutoff thickness are not tested in this sensitivity analysis. The slide margin coefficient is related to the graphic presentation of the modelling, and is not considered relevant for the run-out distance (Hungr, 2010). The stiffness coefficient is defaulted to 200. This value is reported to produce good results and the model results are found not to be sensitive to changes with this coefficient (Hungr, 1995, McDougall and Hungr, 2004).

As mentioned, the effect of running the model with a frictional rheology is tested. The frictional rheology may be more suitable for back-analyses, as it may be difficult to assess reasonable values of the input friction angle. However, the frictional rheology will be tested in order to compare the two rheologies. A study of which input parameters that gives run-out distances in the same order as the Voellmy rheology is also desirable.

Table 5.4: Input parameters and range of friction angles tested with the frictional rheology.

Parameter	Value/Range
Rheology	Frictional
Unit weight [kNm^{-3}]	28
Friction angle, α [deg]	15, 17, 20, 25, 30, 35
Pore pressure coefficient, r_u	0
Internal friction angle [deg]	35

Effect of larger volumes.

After the sensitivity analysis on the input parameters, the parameter that influences the run-out distance the most is tested on larger volumes. The volumes are defined by identified scenarios at Børa (Figure 3.4). The first large scenario tested is Børa C Large. This is an enlargement of scenario Børa C, which is used for the parameter test. The volume of this scenario is 475 650 m^3. The sensitivity test is then repeated on scenario Børa B, with a volume of 2.4 million m^3.

The parameter test indicated that the run-out distance of the smallest scenario is most sensitive to the Voellmy friction coefficient, μ. In order to check the model's sensitivity to larger volumes, the sensitivity analysis of both Voellmy coefficients, μ and ξ are repeated on the larger volumes. The input parameters are kept constant and equal to the reference values (Table 5.1), while the coefficient tested is altered.

The suitability of the frictional rheology for larger volumes is also tested. The findings from the smaller scenario regarding the friction angle, φ_b are tested on the larger scenario. The model is run with the friction angles that gave approximately the same run-out distance of the small scenario as the reference simulation with Voellmy rheology.

5.2.3 Entrainment of debris material

This section gives an overview of the methodology of the analysis of entrainments influence on modelled run-out distance. First, the model is run under dry conditions, meaning pore-pressure coefficient is set to zero. The different parameters influencing entrainment and erosion are tested to check their sensitivity to the modelled run-out distance. The parameters are entrainment rate, E, maximum erosion depth and the friction angle, φ_b. In addition, the effect of the location of the entrained material is tested. This is done by setting the maximum erosion depth to zero in one of the two scree deposit zones.

In a last step, the effect of pore pressure is studied. Using the frictional rheology, the model allows the user to set a pore-pressure coefficient, r_u. By altering this coefficient, the effect of water to the modelled run-out distance is assessed.

Input files and parameters

The smallest scenario, Børa C is used for the study of the effect of entrainment. It is assumed that entrainment will affect the run-out of a small event more than a large, and thus play a more important role in the run-out of a small scenario.

A third input file is required for the model to be run with entrainment. The erosion map file is in the same format as the two other input files, the ASCII grid format (.grd). The file defines the different materials on the slope, and makes it possible to distinguish between materials by giving them different properties. The slope is divided in polygons based on geomorphological mapping carried out as a part of the project by the author (Andresen, 2015). First, a file that divided the slope in eight different materials was used. However, due to long simulation time, the eight classes were merged to four classes (Figure 5.5). The categories are source area, rock outcrops and rock avalanche deposits, deposits on the upper part of the slope and deposits on the lower part of the slope (Table 5.5). The deposits on the slope, meaning the scree material available for entrainment, are divided in different categories based on the thickness estimated from the SLBL analysis. A simplification is made in order to reduce the simulation time. Thus, the scree slope is separated in an upper and lower part, as the upper part contains thicker deposits than the lower part. The average thickness of the material in the upper and lower part are 40 m and 20 m, respectively.

Table 5.5: Input values used in analysis of entrainments influence on modelled run-out distance.

	Rock outcrops/ rock-avalanche deposits	Source area	Scree deposits – Upper part	Scree deposits – Lower part
Rheology	Frictional	Voellmy	Frictional	Frictional
Unit weight, [kNm^{-3}]	28	28	22	22
Friction angle, [deg.]	35	-	20	20
Friction coefficient	-	0.15	-	-
Turbulence coefficient, [$ms^{-2]}$]	-	500	-	-
Internal friction angle, [deg.]	35	35	35	35
Maximum erosion depth, [m]	-	-	40	20

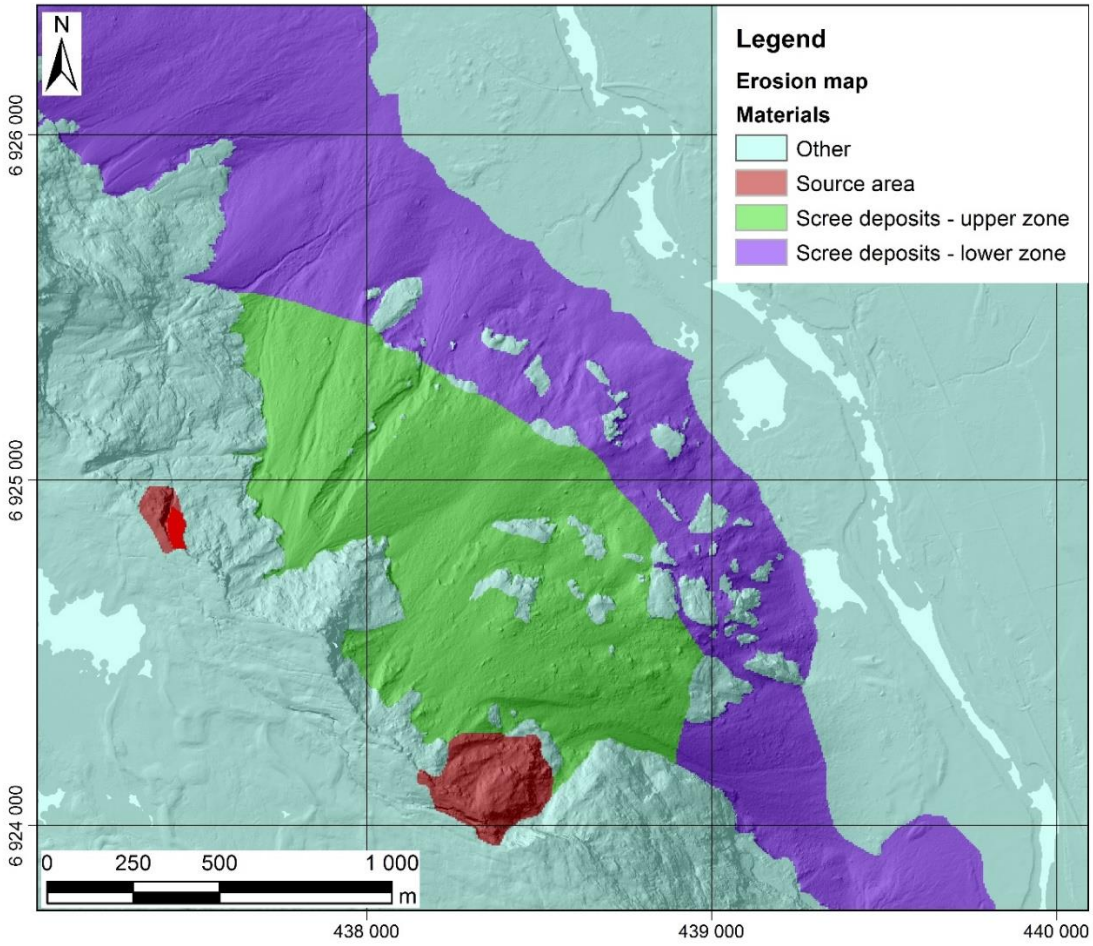

Figure 5.5: Erosion map. Input file required when running the model DAN3D with entrainment. Divides the slope in different materials which may be given different properties. The category "other materials" include rock outcrops and rock-avalanche deposits.

Entrainment rate, E.

Analysis of entrainment rate, E, is split in two. First, situations with little entrainment are studied. The bulk slide porosity, n of the landslide is used to calculate the final slide volume, V_f. The final slide volume is required as an input when the program calculates the entrainment rate, E (Section 4.5.5, Equation 4.17). The range of values of bulk slide porosity ($31\% < n < 43\%$) used in the model developed by Heller et al. (2009) for study of landslide-generated impulse waves, are applied in this analysis. Length of zone, S containing material available for entrainment is measured in ArcMap. In addition, values found in literature are tested (McDougall and Hungr, 2005). Using the bulk slide porosity means that little or no material is entrained, as it only accounts for volume increase due to porosity. However, it may be used to check the models sensitivity to the parameter erosion rate, and the effect of little entrainment.

Table 5.6: Erosion rates tested based on bulk slide porosities from Heller et al. (2009) and values of entrainment rate found in literature (McDougall and Hungr, 2005). ΔV is the desired volume increase in % and equals the bulk slide porosities. The exact estimated volume of the source area, V_0 is used for the calculations.

V_0, [m^3]	75567.5	75567.5	75567.5	75567.5	75567.5	75567.5	75567.5
ΔV , %	20	25	32	35	37	40	43
V_f, [m^3]	90681	94459	99749	102016	103528	105795	108062
S, [m]	1144	1144	1144	1144	1144	1144	1144
E, [m^{-1}]	0.00016	0.00019	0.00024	0.00026	0.00027	0.00029	0.00031

Studying the Norwegian events presented in the theory chapter (Section 4.3.1), one can see that the calculated final volumes based on the bulk slide porosity (Table 5.6) are too low. The Loen-events are reported to increase their volumes with factors of three and six. From SLBL analysis and fieldwork, it is known that a considerable amount of scree deposits is available for entrainment at Børa. Thus, higher erosion rates are tested on the scenario at Børa. Bulking factors from 1.5 up to the extreme value 10 are used to calculate final volumes and thereafter erosion rates (Table 5.7).

Table 5.7: Erosion rates tested based on bulking factors from Norwegian case studies. ΔV is the desired volume increase in %. The exact estimated volume of the source area, V_0 is used for the calculations.

V_0, [m^3]	75567.5	75567.5	75567.5	75567.5	75567.5	75567.5	75567.5
Bulking factor	1.5	2	3	4	5	7	10
ΔV, %	50	100	200	300	400	600	900
V_f, [m^3]	113000	151000	227000	302000	378000	529000	756000
S, [m]	1144	1144	1144	1144	1144	1144	1144
E, [m^{-1}]	0.00035	0.00061	0.000960	0.0012	0.0014	0.0017	0.0020

Maximum erosion depth.

The slope is divided, as described, in four polygons by material character. Two of the polygons represent the scree deposits on the slope, one upper and one lower part. This is the material available for entrainment. The polygons are given values for maximum erosion depths separately (Table 5.8). The maximum erosion depths are based on the debris thickness estimated from the SLBL analysis. The SLBL analysis provides a mean, max and min value of the debris thickness. Mean values are used as standard values for the maximum erosion depths. Extreme situations are checked by adding one and two standard deviations to the mean values. It is desirable to test the effect of where on the slope material is entrained. Meaning at high or low elevations, i.e. from the upper or lower scree deposit zone. The erosion depth is set to zero in the zones where no erosion is wanted.

Table 5.8: Debris thickness in the upper and lower scree deposit zone. The debris thicknesses are estimated by the SLBL technique.

	Mean debris thickness, [m]	Std., [m]
Upper zone	40	30
Lower zone	20	18

Pore-pressure ratio, r_u

The effect of the presence of water in the slope material at Børa is assessed by including the pore-pressure ratio to the modelling. Thus, the effect of water to the run-out may be studied. By altering the pore-pressure ratio, it is possible to study at what ratio the run-out is affected. The scree deposits are divided in an upper and lower zone, which makes it possible to simulate presence of water in one part of the slope. Thus, the difference between water in the upper and lower part of the slope may be assessed. A selection of values of the pore-pressure ratio between 0 – 0.9 are tested.

6 Results

6.1 Estimation of debris thickness and volume

6.1.1 Curvature

Tolerance values, *Δz*, are chosen for each scree deposit zone along the six profile lines (Figure 5.1) in order to find the best fitting curvature for each zone (Table 6.1). The curvature values are chosen based on profiles derived from the SLBL procedure implemented in the CONEFALL software and further analyzed in ArcGIS. The chosen values form the base of the volume computations that will lead to estimates of the thickness and volume of the scree deposits at Børa.

Table 6.1: Overview of the tested and the chosen tolerance values, Δz, for each scree deposit zone along the profile lines. Assessment of values are symbolized: "- -" much too deep, "-" too deep, "~" plausible, "=" chosen, "+" too shallow, "++" much too shallow.

Profile line	Scree deposit zone	Length of zone [m]	Tested curvature tolerance values, -Δz						
			0.04	0.03	0.02	0.015	0.012	0.008	0.006
1	1	710	--	--	-	~	=	+	+
2	1	774	--	-	=	~	+	++	++
	2	370	=	~	+	+	++	++	++
3	1	605	--	-	=	~	+	++	++
	2	134	-	~	=	~	+	++	++
	3	184	~	=	~	+	+	++	
4	1	387	--	--	--	-	-	~	=
	2	162	-	~	=	~	+	+	++
	3	430	~	=	~	+	+	++	++
5	1	481	--	--	--	-	-	~	=
	2	149	=	~	+	+	++	++	++
6	1	391	--	-	~	=	~	+	++

In order to assess the thickness of the debris deposited on the entire slope, the slope is divided into polygons with similar curvature. The polygons are based on the curvature values chosen for each scree deposit zone along the profile lines (Table 6.1). The result is seven polygons with different values of curvature (Figure 6.1).

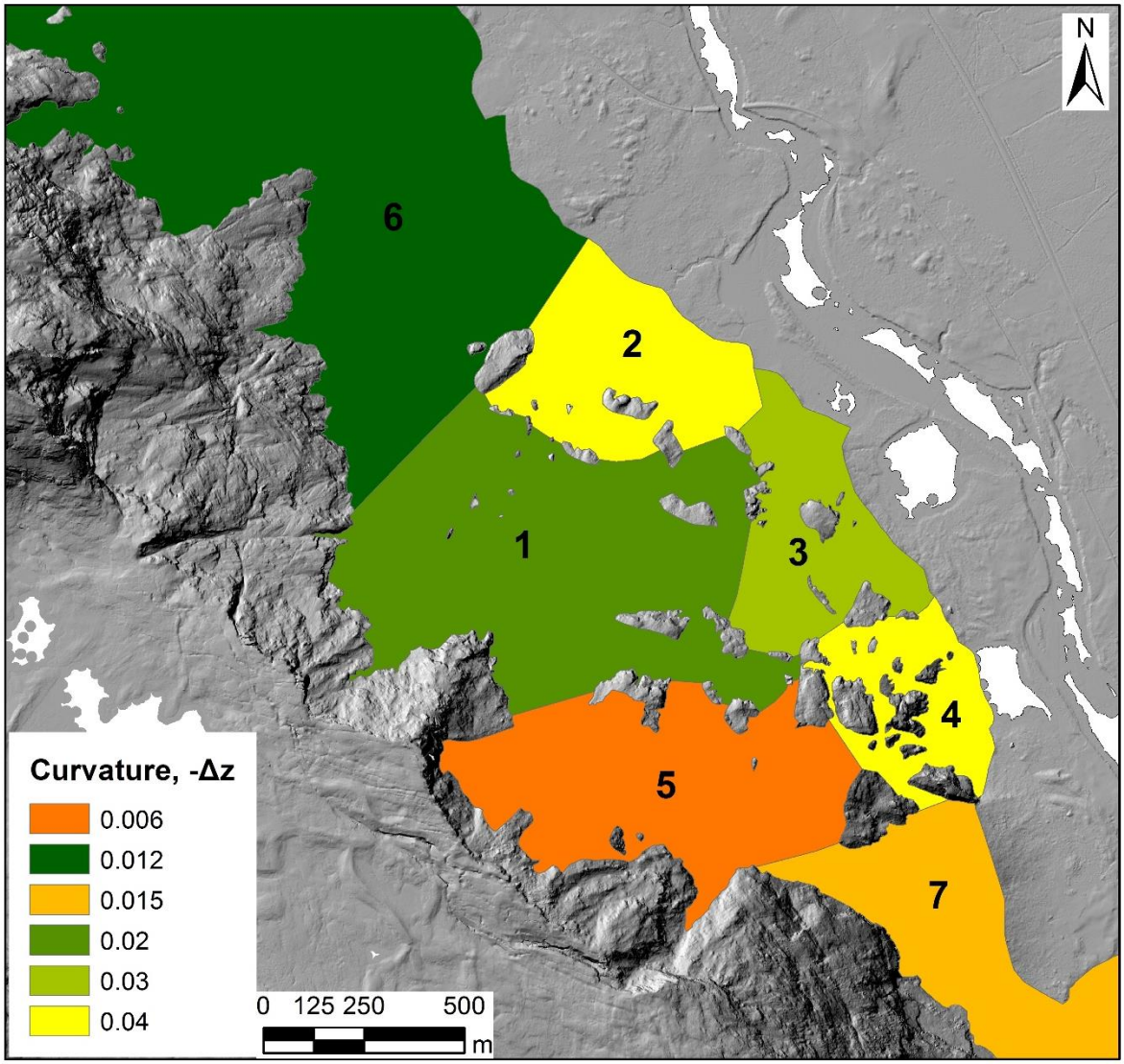

Figure 6.1: Polygons with different curvature, -Δz. Used for calculation of volume of debris.

6.1.2 Volume computation

The volume of the scree deposits is calculated based on the thicknesses, *h*, estimated from the SLBL analysis (Figure 6.2). The estimated total volume of scree deposits at Børa is 56 million m^3 (Table 6.2).

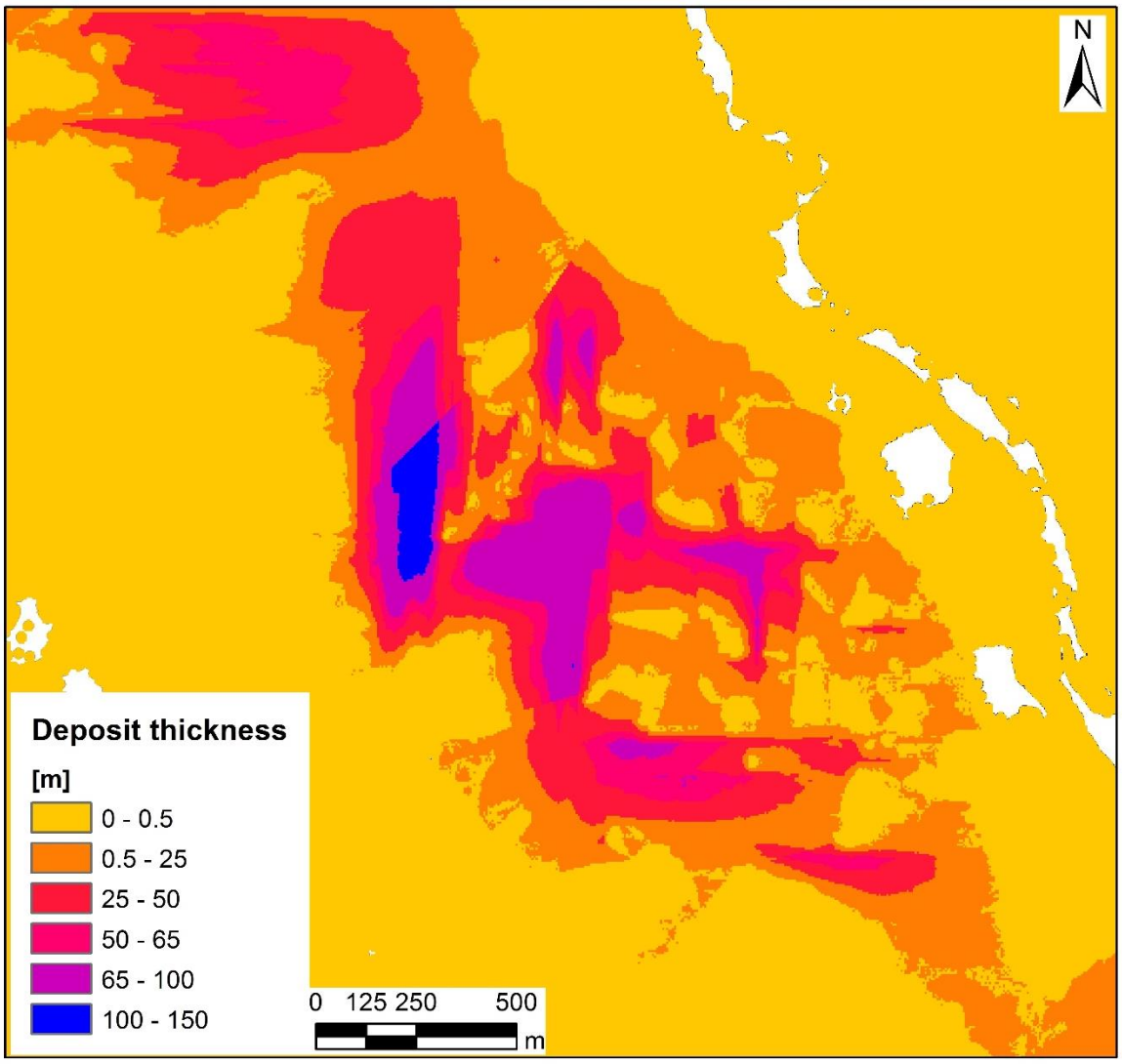

Figure 6.2: Thickness of scree deposits at Børa. Analysis carried out by the SLBL technique.

Table 6.2: Results of debris thickness estimations and volume calculations based on SLBL analysis.

Polygon	Curvature, -Δz	Max. h [m]	Mean h [m]	Volume [Mm^3]
1	0.020	150.74	46.74	26
2	0.040	86.63	22.05	4.56
3	0.030	82.19	17.52	3.10
4	0.040	41.78	5.52	0.67
5	0.006	75.21	23.99	8.62
6	0.012	96.48	27.73	10.57
7	0.015	61.87	14.05	2.11
			SUM	55.62

6.2 Empirical estimation of run-out distance

The relationship between the volume of the unstable area and the ratio *H/L* proposed by Scheidegger (1973) are used to calculate the run-out and Fahrböschung based on the known volumes of the scenarios at Børa (Section 4.2.1, Equation 4.7). According to Corominas (1996) a fixed angle of 31° should be used when applying the relationship to small events, V<250 000 m^3. This applies to scenario Børa C. Run-out distance increase with increasing volume (Table 6.3)

Table 6.3: Empirical estimation of run-out distance and Fahrböschung by the Scheidegger relationship.

	Volume [m^3]	Run-out distance [m]	Fahrböschung [deg.]
Børa C	76 000	1333	-
Børa C Large	476 000	1777	28
Børa B	2 400 000	2173	23

6.3 Analysis of run-out distance: numerical run-out modelling

The objective of this chapter is to present the results from the run-out analyses carried out by numerical modelling in DAN3D. First, results from the sensitivity analysis of the input parameters are given. The sensitivity of the modelled run-out and velocity to chosen rheology, parameters and size of source area are assessed and presented. Sensitivity are given as deviations form reference simulations, the deviations are rounded to integers. Further, the results of the analysis of the effect of erosion and entrainment of path material are presented. Differences in modelled run-out distances are illustrated by the use of figures in combination with tables summarizing the results. The obtained maximum velocity, travel angle and final volume (when entrainment is included) of each simulation are presented in tables. "Fahrböschung" is calculated based on run-out distance and elevation of deposits measured in ArcMap, the results are included in the tables. Complete results and calculations are found in Appendix III.

6.3.1 Sensitivity analysis: Input parameters

The results from sensitivity analysis of the input parameters are presented in this section. The input parameters influence on run-out distance and velocity and their deviation from the reference simulation are given in tables. The reference simulation is the simulation run with input parameters proposed in the paper by Schleier et al. (2015) (Table 5.1). The sensitivity analysis is mainly performed on scenario Børa C with a volume of 76000 m^3. However, the sensitivity to larger volumes and the larger volumes' sensitivity to the input parameters of importance to the run-out are tested and presented in the next section (Section 6.3.2).

The main findings of this sensitivity analyses are presented in the NGU-report by Oppikofer et al. (2016a) describing the methodology for assessing consequences of large rock-slope failures. The results are given here as well.

Friction coefficient, μ.

The modelled run-out is most sensitive to the Voellmy friction coefficient, μ. The modelled run-out distance decreases with increasing friction coefficients (Figure 6.3, Table 6.4).

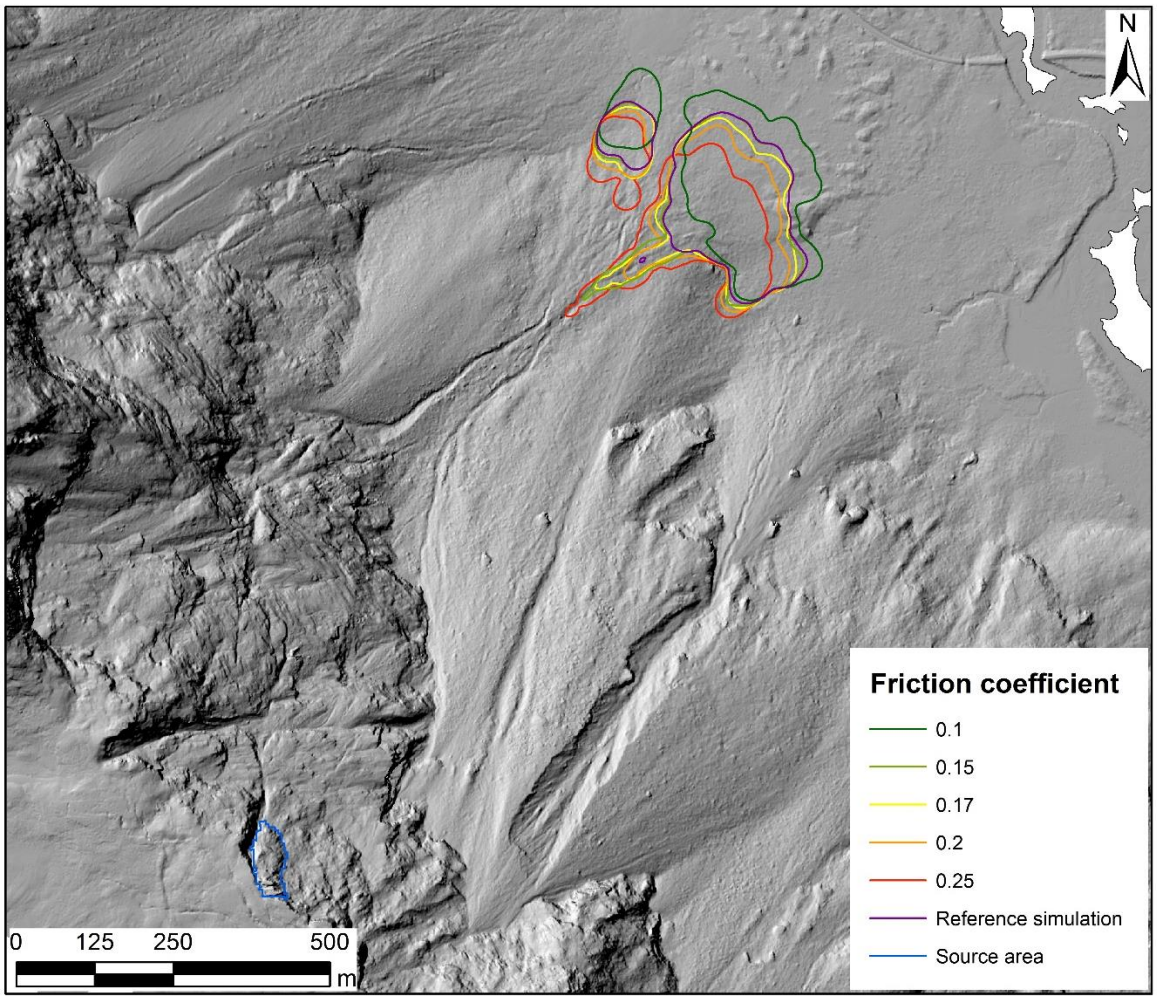

Figure 6.3. Friction coefficient, Voellmy rheology. The run-out is significantly shorter with higher friction coefficients.

The maximum divagation between the calculated Fahrböschung, α and the modelled travel angle, α' is small, with a maximum of 0.8°.

Table 6.4: Friction coefficient, Voellmy rheology. Results from sensitivity analysis of the Voellmy friction coefficient, μ.

Friction coefficient	Fahrbö-schung	Travel angle	Run-out	Max. velocity	Deviation, %	
	[deg.]	[deg.]	[m]	[m/s]	Run-out	Max. velocity
Reference	33.7	33.5	1448	37.3	-	-
0.1	32.9	33.0	1491	38.7	3	4
0.15	33.7	33.5	1448	37.3	-	-
0.17	34.0	33.5	1428	37.1	-1	-1
0.2	34.3	33.8	1409	35.7	-3	-4
0.25	35.0	34.2	1369	32.0	-6	-14

Turbulence coefficient, ξ.

Run-out distance sensitivity to the second Voellmy coefficient, the turbulence coefficient, ξ, is observed to be low (Figure 6.4, Table 6.5). The modelled run-out distance is not affected when the turbulence coefficient is altered.

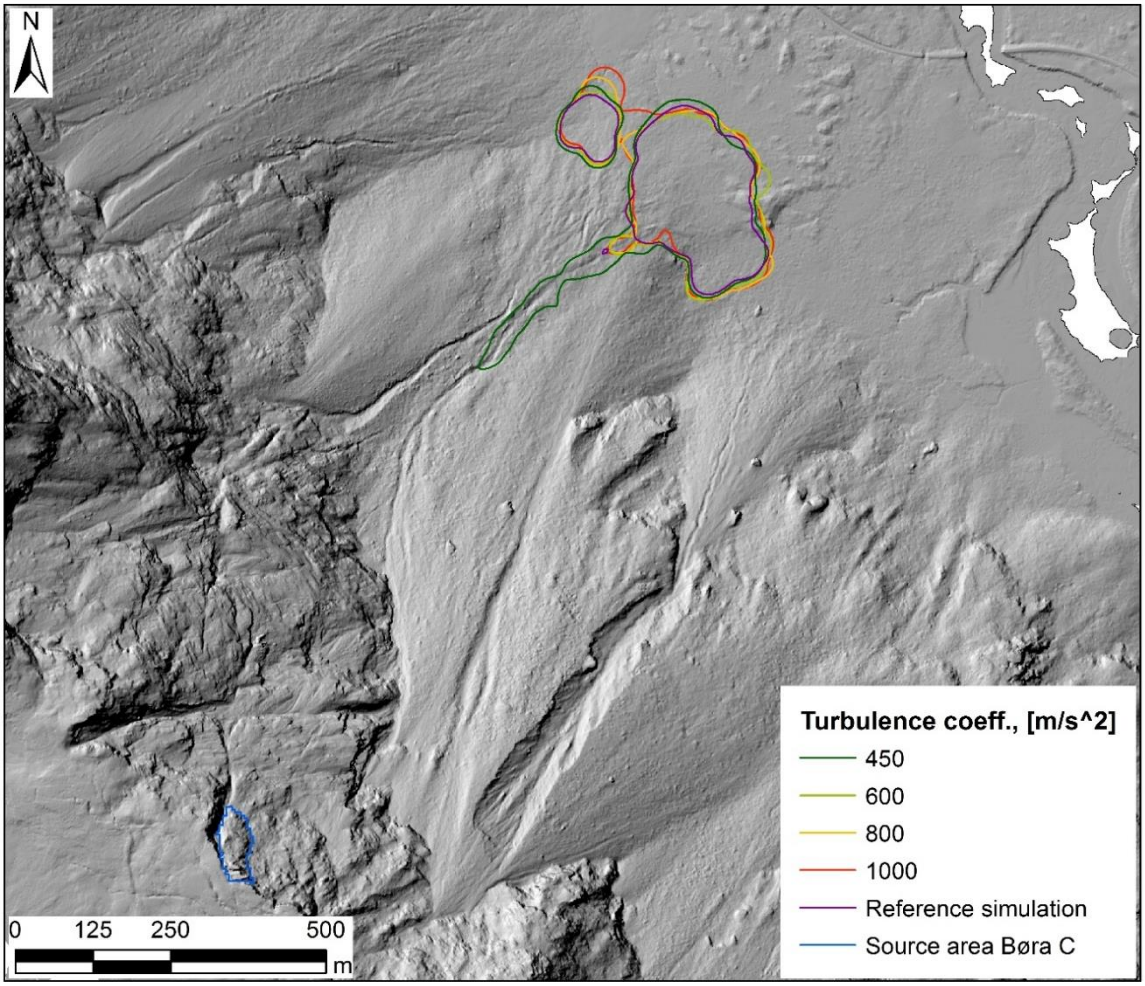

Figure 6.4: Turbulence coefficient, Voellmy rheology. The run-out is not sensitive to changes in the Voellmy turbulence coefficient.

Table 6.5: Turbulence coefficient, Voellmy rheology. Results from sensitivity analysis of the Voellmy turbulence coefficient, ξ.

Turbulence coefficient, [m/s^2]	Fahrbö-schung [deg.]	Travel angle [deg.]	Run-out [m]	Max. velocity [m/s]	Deviation, %	
					Run-out	Max. velocity
Reference	33.7	33.5	1448	37.3	-	-
450	33.9	33.4	1434	35.3	-1	-5
500	33.7	33.5	1448	37.3	-	-
600	33.5	33.5	1456	39.9	1	7
800	33.8	33.6	1442	39.6	0	6
1000	33.6	33.7	1452	43.0	0	15

Frictional rheology, friction angle φ_b

The modelled run-out distance is sensitive to changes in the friction angle. The run-out distance is highly affected when the friction angle is altered, with increasing run-out distances for decreasing friction angles (Figure 6.5, Table 6.6). The size of the deposit increases with decreasing friction angles as well.

To obtain a run-out distance of the same length as the reference simulation run with Voellmy rheology provides, the model requires low friction angles. A friction angle of 20° (red line) gives a run-out distance of approximately the same length as the reference simulation (purple line).

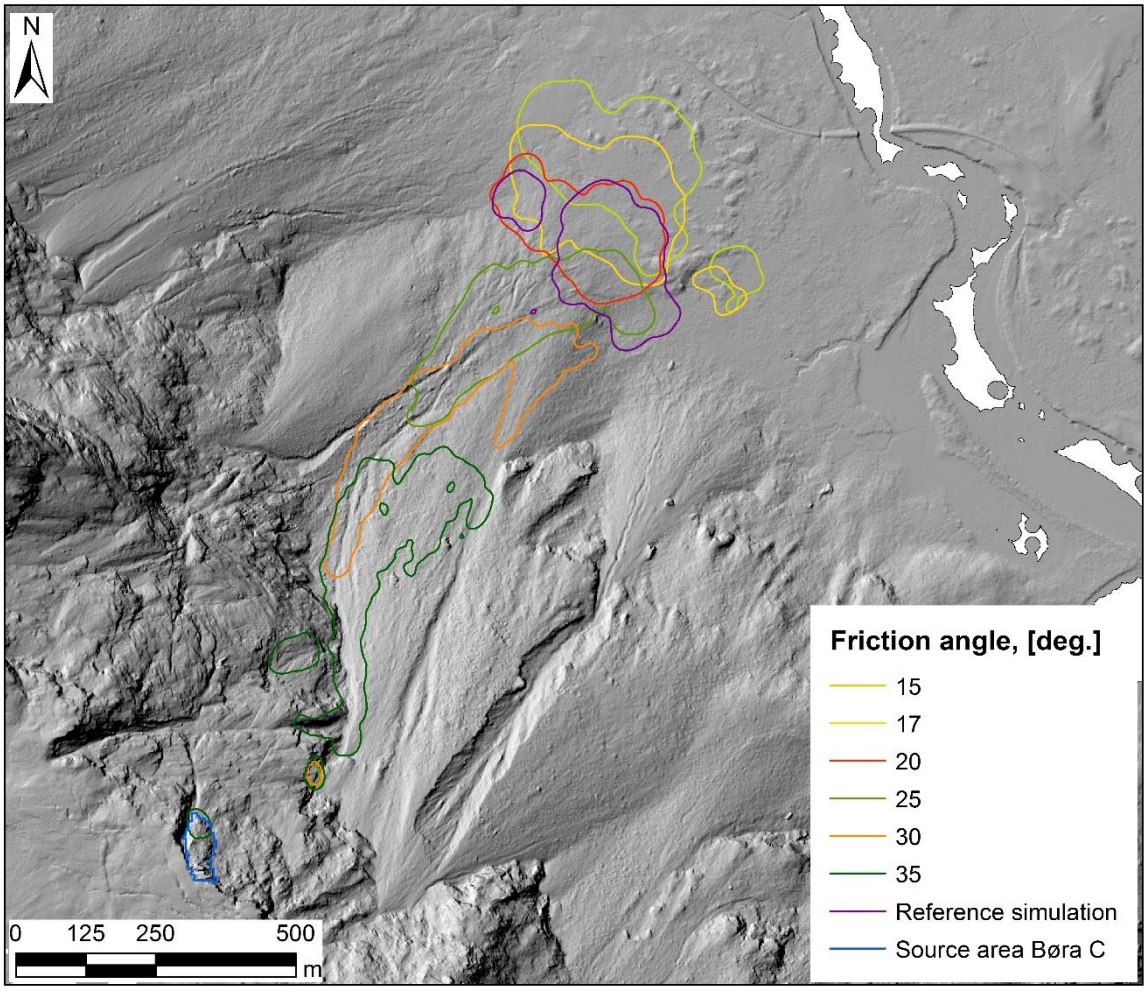

Figure 6.5: Friction angle, frictional rheology. The run-out is sensitive to the friction angle and increases with lower friction angles. A friction angle of 20° (red line) provides a run-out in the same order as the reference simulation (purple line).

The Fahrböschung is slightly lower than the travel angle. The maximum velocity is sensitive to the friction angle and decreases with increasing values. The deviation of the run-out and maximum velocity from the reference simulation is high, with a maximum of 46 % (Table 6.6).

Table 6.6: Friction angle, frictional rheology. Results from analysis of the sensitivity of the run-out of Børa C to the friction angle.

Friction angle, [deg.]	Fahrbö-schung [deg.]	Travel angle [deg.]	Run-out [m]	Max. velocity [m/s]	Deviation, %	
					Run-out	Max. velocity
Reference	33.7	33.5	1448	37.3	-	-
15	30.8	32.0	1624	54.5	12	46
17	31.9	33.1	1552	53.3	7	43
20	33.3	34.2	1467	50.1	1	34
25	35.4	37.0	1350	44.8	-7	20
30	37.5	39.0	1199	40.9	-17	10
35	40.6	42.5	892	36.2	-38	-3

The model run time is shorter when the frictional rheology is assumed compared to the Voellmy rheology.

Internal friction angle

Changes in the internal friction angle of the landslide material does only lead to small differences in the modelled run-out. The deviation in the run-out distance is below 1 % for all values, but the area of run-out are slightly increased with decreasing values (Figure 6.6, Table 6.7).

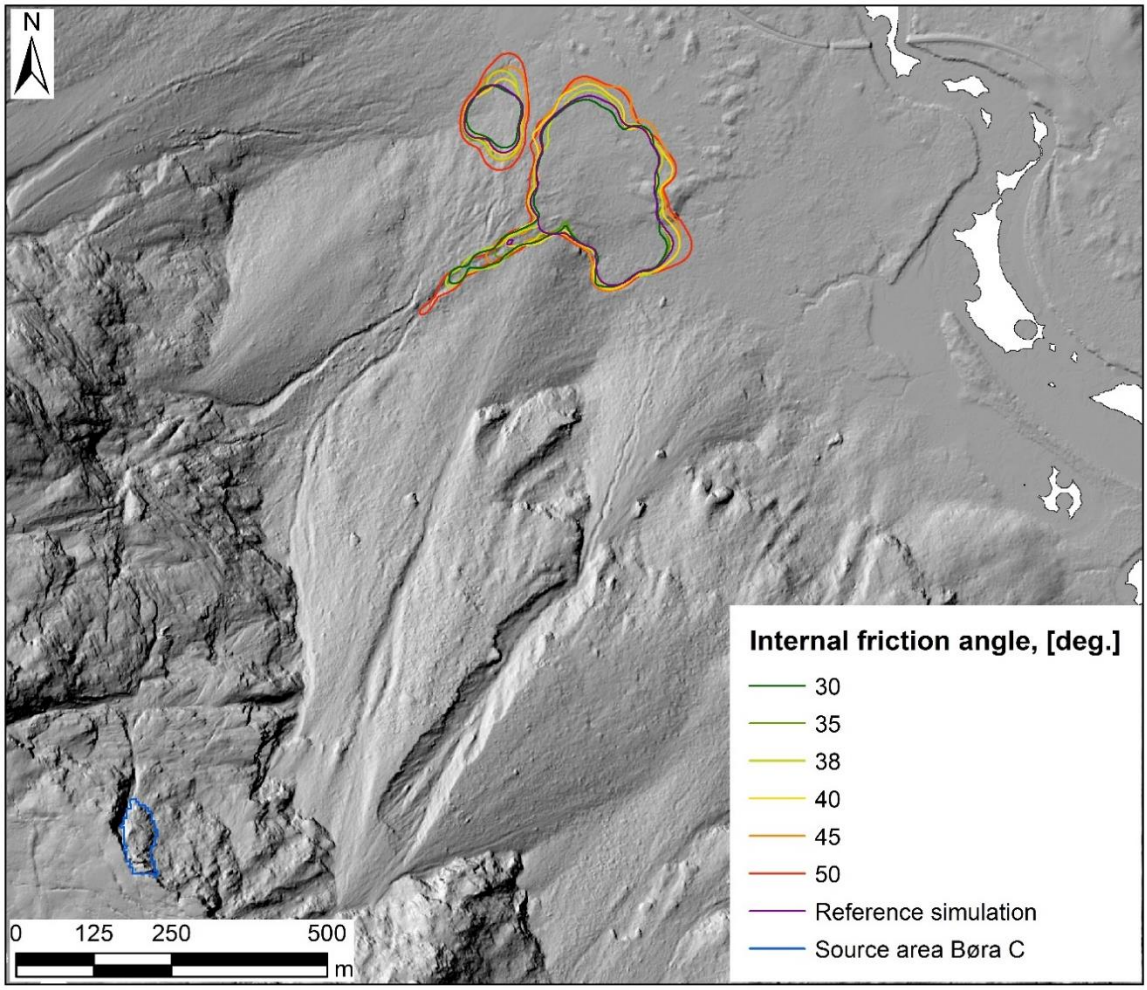

Figure 6.6: Internal friction angle. The run-out distance and area slightly increases with lower values of the internal friction angle of the rock-avalanche material.

The modelled maximum velocity is sensitive to the internal friction angle. Deviations up to 35 % is obtained when altering the values. The difference between Fahrböschung and travel angle is small.

Table 6.7: Internal friction angle. Results from analysis of the run-out of Børa C to the internal friction angle of the material.

Internal friction angle,	Fahrbö-schung	Travel angle	Run-out	Max. velocity	Deviation, %	
[deg.]	[deg.]	[deg.]	[m]	[m/s]	Run-out	Max. velocity
Reference	33.7	33.5	1448	37.3	-	-
30	33.7	33.4	1449	35.6	0	-5
35	33.7	33.5	1448	37.3	-	-
38	33.7	33.4	1449	39.9	0	7
40	33.7	33.4	1445	43.2	0	16
45	33.5	33.3	1459	50.4	0	35
50	33.7	33.5	1446	46.7	0	25

Other parameters tested

The run-out distance is not sensitive to changes in the other input parameters tested (Figure 6.7). The parameters are the unit weight of the landslide material and the program parameters smoothing length constant, velocity smoothing coefficient and the number of particles, i.e. the number of smoothed particles used for numerical modelling. No significant effect to the run-out is observed when the parameters are changed. However, the effect of changing the smoothing length constant to the model time and results are noticeable. The simulation time is observed to be extremely long when the constant is increased to values above the defaulted value four. For values much lower than four, the modelling does not provide the smooth run-out lines as observed for higher values (red line).

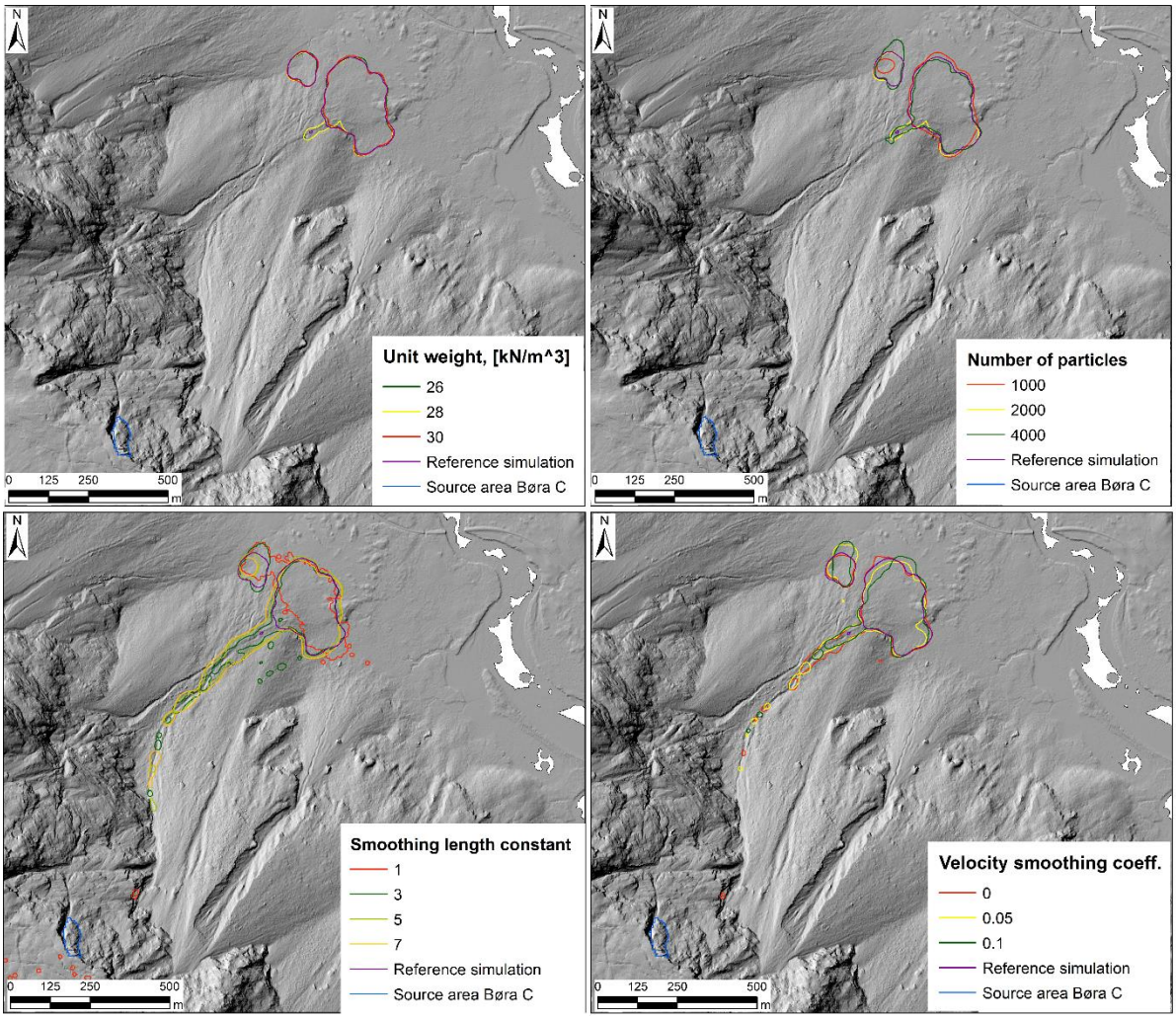

Figure 6.7: Other parameters tested in the sensitivity analysis. The run-out is found to be insensitive to the unit weight of the landslide masses, the number of particles used in the modelling and the program parameters smoothing length constant and velocity smoothing coefficient.

The modelled maximum velocity is found to be more sensitive to the parameters tested than the run-out (Table 6.8). However, the deviation is still low and assumed not to affect the results to such a degree that it should be included in further analyses. The differences in Fahrböschung and travel angle are not of importance.

Table 6.8: Results from sensitivity analysis of the unit weight of the material, the number of particles used when modelling and the program parameters smoothing length constant and velocity smoothing coefficient. X = not realistic results.

Parameter	Fahrbö-schung [deg.]	Travel angle [deg.]	Run-out [m]	Max. velocity [m/s]	Deviation, %	
					Run-out	Max. velocity
Reference	33.7	33.5	1448	37.3	-	-
Unit weight, [kN/m^3]						
26	33.7	33.4	1449	37.3	0	0
28	33.7	33.5	1448	37.3	-	-
30	33.7	33.5	1449	37.3	0	0
Number of particles						
1000	33.6	33.1	1452	35.7	0	-4
2000	33.7	33.5	1448	37.3	-	-
4000	33.8	33.5	1440	40.0	-1	7
Smoothing length constant						
1	33.8	33.9	1443	X	-0	X
3	33.7	33,5	1445	39.7	-0	7
4	33.7	33.5	1448	37.3	-	-
5	33.5	33.5	1456	36.6	1	-2
7	33.7	33.7	1448	34.8	0	-7
Velocity smoothing coefficient						
0	33.9	33.5	1436	38.5	-1	3
0.01	33.7	33.5	1448	37.3	-	-
0.05	33.9	33.6	1437	34.4	-1	-8
0.1	33.8	33.4	1441	34.5	-1	-7

6.3.2 Sensitivity analysis: Larger scenarios

The sensitivity of the modelled run-out distance and flow velocity to larger volumes are tested. Børa C Large is an enlargement of the original scenario Børa C with a volume of approximately 480 000 m^3. Børa B is a limited unstable area with a volume of 2.4 Mm^3. From the parameter test carried out on scenario Børa C, the run-out is found to be most sensitive to the Voellmy coefficients, μ and ξ and the friction angle, φ_b. Thus, the sensitivity of the larger volumes to these parameters are assessed. The output maximum velocities of the analyses of the larger scenarios are high, for Børa B extremely high. This is discussed in the discussion chapter (Section 7.2.1, Section 7.2.3).

Børa C Large: 476 000 m^3

Voellmy coefficients, μ and ξ.

The sensitivity of the run-out of scenario Børa C Large to the Voellmy friction coefficient is high. The run-out distance and area are increasing with decreasing friction coefficients (Figure 6.8, Table 6.9).

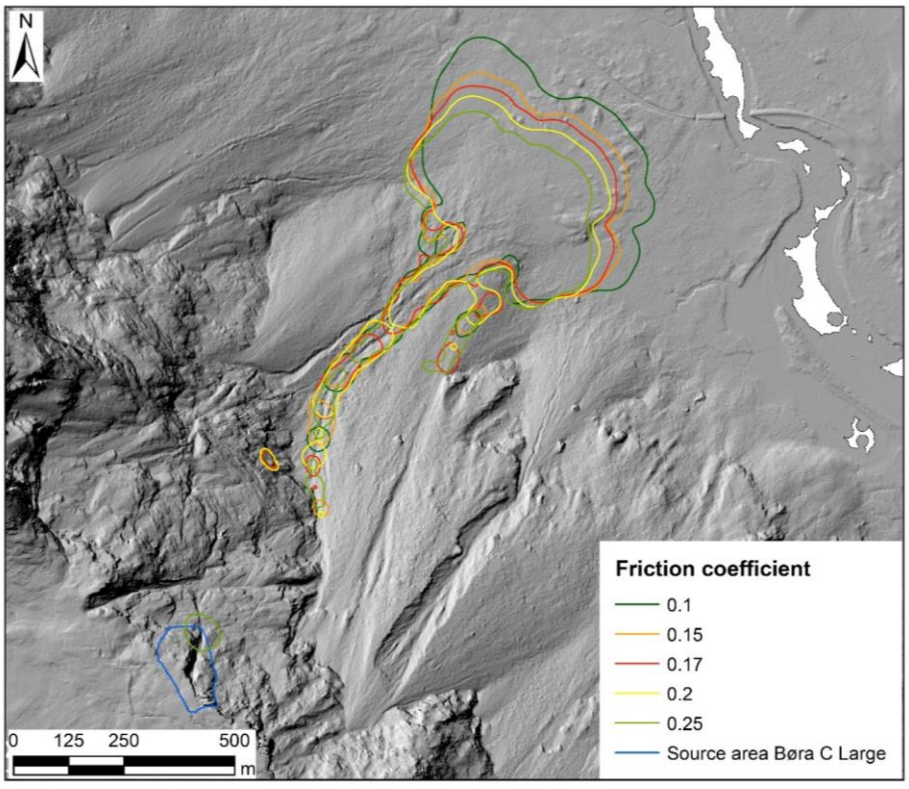

Figure 6.8: Friction coefficient, Voellmy rheology. Run-out distance is highly affected by the Voellmy friction coefficient. Run-out is increasing with decreasing values of the friction coefficients.

The velocity of the landslide is lower for friction coefficients higher and lower than the reference value (μ = 0.15). The travel angle is approximately 2° higher than the calculated Fahrböschung or angle of reach (Table 6.9).

Table 6.9: Friction coefficient, Voellmy rheology. Results from sensitivity analysis carried out on scenario Børa C Large.

Friction coefficient	Fahrbö-schung	Travel angle	Run-out	Max. velocity	Deviation, %	
	[deg.]	[deg.]	[m]	[m/s]	Run-out	Max. velocity
Reference	31.1	33.1	1598	140.6	-	-
0.1	30.3	32.5	1655	96.6	4	-31
0.15	31.1	33.1	1598	140.6	-	-
0.17	31.5	33.3	1576	107.0	-1	-24
0.2	31.9	33.6	1552	80.7	-3	-43
0.25	32.6	34.0	1512	83.0	-5	-41

The run-out distance of larger volumes (Børa C Large and Børa B) are found to be more sensitive to the Voellmy turbulence coefficient, ξ than the small volume (Børa C). The run-out distance increases with increasing values of the turbulence coefficient (Figure 6.9). However, the deviation from the reference simulation (ξ = 500 m/s^2) is relatively low, with a maximum of 6 % (Table 6.10).

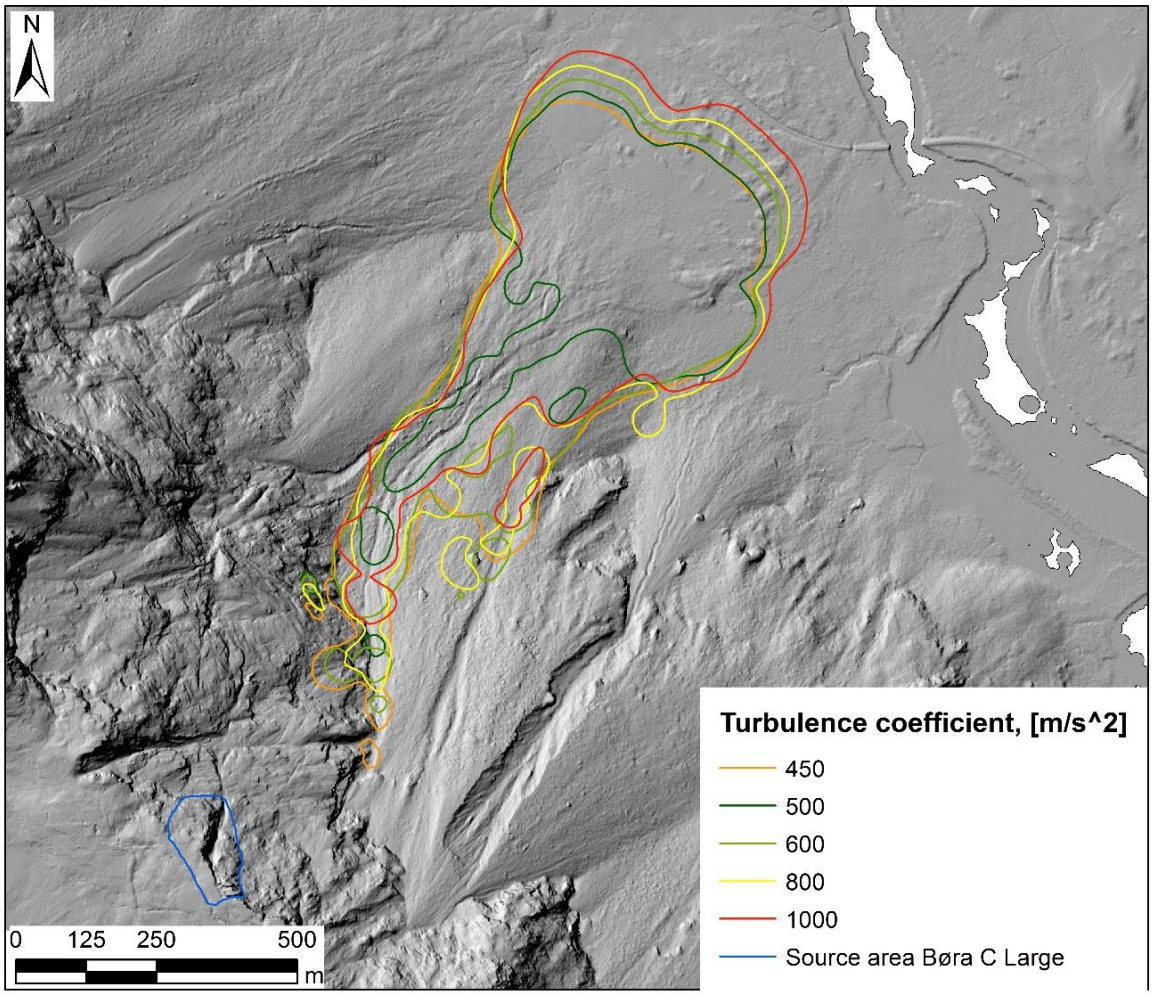

Figure 6.9: Turbulence coefficient, Voellmy rheology. The run-out distance of the scenario Børa C Large increases when the turbulence coefficient is increased.

The maximum velocity is sensitive to changes in the turbulence coefficient. The velocity is lower for values both higher and lower than the reference value (ξ = 500 m/s^2). The difference between the travel angle and Fahrböschung is approximately 2°.

Table 6.10: Turbulence coefficient, Voellmy rheology. Results from sensitivity analysis carried out on scenario Børa C Large.

Turbulence coefficient	Fahrbö-schung	Travel angle	Run-out	Max. velocity	Deviation, %	
[m/s^2]	[deg.]	[deg.]	[m]	[m/s]	Run-out	Max. velocity
Reference	31.1	33.1	1598	140.6	-	-
450	31.1	33.1	1597	88.8	0	-37
500	31.1	33.1	1598	140.6	-	-
600	30.7	32.9	1627	84.2	2	-40
800	30.3	32.8	1654	89.4	4	-36
1000	29.8	32.5	1691	120.9	6	-14

Friction angle, φ_b

The run-out of Børa C Large is sensitive to changes in the friction angle, as observed for the small volume Børa C. The run-out distance is increasing with decreasing friction angles (Figure 6.10). To obtain the same run-out distance as the reference simulation based on input parameters from Schleier et al. (2015), a friction angle of 17° is sufficient.

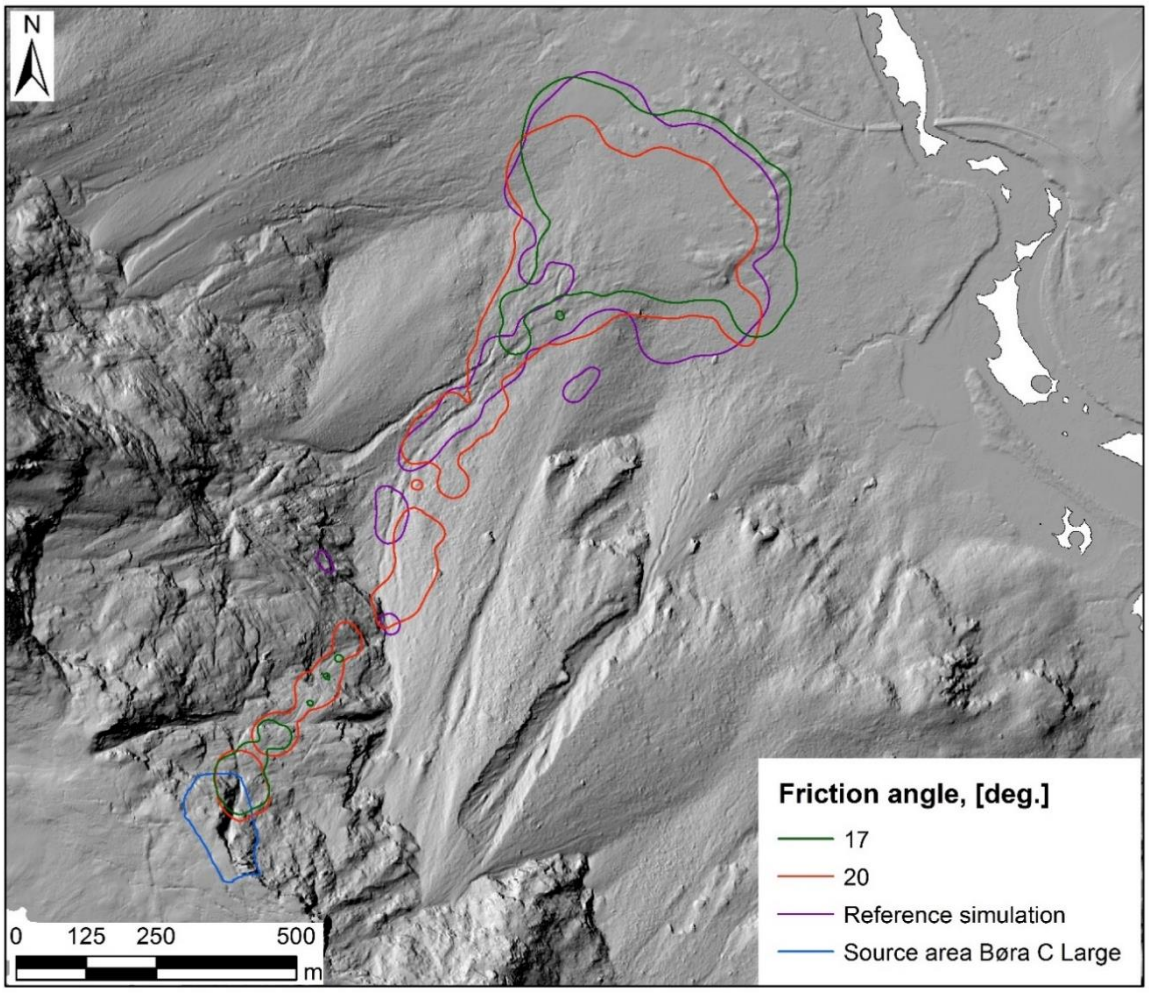

Figure 6.10: Friction angle, frictional rheology. The run-out distance of scenario Børa C Large increases with decreasing friction angle. A friction angle of 17° provides approximately the same run-out (deviation of 1.1%) as the reference simulation run with Voellmy rheology and reference parameters from Schleier et al. (2015).

The modelled maximum velocity is sensitive to the friction angle (Table 6.11). Running the model with assumed frictional rheology provides lower velocities than the Voellmy rheology. The difference between the Fahrböschung and the travel angle varies, in contrast to the constant difference observed for the Voellmy coefficients.

Table 6.11: Friction angle, frictional rheology. Results from sensitivity analysis carried out on scenario Børa C Large.

Friction angle	Fahrbö-schung	Travel angle	Run-out	Max. velocity	Deviation, %	
[deg.]	[deg.]	[deg.]	[m]	[m/s]	Run-out	Max. velocity
Reference	31.1	33.1	1598	140.6	-	-
17	30.9	32.8	1615	76.3	1	-46
20	32.1	33.6	1541	58.0	-4	-59

Børa B: 2.4 Mm³

The results of the sensitivity analysis performed on scenario Børa B are presented in terms of figures and tables in this section. The modelled maximum velocities are unrealistically high. See Section 7.2.3 for possible explanations.

Voellmy coefficients, μ and ξ.

The run-out of the largest scenario, Børa B is sensitive to the Voellmy coefficients. The sensitivity to the friction coefficient is observed to be highest, with a significant increase in run-out when the friction coefficient is lowered (Figure 6.11).

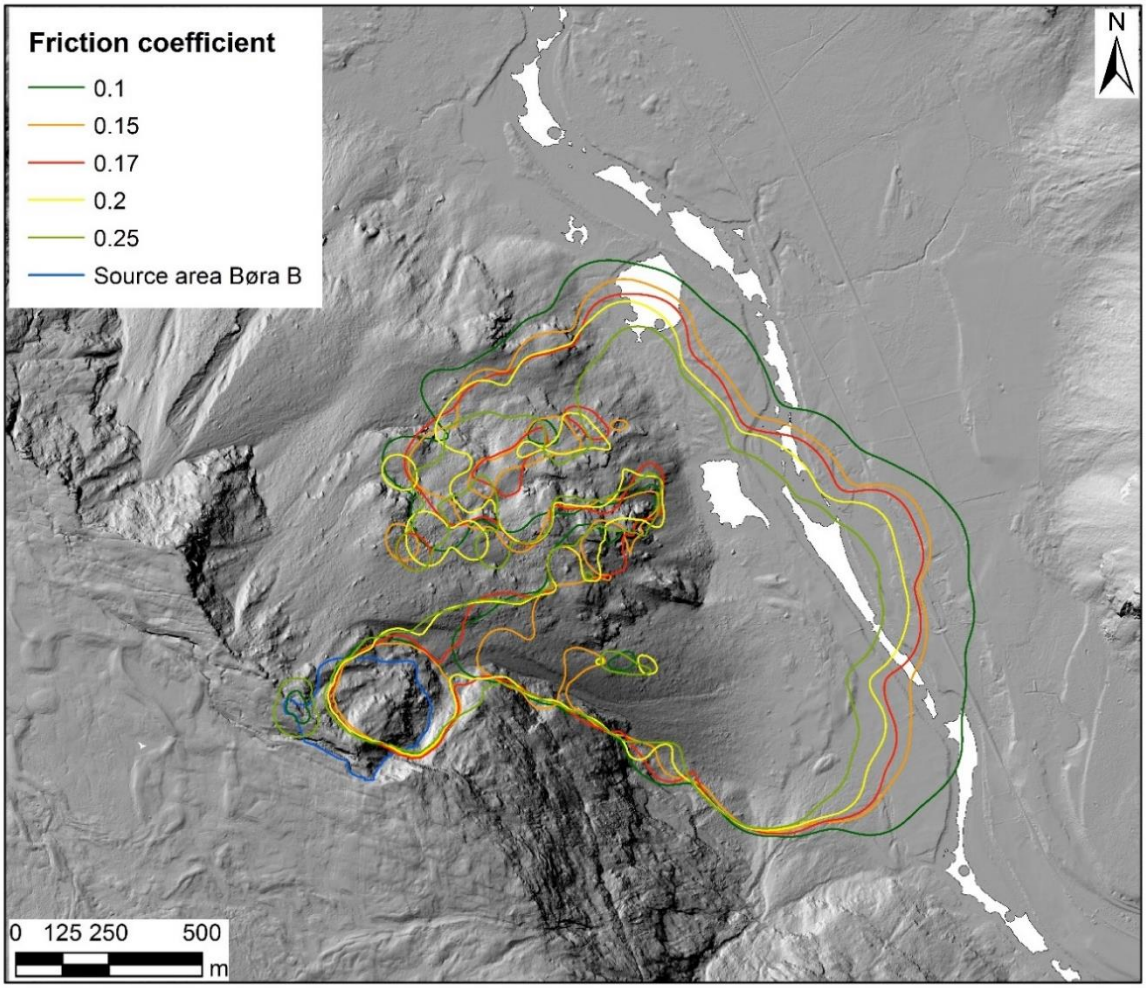

Figure 6.11: Friction coefficient, Voellmy rheology. The run-out distance and area of scenario Børa B are highly affected by the friction coefficient. The run-out increases with decreasing values of the friction coefficient.

Altering the friction coefficient leads to changes of both run-out distance and velocity (Table 6.12). The maximum velocity is significantly affected by changes in the friction coefficient.

The difference between Fahrböschung and travel angle is increased compared to the smaller volumes. The difference is 5-6°.

Table 6.12: Friction coefficient, Voellmy rheology. Results from sensitivity analysis carried out on scenario Børa B.

Friction coefficient	Fahrbö-schung	Travel angle	Run-out	Max. velocity	Deviation, %	
	[deg.]	[deg.]	[m]	[m/s]	Run-out	Max. velocity
Reference	27.4	33.5	1767	791.4	-	-
0.1	26.2	32.3	1861	1259.6	5	59
0.15	27.4	33.5	1767	791.4	-	-
0.17	27.8	33.9	1740	634.0	-2	-20
0.2	28.9	34.3	1675	856.1	-5	8
0.25	29.9	34.9	1610	1187.0	-9	50

Increasing the turbulence coefficient results in a small increase of run-out distance for scenario Børa B (Figure 6.12). However, the sensitivity of the run-out distance to the turbulence coefficient is higher for scenario Børa C Large.

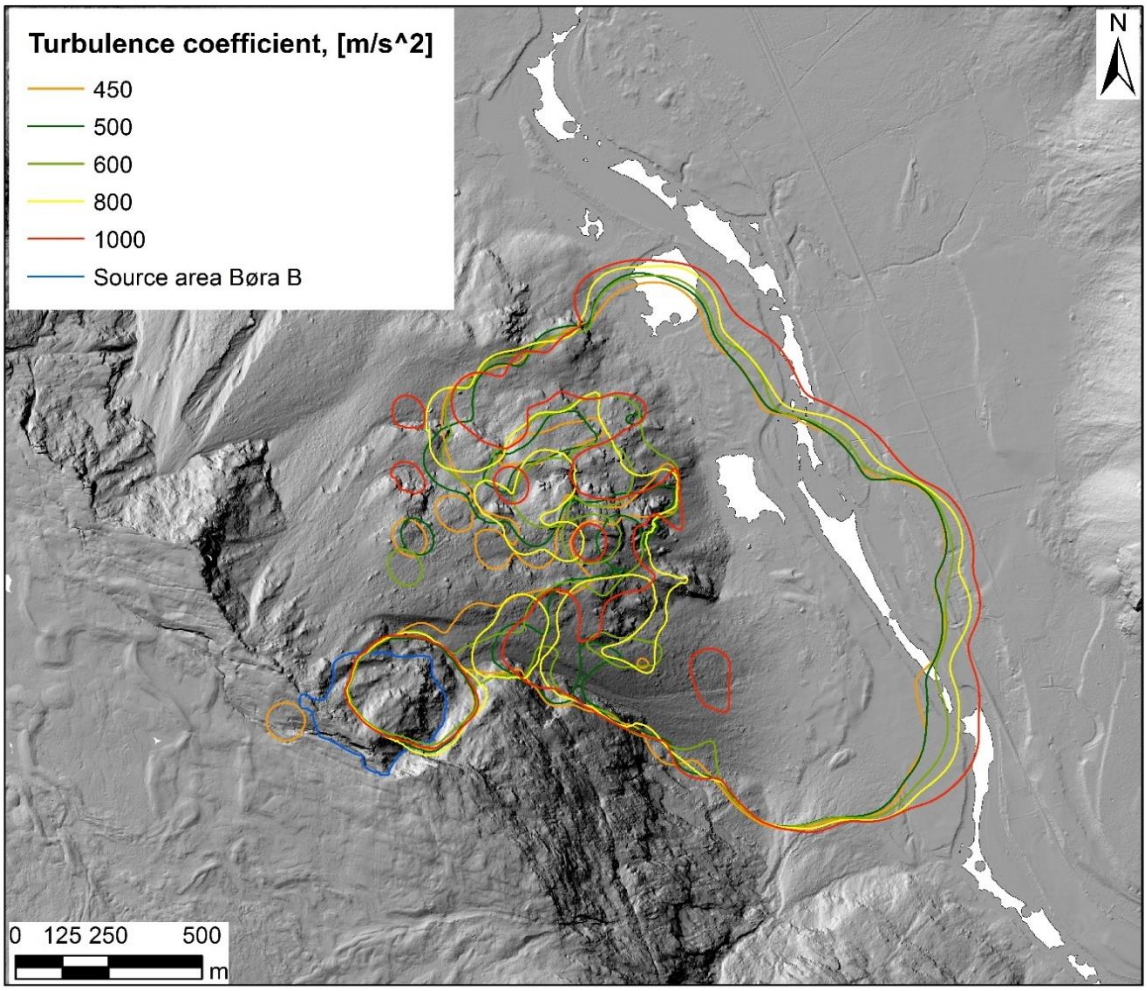

Figure 6.12: Turbulence coefficient, Voellmy rheology. The run-out distance of scenario Børa B increases with increasing values of the turbulence coefficient.

The difference between the Fahrböschung and the travel angle is approximately constant at 5°. The maximum velocity is highly sensitive to changes in the turbulence coefficient, ξ (Table 6.13).

Table 6.13: Turbulence coefficient, Voellmy rheology. Results from sensitivity analysis carried out on scenario Børa B.

Turbulence coefficient	Fahrbö-schung	Travel angle	Run-out	Max. velocity	Deviation, %	
[m/s^2]	[deg.]	[deg.]	[m]	[m/s]	Run-out	Max. velocity
Reference	27.4	33.5	1767	791.4	-	-
450	27.4	33.3	1767	1243.1	0	57
500	27.4	33.5	1767	791.4	-	-
600	27.3	33.3	1776	1057.0	1	34
800	27.0	32.9	1805	2263.2	2	186
1000	26.7	32.5	1821	1790.7	3	126

Friction angle, φ_b.

The run-out distance increases with lower friction angles (Figure 6.13). Friction angles that provide a run-out distance in the same order as the reference simulation did for scenario Børa C, are tested for scenario Børa B. It can be seen that a run-out distance in the same order as the reference simulation, is not obtained with these angles.

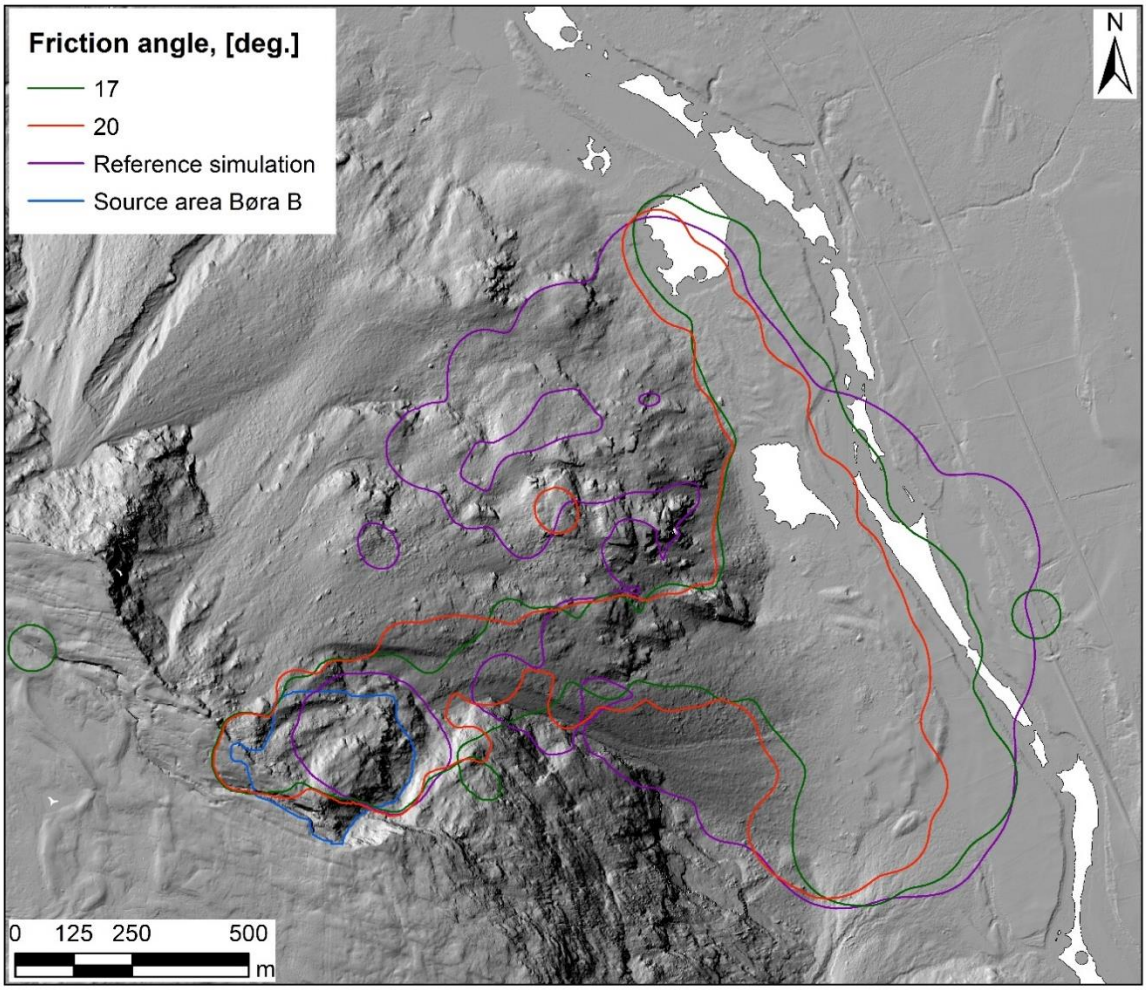

Figure 6.13: Friction angle, frictional rheology. The run-out distance is increasing with decreasing values of the friction angle. A run-out distance that corresponds to what the Voellmy rheology provides is not obtained with the tested values.

The run-out and maximum velocity of Børa B are sensitive to changes in the friction angle. The difference between the Fahrböschung and the travel angle is 3-4°.

Table 6.14: Friction angle, frictional rheology. Results from sensitivity analysis carried out on scenario Børa B.

Friction angle	Fahrbö-schung	Travel angle	Run-out	Max. velocity	Deviation, %	
[deg.]	[deg.]	[deg.]	[m]	[m/s]	Run-out	Max. velocity
Reference	27.4	33.5	1767	791.4	-	-
17	30.2	34.1	1592	833.3	-10	5
20	32.2	35.0	1473	212.2	-17	-73

6.3.3 Summarized results of sensitivity analyses.

Run-out distance.

Altering the friction coefficient, μ, leads to significant changes of the run-out distance. When increasing μ the run-out was decreased for all scenarios. The size of the deviation, hence the sensitivity, is highest for the largest volume, Børa B (Table 6.18).

The sensitivity of the run-out to the Voellmy turbulence coefficient, ξ is relatively low, but the larger scenarios are both more sensitive than the small scenario. An increase in ξ leads to slightly longer run-outs for scenario Børa C Large and Børa B. The run-out of Børa C Large increased more than the run-out of Børa B.

When modelling with assumed frictional rheology, the sensitivity of the run-out to the friction angle is assessed. The sensitivity of the run-out to changes in the friction angle is significant. When increasing the friction angle, the run-out distance is reduced. Running the model with friction angles of 20° and 17° for scenario Børa C and Børa C Large respectively, provides run-out distances similar to the reference simulation. This result was not obtained for scenario Børa B, meaning that the friction angles checked did not provide a run-out similar to the reference.

The other parameters tested on Børa C do not influence the modelled run-out distance significantly, and are therefore not tested on the larger volumes (Table 6.15).

Table 6.15: Summarized results of the analysis of the sensitivity of the run-out to the input parameters.

Parameter	Reference	Tested values Børa C	Tested values Børa C L., Børa B	Effect to run-out, increasing values
Friction coefficient, μ	0.15	0.1/0.15/0.17/ 0.20/0.25	0.1/0.15/0.17/ 0.20/0.25	Shorter
Turbulence coefficient, ξ [m/s^2]	500	450/500/600/ 800/1000	450/500/600/ 800/1000	No effect for small volumes Longer for larger volumes
Friction angle, φ_b [deg.]	-	15/17/20/ 25/30/35	17/20	Shorter
Internal friction angle, [deg.]	35	30/35/38/ 40/45/50	-	Slightly longer
Unit weight, [kN/m^3]	28	26/28/30	-	No significant effect
Particles	2000	1000/2000 /4000	-	No significant effect
Velocity smoothing coefficient	0.01	0.00/0.05/ 0.10	-	No significant effect
Smoothing length constant	4	1/3/5/7	-	No significant effect

Maximum velocity.

The maximum slide velocity is observed to be more sensitive, i.e. the size of the deviations are higher, to changes in the input parameters compared to the run-out distance (Table 6.18). For the smallest scenario, Børa C the frictional rheology provides higher velocities than when Voellmy rheology is assumed. For the larger scenarios, the opposite is observed. The modelled maximum velocity do vary and no clear overall coherence with the input parameters is found for the three scenarios. However, the results from scenario Børa C are consistent and a trend can be seen (Table 6.16). For scenario Børa C the velocity decreases with increasing values of μ, decreasing values of ξ and increasing friction angles, φ_b. Increasing the internal friction angle significantly increases the modelled velocity. The impact of the program parameters tested are small compared to the above-mentioned parameters. However, they do affect the velocity (Table 6.8, Table 6.18). The velocity is found to be insensitive to changes in the unit weight of the material. The modelled maximum velocities for the larger scenarios, especially Børa B, are extremely high, showing unrealistic values for some simulations. See Section 7.2.1 and Section 7.2.3 for discussion and possible explanations.

Table 6.16: Summarized results of the analysis of the sensitivity of the velocity to the input parameters.

Parameter	Reference	Tested values Børa C	Effect to max. velocity, increasing values
Friction coefficient, μ	0.15	0.1/0.15/0.17/ 0.20/0.25	Lower
Turbulence coefficient, ξ [m/s^2]	500	450/500/600/800/1000	Higher
Friction angle, φ_b [deg.]	-	15/17/20/25/30/35	Lower
Internal friction angle, [deg.]	35	30/35/38/40/45/50	Higher
Unit weight, [kN/m^3]	28	26/28/30	No significant effect
Number of particles	2000	1000/2000/4000	Slightly higher
Velocity smoothing c.	0.01	0.00/0.01/0.05/0.10	Slightly lower
Smoothing length c.	4	1/3/4/5/7	Slightly lower

Fahrböschung, α and travel angle, α'

The difference between Fahrböschung and travel angle increases with increasing landslide volume (Table 6.17). See Section 7.2.1 for discussion. The difference is negligible for Børa C.

Table 6.17: Average difference between Fahrböschung α and travel angle α' for the three scenarios.

Scenario	Børa C	Børa C Large	Børa B
Volume, [m^3]	76000	476000	2 400 000
α'- α, [deg]	0.1	2.0	5.4

Table 6.18: Summarized deviations of the parameters of impact.The deviations are based on the reference simulation (μ=0.15, ξ=500 m/s^2) with parameters from Schleier et al. (2015). Velocity is the output maximum velocity. The velocity results from Børa C Large and Børa B should be carefully considered. See Section 7.2.1 and Section 7.2.3. "-" = reference.

Parameter	Deviations Børa C, %		Deviations Børa C L., %		Deviations Børa B, %	
	Run-out	Velocity	Run-out	Velocity	Run-out	Velocity
Friction coefficient, μ						
0.1	3	4	4	-31	5	59
0.15	-	-	-	-	-	-
0.17	-1	-1	-1	-24	-2	-20
0.20	-3	-4	-3	- 43	-5	8
0.25	-6	-14	-5	-41	-9	50
Turbulence coefficient, ξ [m/s^2]						
450	-1	- 5	0	-37	0	57
500	-	-	-	-	-	-
600	1	7	2	-40	1	34
800	0	6	4	-36	2	186
1000	0	15	6	-14	3	126
Friction angle, φ_b [deg.]						
15	12	46				
17	7	43	1	-46	-10	5
20	1	34	-4	-59	-17	-73
25	-7	20				
30	-17	10				
35	-38	-3				

6.3.4 Entrainment of debris material

Two of the aims of this thesis is to assess the effect of entrainment to the run-out distance and to study what factors that influence the entrainment potential. Scenario Børa C is used for this purpose. The results of the analysis of these features are presented in this section. The slope is divided in an upper and lower scree deposits zone, source area and rock outcrops and rock avalanche deposits (Section 5.2.3, Table 5.5). The sensitivity of the run-out to the parameters influencing entrainment is analyzed. Further, the effect of where on the slope entrainment occur are studied. Last, the effect of pore pressure, i.e. the presence of water, in the scree deposits are assessed. The results are presented in terms of figures and tables.

The travel angle is one of the program outputs. When entrainment is included to the model, DAN3D does not provide reasonable values of the angle. The values are in the range 0.003 – 0.016. This applies to all simulations with entrainment included. The travel angle is therefore not included in this result chapter.

The study of the effects and processes of entrainment were first carried out based on small final volumes, calculated from the bulk slide porosity, n (Section 5.2.3). This means low entrainment rates, E and little material allowed to be entrained. Most of the results from the study are not included in the text, but presented in Appendix V, as the values of E were found to be too low for the scenario at Børa. However, the results have been useful to compare the differences between low and high entrainment rates, i.e. little or much entrainment.

Entrainment rate, E

The run-out distance decreases when entrainment is included in the model. However, altering the entrainment rate does not lead to changes in the shortened run-out distance (Figure 6.14). The run-out area is, on the other hand, affected meaning more deposits on the slope and an increased lateral spread of the material.

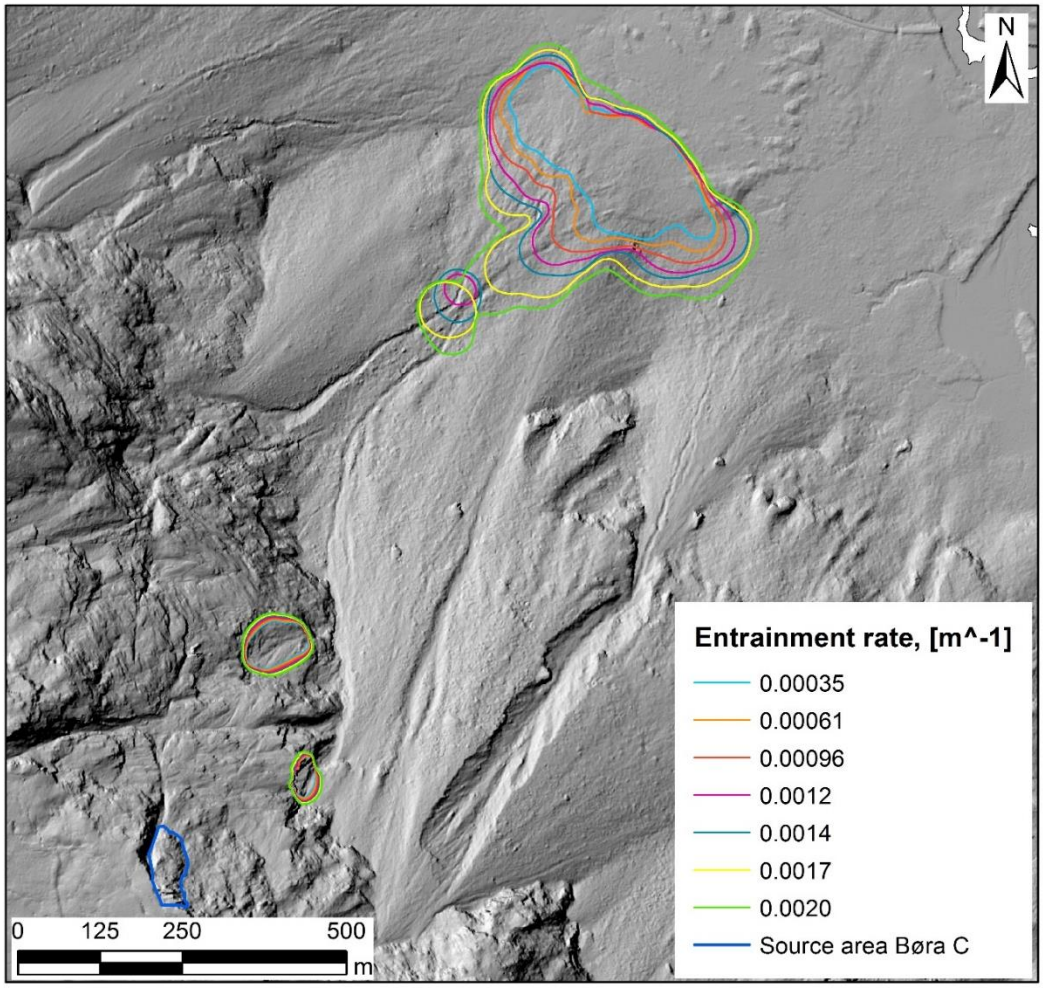

Figure 6.14: Entrainment rate, E. The run-out distance is not sensitive to the entrainment rate, but the area and lateral spread increases with increasing E.

The final volume increases with increasing entrainment rate because the increased entrainment rate allows more material to be entrained (Table 6.19). The final volumes obtained by modelling are significantly lower than the input final volumes required as an input to calculate the entrainment rate. The deviation increases with increasing *E*. Based on the study of Norwegian events known to have entrained significant volumes (Section 4.3.1), a volume increase by a factor of four are considered realistic at Børa. Results show that to obtain this, the initial volume should be increased by a factor of five (Table 6.19). An entrainment rate representing expected volume increase by a factor of four (E = 0.0012 m^{-1}) are used in further analyses. Other values are used and presented where this is considered necessary.

When including the low values of entrainment rate the obtained maximum velocity of the landslide decreases with increasing *E*. This is not the fact for the values presented here in this section, where a constant maximum velocity is observed. For larger entrainment rates, the maximum velocity if insensitive to changes. Results from simulations with low entrainment rates are found in Appendix IV and Appendix V.

Table 6.19: Results from analysis of entrainment rate, E. The analysis is carried out on scenario Børa C, V = 76 000 m^3. Deviations are calculated from the input and modelled final volumes, m^3. The expected factor of volume increase equals the increase applied to the input final volume.

Entrainment rate	Run-out	Max. velocity	Factor of volume increase		Deviation final volume
[m^{-1}]	[m]	[m/s]	Expected	Modelled	%
0.00035	1400	34.5	1.5	1.4	- 6
0.00061	1400	34.5	2.0	1.8	- 8
0.00096	1400	34.5	3.0	2.6	- 13
0.0012	1400	34.5	4.0	3.3	- 17
0.0014	1403	34.4	5.0	4.1	- 19
0.0017	1408	34.3	7.0	5.4	- 22
0.0020	1413	34.2	10.0	7.3	- 27

Maximum erosion depth

The run-out distance is not sensitive to changes in the set maximum erosion depth. The same holds for the final volume, meaning that the volume of material entrained, is not affected by the set maximum erosion depth. The maximum velocity is also insensitive to the maximum erosion depth. Therefore, no table with results are included. The interested reader is referred to Appendix IV.

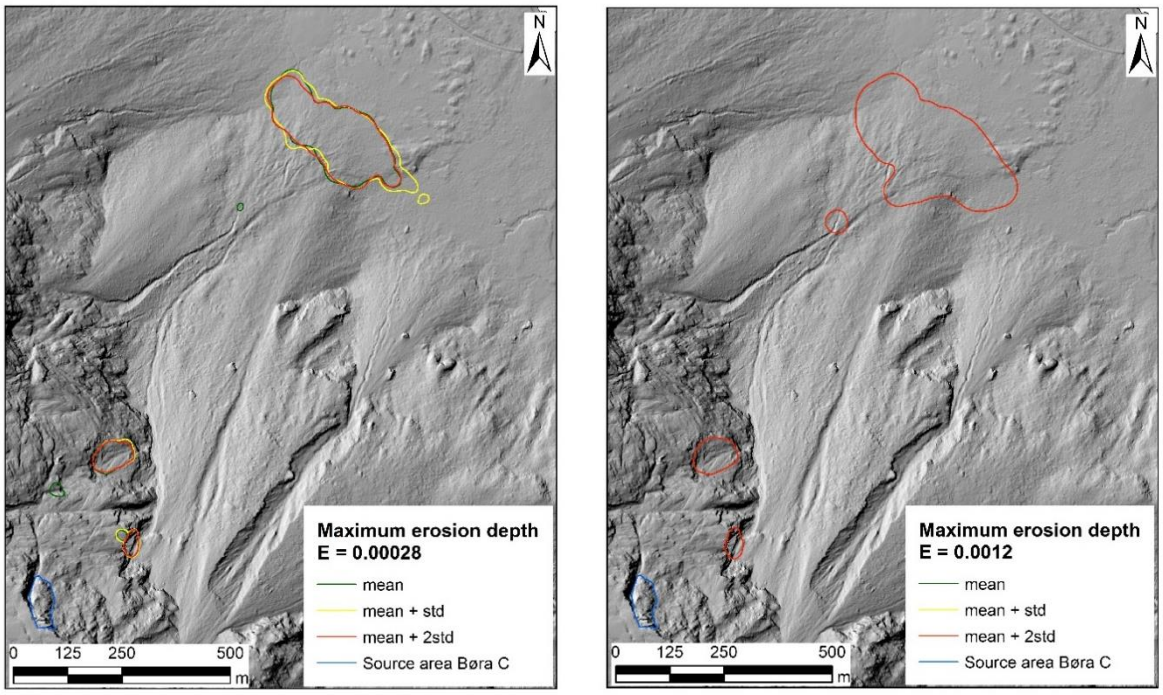

Figure 6.15: Maximum erosion depth. Left: Erosion rate, E = 0.00028 m^{-1}. Right: Erosion rate, E = 0.0012 m^{-1}. The set maximum erosion rate does not lead to changes in run-out.

Friction angle, φ_b

The run-out distance is sensitive to changes in the friction angle. Increasing the friction angle decreases the run-out distance (Figure 6.16). A figure showing the results for E = 0.00028 m^{-1} is found in Appendix V.

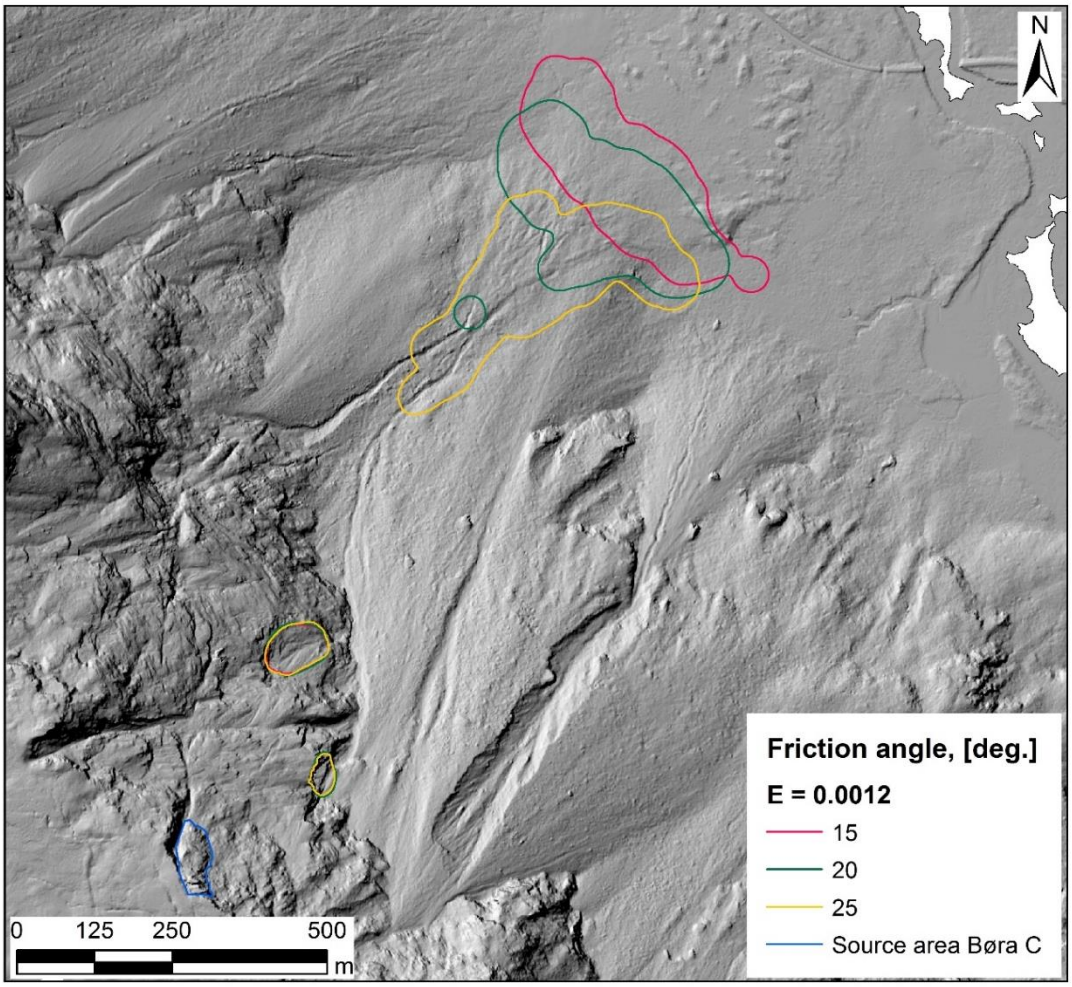

Figure 6.16: Friction angle, E = 0.0012 m^{-1}. The run-out increases when the friction angle is decreased.

The final volume decreases with increasing friction angles, meaning less material is entrained for larger friction angles (Table 6.20). The maximum velocity decreases with increasing friction angles. Fahrböschung increases when the friction angle is decreased.

Table 6.20: Friction angle of the scree deposits, E = 0.0012 m^{-1}. Results from analysis of the impact of the friction angle of the scree deposits.

Friction angle [deg.]	Run-out [m]	Max. velocity [m/s]	Modelled final volume [m^3]	Fahrböschung [deg.]
15	1439	40.7	266193	33.8
20	1400	38.2	251935	34.5
25	1331	38.2	197903	35.7

Erosion from separate zones

The effect of erosion from different elevations is assessed by allowing entrainment from one scree deposit zone at the time. For small erosion rates, the run-out distance is not affected by the elevation of the entrainment processes (Appendix IV, Appendix V). Higher erosion rates allows more material to be entrained. When applying a higher erosion rate, the run-out is sensitive to where on the slope the material is entrained (Figure 6.17, Figure 6.18). Entrainment from the lower part of the slope leads to shorter run-out distances than entrainment from the upper part. However, the obtained final volumes when entraining from the lower part are higher than when entrainment is allowed on the upper part. Even though the maximum erosion depth is higher in the upper part and the fact that the upper scree deposit zone is longer than the lower. Assessing the effect of the elevation of the material available for entrainment is one of the main interests of this study. Thus, the extreme value $E = 0.002$ m^{-1} (volume increased by a factor of 10) is tested in addition to $E = 0.0012$ m^{-1}.

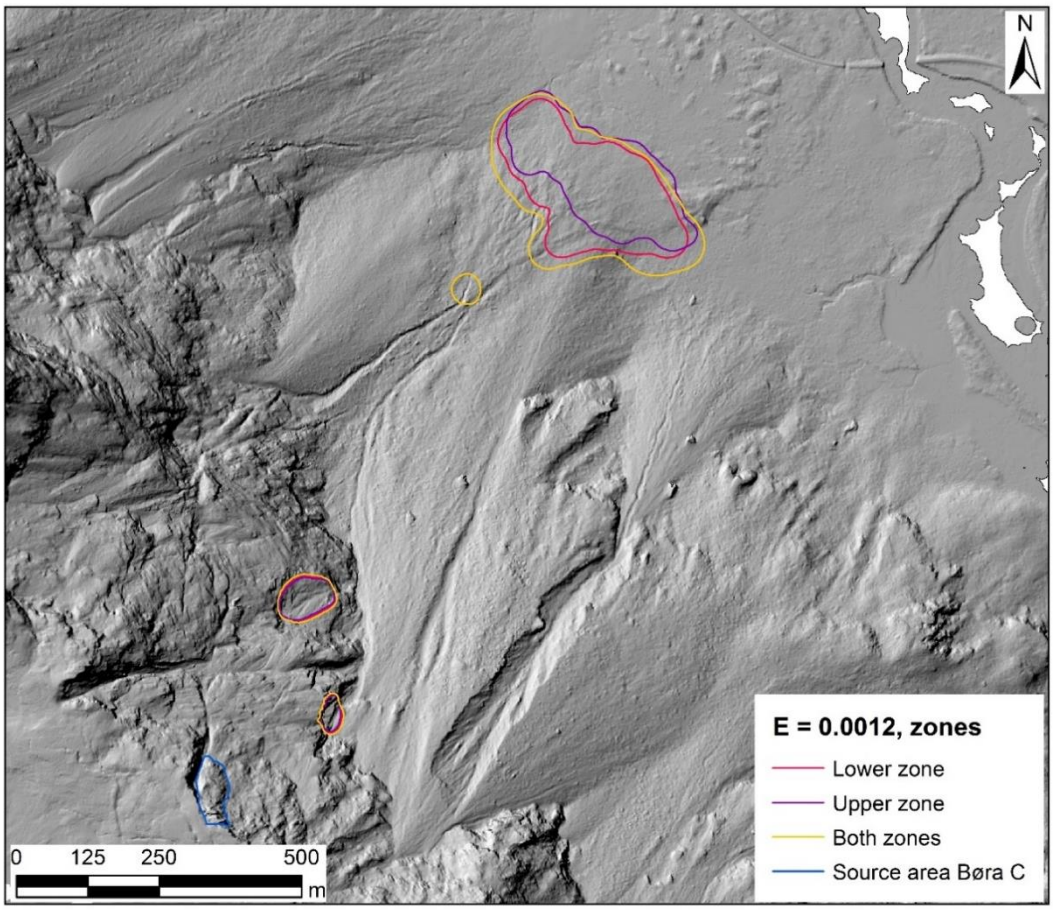

Figure 6.17: Entrainment of debris material from separate zones, $E = 0.0012$ m^{-1}. Results of the study of the elevation of entrainment processes.

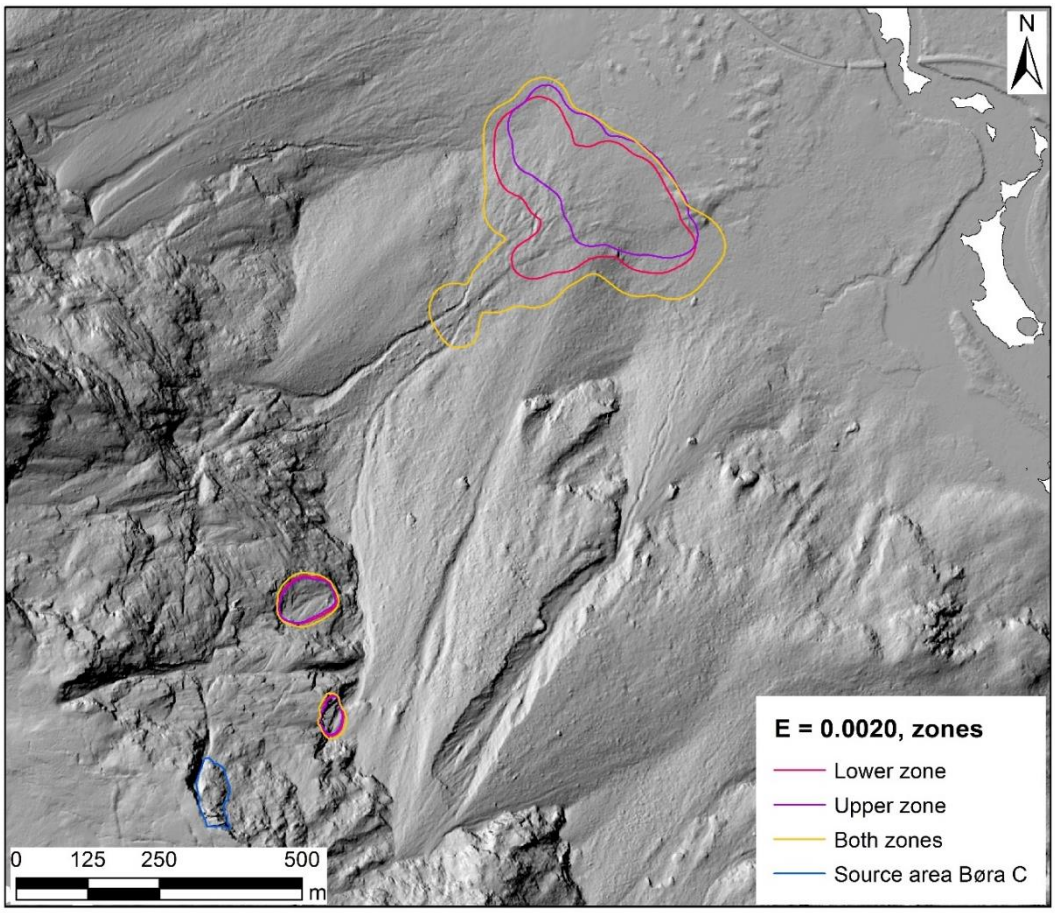

Figure 6.18: Entrainment of debris material from separate zones, E = 0.002 m^{-1}. Results of the study of the elevation of entrainment processes.

The obtained final volumes when entraining from the lower part are higher compared to when entrainment is allowed on the upper part (Table 6.21). This is not consistent with the maximum erosion depth being higher in the upper part and the upper scree deposit zone being longer than the lower. Fahrböschung remains constant at 34° when changing the zones of entrainment.

Table 6.21: Results from analysis of the effect of the elevation of where entrainment occurs.

Parameter	Run- out [m]	Maximum velocity [m/s]	Modelled final volume [m^3]
E = 0.0012 m^{-1}			
Lower zone	1397	43.6	139302
Upper zone	1414	39.0	133486
Both zones	1400	38.2	251935
E = 0.0020 m^{-1}			
Lower zone	1395	43.6	205103
Upper zone	1410	38.2	200776
Both zones	1413	38.2	553742

6.3.5 Pore pressure in the scree deposits

Pore pressure ratio, r_u

Adding water to the model affects the modelled outputs. The run-out is significantly influenced by the pore pressure ratio, r_u. When increasing r_u the run-out is increased, in terms of both distance and lateral spread (Figure 6.19).

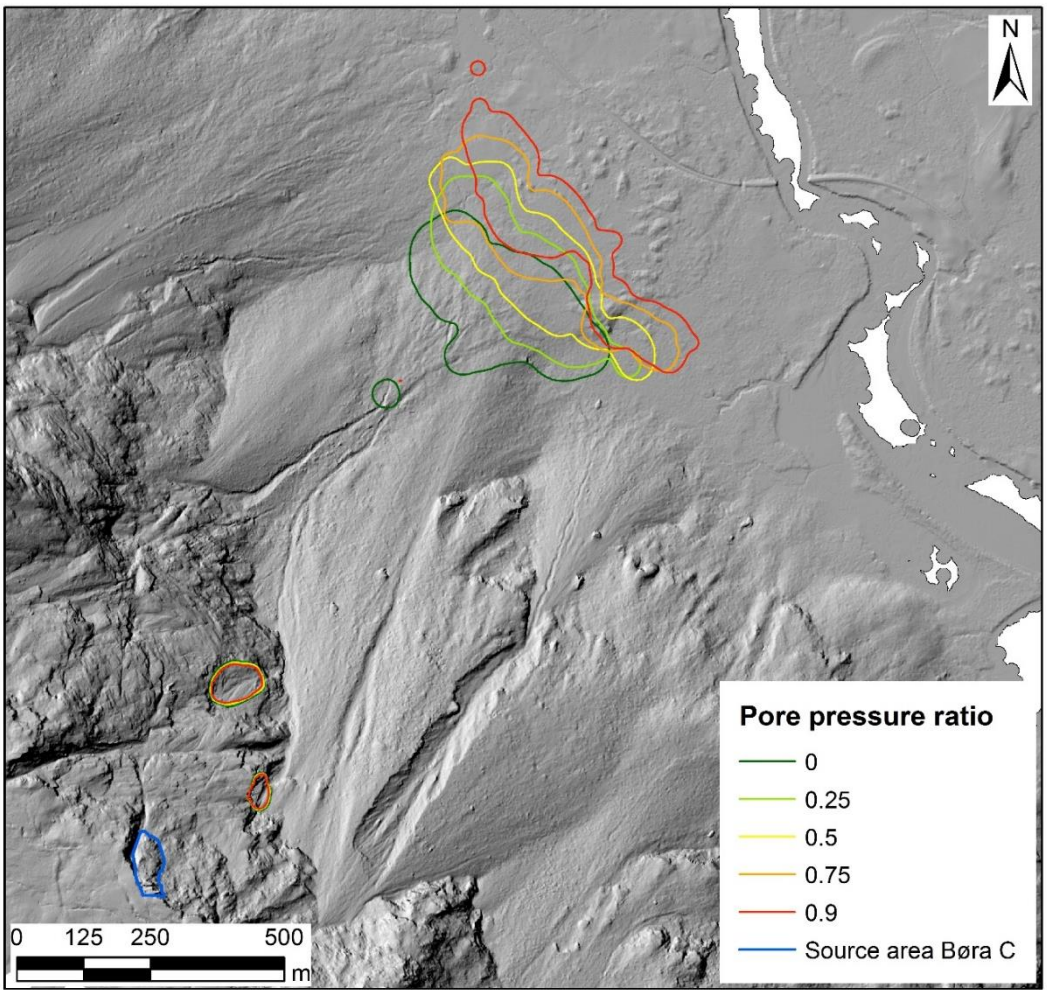

Figure 6.19: Pore-pressure ratio, r_u. E = 0.0012 m^{-1}.

The final volume increases with increasing values of r_u up to r_u =0.5 (Table 6.22). For higher values, the final volume starts to decrease. The maximum velocity is increasing when water is included compared to dry conditions. Fahrböschung is decreasing with increasing values of the pore-pressure ratio due to the increase in run-out.

Table 6.22: Pore-pressure ratio, r_u, E = 0.0012 m^{-1}. Results from simulations with different pore-pressure ratios.

Pore – pressure ratio	Run-out [m]	Max. velocity [m/s]	Modelled final volume [m^3]	Fahrböschung [deg.]
0	1400	38.2	251935	34.3
0.25	1437	40.1	265467	33.9
0.5	1477	46.3	272688	33.2
0.75	1522	53.6	272029	32.4
0.9	1550	60.2	267285	32.0

Pore pressure at different elevations

The effect of where on the slope pore pressure is present, is assessed by setting the pore pressure ratio, r_u to zero in one scree deposit zone. The run-out is observed to be sensitive to where in the slope pore pressure is present (Figure 6.20). Presence of water in the lower part leads to longer run-outs compared to water in the upper part. This holds for both low and high entrainment rates.

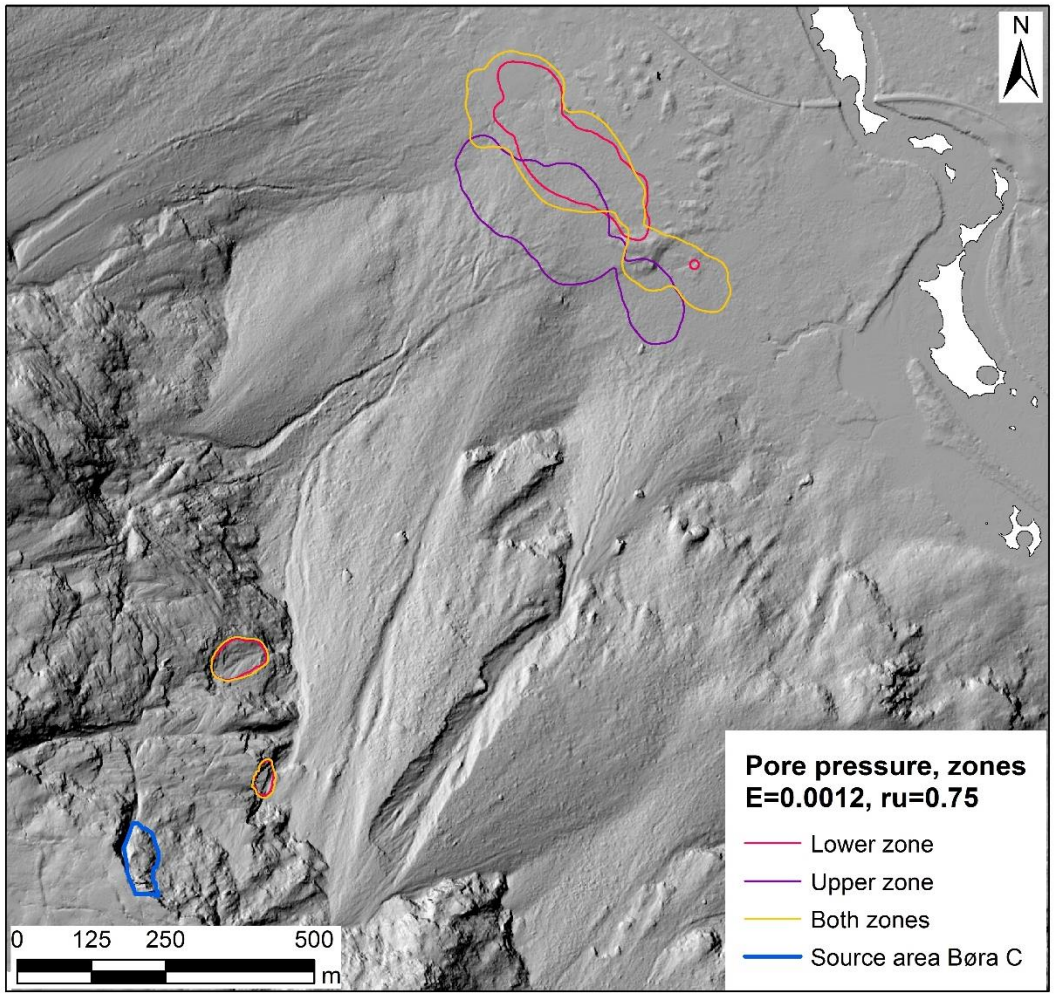

Figure 6.20: E = 0.0012 m^{-1}, r_u = 0.75. Entrainment and presence of water are allowed in separate zones.

Figure 6.20 shows results from simulations where entrainment and pore pressure are allowed in one of the two scree deposit zones. Results from simulations where entrainment is allowed from the entire slope, but pore-pressure is only added in one zone at the time are found in Appendix V and Table 6.23.

The obtained final volumes are higher when erosion and pore pressure occur in the lower part of the slope compared to the upper part (Table 6.23). The opposite is observed for the maximum velocity.

Table 6.23: E= 0.0012 m^{-1}, r_u = 0.75. Results from analysis of the impact of the location of water.

	Run-out [m]	Max. velocity [m/s]	Modelled final volume [m^3]	Fahrböschung [deg.]
Erosion from both zones, pore pressure in separate zones				
Lower zone	1511	45.4	275249	32.8
Upper zone	1415	56.2	244043	33.9
Erosion and pore pressure in separate zones				
Lower zone	1498	47.3	150815	32.6
Upper zone	1435	54.6	135472	34.2

6.3.6 Summarized results of entrainment analyses

When including entrainment to the model, the run-out distance decreases compared to modelling without entrainment. The run-out distance is not significantly affected by the entrainment rate, *E*. However, the run-out is affected in terms of lateral spread and area because of increased volume of material. The maximum velocity is slightly decreasing when the entrainment rate is increased. The maximum erosion depth is of no importance to the modelled results. On the other hand, the run-out and maximum velocity are sensitive to changes in the input friction angle, φ_b of the scree deposits. The angle is not the friction angle of the material, but the friction angle of the sliding masses. The run-out and maximum velocity are decreasing with increasing values of the friction angle.

The effect of the elevation of material available for entrainment is assessed. When running the model under dry conditions, i.e. no pore pressure $R_u = 0$, entrainment from the upper part provides the longest run-outs. The modelled final volume of the landslide is nevertheless higher when material is entrained from the lower part compared to the upper part. The maximum velocity of the landslide is higher when material is entrained from the lower part of the slope. Entrainment from one part of the slope does not provide shorter run-out distances than entrainment from the entire slope.

When including pore pressure to the simulations, the run-out increases. The run-out distance is significantly increased when r_u is increased. This leads to a decrease in Fahrböschung. The maximum velocity of the landslide is highly sensitive to changes in the pore-pressure coefficient and degree of water saturation. When increasing r_u , the maximum velocity increases.

When adding pore pressure to one scree deposit zone at the time, it is possible to study the effect of the elevation of the presence of water, i.e. the pore pressure. It is seen that water in the lower part of the slope leads to longer run-outs and higher final volumes compared to presence of water in the upper part. Nevertheless, the landslide obtains a higher maximum velocity if entrainment of saturated material occurs in the upper part of the slope.

Generally, the maximum velocity slightly decreases when entraining unsaturated material compared to no entrainment. On the other hand, the maximum velocity increases when saturated material is entrained.

6.4 Estimation of debris available for entrainment

In order to compare the modelled volume entrained to the estimated volume available for entrainment, the volume of deposits in the path of the landslide is calculated based on the simulations with entrainment rate E = 0.0012 m^{-1} and pore pressure ratio r_u = 0.75 and r_u = 0. Both the total volume of deposits in the extent of the landslide and the volume of deposits in the area were entrainment actually occur, are calculated (Figure 6.21, Table 6.24). The volumes are calculated by using the same principles as applied when the total volume of deposits at Børa was estimated (Section 5.1.3). The raster file with estimated thickness of the deposits (Figure 6.2) is used for the calculation. Material is mainly entrained in the central part of the extent of the landslide (Figure 6.21).

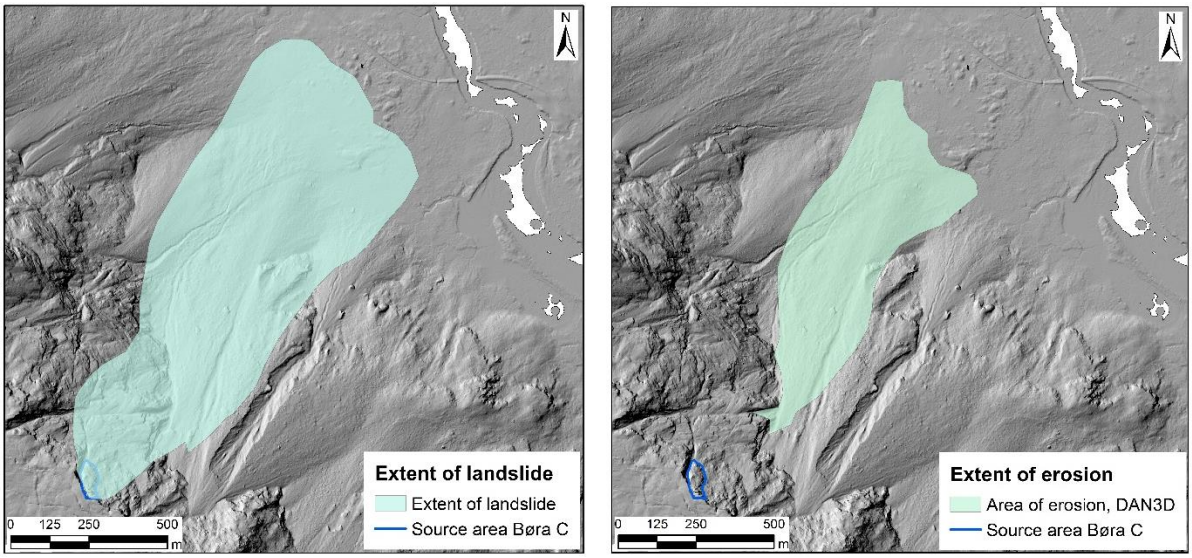

Figure 6.21: Areas used for calculation of volumes of deposits available for entrainment. The extent of the landslide and the area of where erosion occurs are found from output files from DAN3D. (Simulation: E= 0.0012 m^{-1}, r_u = 0.75)

The difference between the estimated volume of deposits in the path (18 Mm^3 and 14 Mm^3) and the area where entrainment actually occur (11 Mm^3) are noticeable (Table 6.24).

Table 6.24: Volume available for entrainment. Thickness of deposits from SLBL analyses (Figure 6.2), areas from modelling in DAN3D (Figure 6.21).

Area of deposits	Volume [Mm^3]
Total extent of landslide, (E=0.0012 m^{-1}, r_u= 0.75)	18
Total extent of landslide, (E=0.0012 m^{-1}, r_u= 0)	14
Area where entrainment occur	11

7 Discussion

7.1 Estimation of debris thickness and volume

The estimated total volume of deposits at Børa is 56 Mm^3 (Table 6.2). This is in the same order of size as found on a nearby, similar slope in terms of debris fan size. Nilsen (2016) did a volume estimation of debris by the SLBL technique in his study of the periglacial processes at Gråhøa, Sunndal Valley, western Norway. The estimated volumes of debris are 58-95 Mm^3, depending on the chosen limits of the deposits. The maximum thicknesses of the deposits at Børa are 42-150 m. At Gråhøa the maximum thicknesses are estimated to 95-97 m. It can be seen that both the estimated debris volumes and thicknesses at Børa are in the same order of size as at Gråhøa. The results are not verified by this comparison, but the observation of similar conditions in a nearby similar slope may indicate that the results are reliable. The total volume of the unstable rock slope is approximately 400 Mm^3. The 400 Mm^3 includes the deposits, meaning that approximately 345 Mm^3 is left of the initial unstable volume and 56 Mm^3 is scree deposits possibly available for entrainment. However, a collapse of the entire slope is not considered a realistic scenario, but an estimation of debris volume may be useful to assess the potential for entrainment.

The output profiles from the SLBL analyses in CONEFALL are used to find the best-fit curvature for each scree deposit zone. This is a subjective method, which depends on the user. The user is in this case the author of the thesis. Several values and models are checked, and the most appropriate values are chosen in each case (

Table 6.1, Appendix I). However, as the method is based on subjective assessments, other values of curvature may be found more appropriate by a different user. Advantageously, estimation of debris thickness by the SLBL technique may be complemented by geophysical methods in order to verify the results.

The slope is divided into seven polygons with different curvature values (Figure 6.1). This is used to estimate the thickness of the scree deposits and later to calculate the volume of the deposits. Each polygon is given its respective curvature based on the chosen values from the profiles created by the SLBL analysis (Figure 6.1). This leads to an unnatural and abrupt change in curvature along the margins of the polygons, seen as a thick, black line on the hill shade (Figure 7.1). No gradual transition in curvature is possible, which means that sudden jumps in deposit thickness are initiated along the margins. This is unrealistic and not the case in real life.

The differences in deposit thickness is somewhere quite significant, as the curvatures of the adjacent polygons are different. The error is due to the method applied, and the fact that no smooth transition in curvature between the polygons is created. No sufficient and effective way of doing this in ArcGIS was found.

The error is affecting the estimate of the total volume of the scree deposits, as the mean thickness of the debris in each polygon is used for this purpose. However, this is assumed not to be of importance for further use of the results. The results are not implemented directly in the numerical run-out modelling, as only the maximum erosion depth, meaning the maximum debris thickness, of certain areas are needed to run the entrainment model. The total volume of the scree deposits is not required as direct input at any stage.

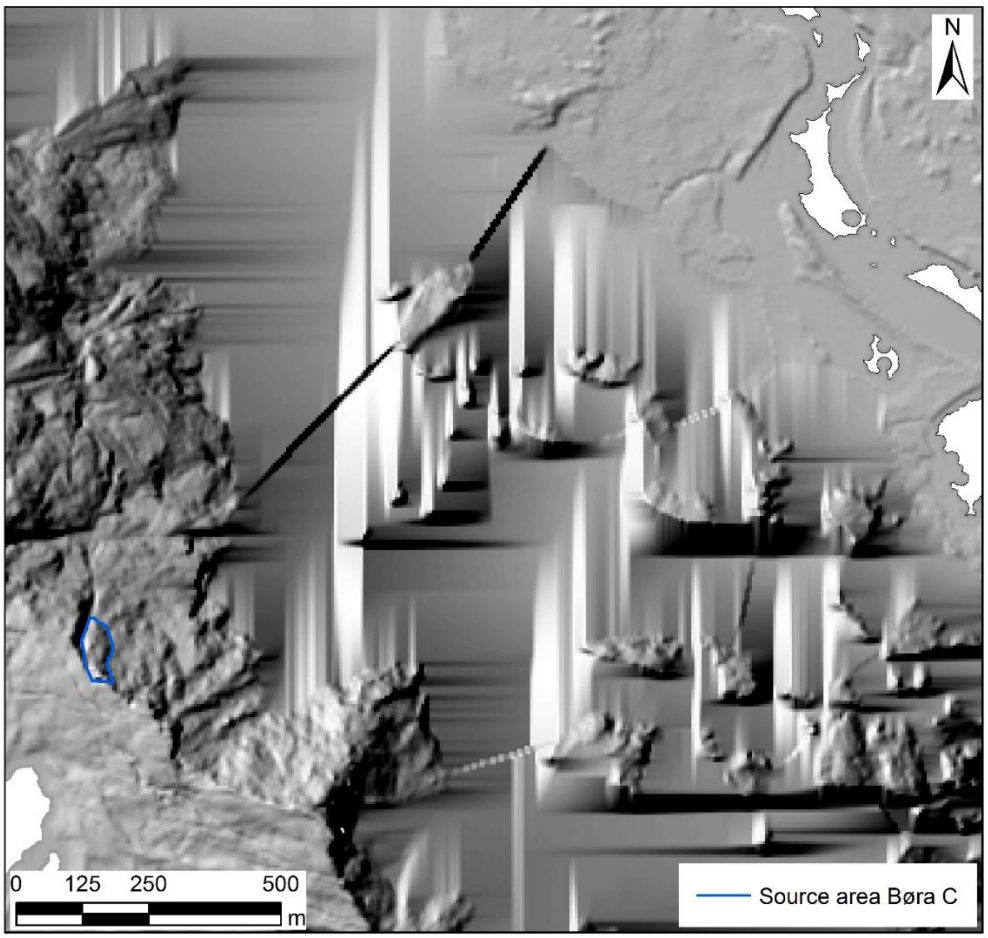

Figure 7.1: Hill shade. Based on debris thickness estimated by the SLBL technique. The thick, black line cutting the area of deposits is located on the margin of polygons and is caused by the difference in curvature between the polygons.

7.2 Analysis of run-out distance

A numerical run-out model is based on assumptions and governing equations simplifying the processes of run-out, however most models are able to simulate the main characteristics of a real landslide (McDougall et al., 2012). Studies have shown that modelled results are highly affected by the set input parameters. Chosen rheology and values of parameters both influence the modelled results significantly (Hungr and McDougall, 2009). Thus, the results should not be directly transferred to reality without critical review. Many input parameters are required to run the model. The input files are somewhat complicated to produce, and the files their self, constitute a source of error. The reader should keep that in mind when the results are discussed.

This section aims to discuss the results carried out by numerical run-out modelling in DAN3D. First, a discussion of the sensitivity analysis will be given, including parameter assessment, and the sensitivity of run-out and velocity to the different parameters. The modelled run-out distances are compared to empirical estimates. Fahrböschung is compared to empirical estimates and the travel angle. The discussion of the results from the study of entrainment and involved processes comprise comparisons of estimated debris thickness and volume to modelled erosion depth and final volume. This is considered relevant information for future analyses of the debris entrainment potential and are important to optimize modelling of entrainment events by DAN3D. Comparison of expected and modelled final volume is also given in order to highlight important aspects of how DAN3D handles the two volumes. Expected final volume refers to the input final volume needed to calculate the entrainment rate, *E*. Last, possible explanations to the unrealistic output values are discussed before the challenges by including results from field- and laboratory work are addressed.

7.2.1 Sensitivity analysis

Parameter test

The parameter test is carried out to determine reasonable input parameters for numerical run-out modelling in DAN3D and to assess the different parameters' influence to the run-out distance. The modelled maximum velocity is also considered. Parameter assessment is best done by back-calculation of a nearby event (Molina et al., 2015). A sensitivity analysis will assess the influence of each parameter. By that, one can chose parameters based on trial-and-error. However, it is difficult to validate the parameters without a back-calculation. The results should accordingly be carefully considered.

The tested values are based on parameters used by Schleier et al. (2015) in combination with the range of parameters suggested by Sosio et al. (2008) (Section 5.2.2). The parameters considered the most suitable and used as reference simulations, are coincident with the parameters suggested by Schleier et al. (2015). The assumed rheology is Voellmy with friction coefficient $\mu = 0.15$ and turbulence coefficient $\xi = 500$ m/s^2. Schleier did succeed in reproducing the run-out of the back-calculated event in Innerdalen, western Norway. Thus, the parameters are known to have produced sufficient results in what is considered similar, geological conditions. The sensitivity analysis of the program parameters states that the defaulted values are suitable for studies at Børa.

McDougall (2006) recommends Voellmy rheology with $\mu = 0.1$ and $\xi = 500$ m/s^2 for simple rock avalanches. Back-calculations and analyses of Canadian landslides showed that best results were obtained with Voellmy rheology as the dominant rheology and μ range of 0.02-0.15 and a ξ from 250-500 m/s^2 (McKinnon et al., 2008). The Voellmy rheology is assumed most suitable at Børa. The chosen coefficients used as a reference simulation for this analysis are in the upper part of the suggested ranges ($\mu = 0.15$, $\xi = 500$ m/s^2). Differences in geology and local conditions play a huge role, and the chosen values are considered suitable for the conditions at the study area of these analyses.

The experienced shorter flow duration, i.e. simulation time, with the frictional model compared to the Voellmy rheology is consistent with observations by McDougall (2006) in the back analysis of the Frank Slide, Alberta, Canada.

Run-out

The run-out is sensitive to changes in the Voellmy friction coefficient, μ. Increasing μ results in shorter run-out distances. This is due to an increased surface friction. The deviations from the reference simulation, hence the sensitivity, is highest for the largest volume. Larger volume implies more masses and thus more spreading. The results showing the run-out being most sensitive to the Voellmy friction coefficient, is consistent with findings by Frekhaug (2015).

Børa C is insensitive to changes in the Voellmy turbulence coefficient, ξ regarding run-out. The sensitivity of the run-out of the larger scenarios to the Voellmy turbulence coefficient, ξ is small. However, scenario Børa C Large and Børa B are slightly affected, indicating that the sensitivity of the run-out to the turbulence coefficient should be taken into account for larger volumes.

The run-out is found to be sensitive to the friction angle (frictional model). Increasing values of the friction angle leads to shorter run-out distances. The friction angle counts for the highest deviations, i.e. the run-out is most sensitive to this parameter (Table 6.18). This emphasize the importance of carefully consider the frictional rheology and required parametrization.

According to McKinnon et al. (2008) and their analyses of Canadian landslides a bulk friction angle, φ_b of 20° provided the best results when assuming a frictional model. This is as observed for scenario Børa C, where a model with friction angle of 20° produces a run-out distance in the same order as the reference simulation with Voellmy rheology. However, the scenarios of larger volumes at Børa require lower friction angles to obtain the same run-out distance. The largest scenario, Børa B did not produce run-outs of the same length as the reference simulation with the tested values (17° and 20°). Lower friction angles are probably required to produce run-outs similar to the reference, but as lower values were not considered realistic lower values are not tested.

When comparing the modelled run-out distances to the run-out distances estimated by the Scheidegger relationship one can see that they are shorter (Table 7.1). The Scheidegger relation is considered a conservative estimate for Norwegian events, meaning that the estimated maximum run-out distances based on Scheidegger are too long (Blikra et al., 2001, Oppikofer et al., 2016a). The numerical modelling of the scenarios at Børa indicate the same.

Table 7.1: Comparison of run-out distances modelled by DAN3D and estimated by the Scheidegger relation. The modelled run-out distances are from reference simulations with input parameters based on Schleier et al. (2015) (Voellmy rheology, $\mu = 0.15$, $\xi = 500$ m/s^2).

	Volume [m^3]	Run-out, DAN3D [m]	Run-out, Scheidegger [m]
Børa C	76 000	1448	1333
Børa C Large	476 000	1598	1777
Børa B	2 400 000	1767	2173

Velocity

Børa C

The modelled maximum velocity is sensitive to more input parameters than the run-out. The size of the deviations, i.e. the sensitivity, are also generally higher. This implies that the velocity is more complicated to model, as more parameters need to be considered and calibrated. However, the Voellmy coefficients, μ and ξ, the friction angle, φ_b (frictional rheology) and the internal friction angle of the material, yield the highest sensitivity, which implies that these parameters should be payed most attention.

The velocity decreases with increasing values of μ, decreasing values of ξ and increasing friction angles, φ_b. Increasing the internal friction angle significantly increases the modelled velocity. The unit weight of the material is of no importance to the modelled maximum velocity. The program parameters slightly affects the modelled maximum velocity, but the deviations are lower than what is recorded for the above-mentioned parameters. Thus, the material parameters, excepting the unit weight, are the parameters of most importance to the modelled velocity.

The Thurwieser rock avalanche in the Italian Central Alps was recorded on video and relatively precise measurements of the flow velocity is available (Sosio et al., 2008). Back calculations showed that numerical modelling with the Voellmy rheology assumed, underestimated the flow velocity. However, the frictional rheology did reproduce flow velocities in a satisfactory range (Sosio et al., 2008). The sensitivity analysis performed on scenario Børa C clearly shows that the frictional model provides higher flow velocities than the Voellmy model (tables in Section 6.3.1). This is consistent with what McDougall (2006) describes; a frictional model will

calculate high velocities and predict forward-tapering deposits and a model with Voellmy rheology will result in lower velocities and a forward bulging deposit. However, Schleier et al. (2015) did reproduce satisfactory velocities modelling with the Voellmy rheology. Calculated velocity based on mean run-up was 40 m/s and modelled maximum velocity at the time-step marking the maximum run-up is 36 m/s. The modelled velocities of a possible collapse of Børa C are 32- 50 m/s for simulations with the Voellmy rheology and 36 – 54 m/s for the frictional rheology. The velocity of the reference simulation is 37 m/s.

Scenario Børa C Large and Børa B

For the larger volumes Børa C Large and Børa B, no clear coherence between input parameters and modelled maximum velocity is found. The output maximum velocities for simulations of Børa B are, as distinct from the smallest scenario, unrealistically high. Maximum velocities up to 2000 m/s are obtained. When analyzing the output velocity files from different time steps, it is found that this is probably due to extremely high velocities in one or two particles. This is further discussed in Section 7.2.3.

The maximum velocity results from scenario Børa B are considered not realistic and may therefore not be used for further analyses. Some of the modeled maximum velocities for scenario Børa C Large are also too high to be considered realistic, and the results are not considered reliable. In order to compare the sensitivity of the velocity to the input parameters for all scenarios, the velocity after 10 s is studied. DAN3D allows the user to get outputs during the modelling and to set the interval for the outputs. In this case, the interval is set to 10 s. This is done with results from sensitivity analysis of the Voellmy coefficients and the friction angle (frictional model) for the three scenarios. The velocity after 10 s are in all cases lower than the maximum velocity. Further, the velocities after 20, 30, 40 and 50 s are studied to see if higher velocities are obtained later in the simulation. For the majority of the simulations, the velocity after 10 s are highest. Some simulations are found to have a slightly higher velocity after 20 s, but in order to check the sensitivity of the velocity to the input parameters, the velocity after 10 s are considered a sufficient representation. The velocities after 10 s for Børa C, were studied first, as the maximum velocities are reliable for this scenario. However, no clear tendencies are found. The velocities after 10 s for Børa C do not replicate the results of the sensitivity analysis of the maximum velocity. In the case of the larger scenarios, the velocity after 10 s do not increase/decrease with increasing/decreasing values of input parameters (Appendix III). Further analysis are needed to conclude on the sensitivity of the velocity to the input parameters for the larger scenarios.

Fahrböschung and travel angle

The calculated values of Fahrböschung, α from all simulations of events at Børa are 26°-41°. The wide range is mainly caused by the run-outs sensitivity to the friction angle (frictional rheology). Looking at the results from the simulations with the reference values (Voellmy rheology, μ =0.15, ξ = 500 m/s^2), the Fahrböschung is between 27°-34°, for the three scenarios at Børa (Table 7.2). According to Domaas and Grimstad (2014) a common range of α for Norwegian events is 11°-35°. Børa is in the upper part of this range, which are reasonable considered relatively small volumes.

As one can see, the Fahrböschung angles based on the known volumes and the Scheidegger relationship are lower than the Fahrböschung based on the modelled run-out (Table 7.2). A lower Fahrböschung implies a longer run-out. As mentioned, the Scheidegger relation is considered a conservative estimate for Norwegian events.

Table 7.2: Fahrböschung, α and travel angle, α' for the modelled scenarios at Børa. The results are from simulations with reference values (Voellmy rheology, μ=0.15, ξ=500 m/s^2). Fahrböschung is calculated from modelled run-out (DAN3D) and from the known volume of the events, Equation 4.7.

Scenario	Volume [m^3]	Fahrböschung, DAN3D [deg.]	Fahrböschung, Volume [deg]	Travel angle, DAN3D [deg.]
Børa C	76000	34	-	34
Børa C Large	476 000	31	28	33
Børa B	2 400 000	27	23	33

The difference between the Fahrböschung (based on DAN3D simulation results) and travel angle increases with increasing volume of the scenario (Table 6.17, Table 7.2). This is because an increased volume means larger masses and more spreading of the material. According to Bowman et al. (2012) the travel angle emphasize the motion efficiency of the centers of gravity, not the effect of spreading to the same extent as the Fahrböschung. This means that an expansion of volume and following increased spreading of material will affect the Fahrböschung more than the travel angle. This is as observed at Børa (Table 7.2). Nevertheless,

a low Fahrböschung or travel angle are both taken to indicate a mobile, long run-out landslide (Bowman et al., 2012).

The results from analyses of a rock avalanche into an ice-free valley (Innerdalen, western Norway) presented in the paper by Schleier et al. (2015), indicates that modelled (DAN3D) and field-derived values of the Fahrböschung are consistent. Fahrböschung is estimated to 22° for the mapped deposits and 23° for the modelled particles. The DAN3D travel angle is 27°. The volume of the modelled event is 23.5 Mm^3 while the largest scenario modelled at Børa is 2.4 Mm^3. Higher values of the Fahrböschung at Børa is therefore as expected. The results from Schleier et al. (2015) indicates that the Fahrböschung calculated from results modelled by DAN3D are reliable.

7.2.2 Entrainment of debris material

The travel angle, α' is one of the output values from DAN3D. As mentioned, reasonable output values are not produced when entrainment is included. The values are between 0.003 – 0.016. Thus, the travel angle is not included in the analyses of entrainment processes. The problem is further discussed in Section 7.2.3.

Assessing the entrainment rate, E

The entrainment rate, *E* is the parameter in control of the entrainment algorithm in DAN3D. *E* is a difficult parameter to assess. Nevertheless, it is required as an input if entrainment is to be included in the modelling. The expected or desired final volume of the landslide is one of the parameters needed to calculate the entrainment rate. It is extremely difficult to assess the final volume, which includes the amount of material entrained. This is the main reason why the entrainment rate is so challenging to set. Obviously, this especially applies to forward analyses of unstable rock slopes, as in this thesis. When entrainment is to be included in a forward run-out analysis of an unstable rock slope, the challenges of assessing the entrainment rate should be taken into account if DAN3D are among the considered models. There might be models more suitable for the purpose.

Due to the challenges described in the above section, including difficulties in validating the results, the results of the analysis of the debris entrainment potential should be carefully considered. Back-calculation of a previous event, which is reported to have entrained significant volumes of debris, should be carried out as a part of further analyses of the entrainment potential. A back-calculation may lead to definitions of the entrainment rate that are more precise and enhance the understanding of the processes involved.

Run-out of entrainment events

The run-out distance is decreasing when entrainment of unsaturated material is included in the modelling (Table 7.3). The mobility of a rock avalanche were expected to enhance by entrainment (Hungr and Evans, 2004). From the study at Børa it may be seen that this is not the fact when entrained material is unsaturated (Table 7.3). The observed decrease in run-out distance might be caused by increased friction. However, entrainment of completely unsaturated scree material is most likely not realistic at Børa (Hermanns, 2017). The amount of scree material available for water saturation is significant and the climate generally wet. Thus, water will most likely be present. The amount will vary due to season and weather, and it is extremely difficult to assess a correct pore pressure ratio, as it is influenced by many factors. A pore pressure ratio in the scree deposits of between 0.25 – 0.5 are needed to obtain a run-out distance similar to the simulation without entrainment included (Table 6.22).

The increase in run-out when saturated material is entrained is consistent with Hungr and Evans (2004) assumptions (Table 7.3). The mobility of the landslide increases with increasing pore pressure ratio, r_u (Table 6.22). Run-out distance and the lateral spread of material increases. This is due to reduction of the frictional term (Equation 4.13, Equation 4.14). However, the change in the modelled final volume is quite small.

Table 7.3: Overview of modelled run-out and maximum velocity to compare results. Simulations run with Børa C and reference input parameters (Table 5.1, Table 5.5).

	Entrainment rate [m^{-1}]	Pore pressure ratio	Run-out [m]	Max. velocity [m/s]
Børa C	-	-	1448	37.3
Børa C	0.0012	-	1400	34.5
Børa C	0.0012	0.75	1522	53.6

The run-out of an entrainment event is highly sensitive to the friction angle, φ_b of the sliding scree deposits (Figure 6.16). Both the final volume and the run-out decrease with increasing values of the friction angle. This is consistent with Crosta et al. (2009), stating that modelled run-out distance is highly affected by the properties of the material entrained.

Modelled erosion depth compared to estimated debris thickness.

The run-out and modelled final volume are not sensitive to the set maximum erosion depth. Thus, this parameter seems to have no impact on the erosion process at Børa.

When trying to find an explanation to the run-out being completely insensitive to the set maximum erosion depth, the output erosion thickness was studied. When running the model with an input final volume increased by a factor 4, the modelled erosion depth was approximately 2 m (Figure 7.2).

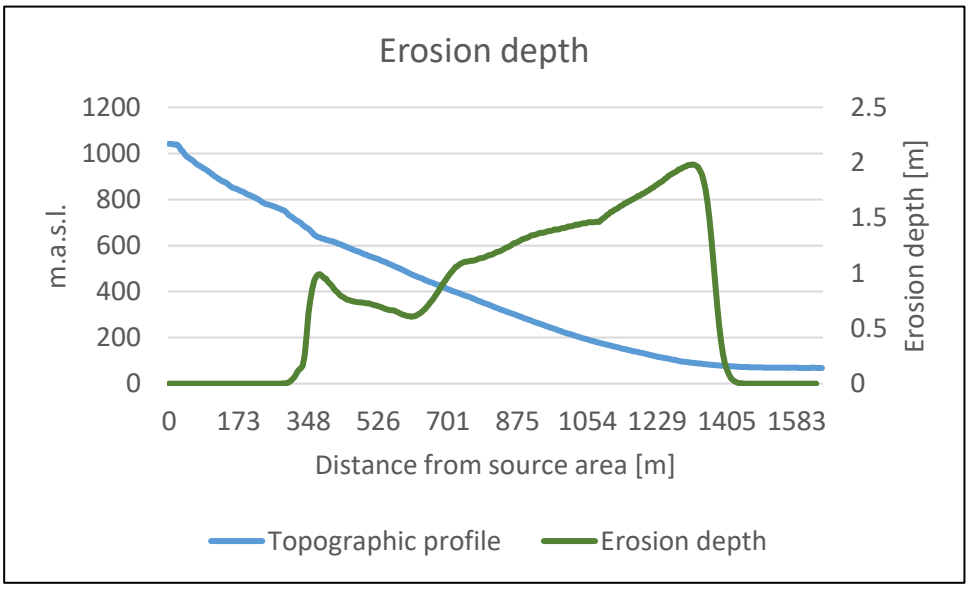

Figure 7.2: Modelled erosion depth. Erosion depth is found from output files from numerical run-out modelling in DAN3D (Simulation: E =0.0012 m^{-1}, r_u = 0.75).

Compared to the set maximum erosion depths of 40 and 20 m for the upper and lower debris zone respectively, this is extremely small (Figure 7.3). As the investigated values of maximum erosion depth were higher than the above-mentioned values, it is obvious that the run-out distance was insensitive to changes in this parameter. The input maximum erosion depth equals the estimated debris thickness from the SLBL analysis. Thus, the estimated thickness of debris available for entrainment and the modelled erosion depth are not in the same order of magnitude.

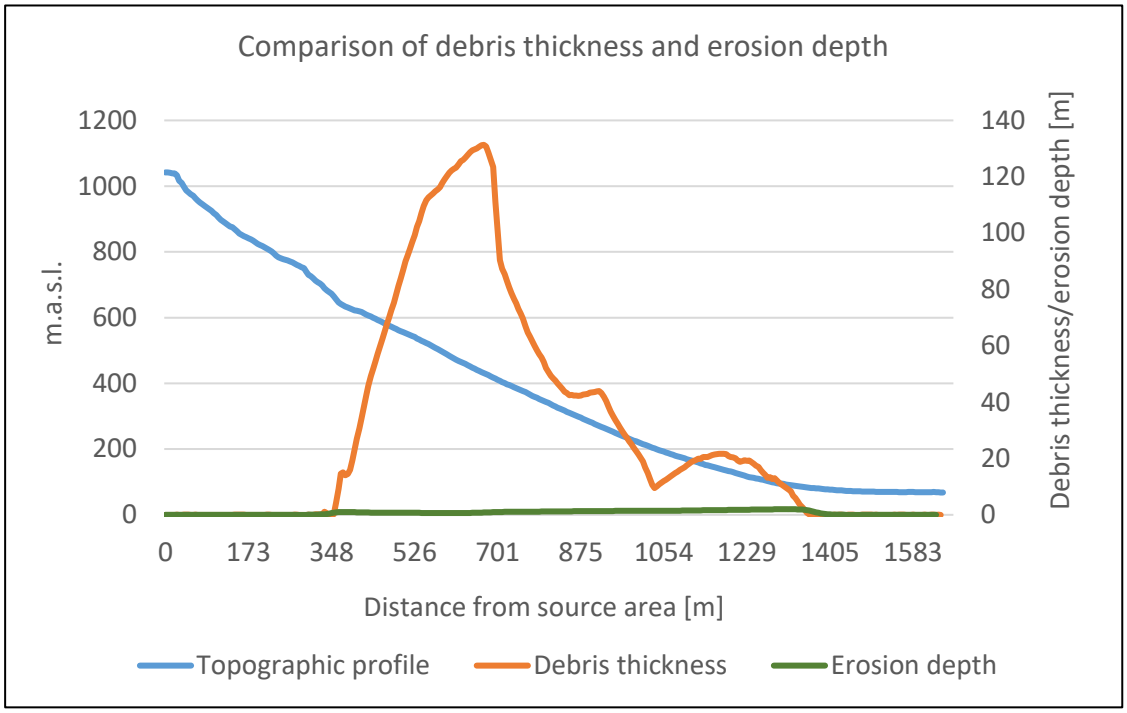

Figure 7.3: Comparison of estimated debris thickness and modelled erosion depth. Erosion depth is output from DAN3D (Simulation: E =0.0012 m^{-1}, r_u = 0.75).

Modelled final volume compared to expected final volume.

DAN3D requires expected final volume as an input in the build-in entrainment rate calculator. However, the expected final volumes are not obtained in the modelling of events at Børa. The modelled final volumes are generally smaller than the expected final volumes. To obtain a modelled final volume increased by a factor of four (E = 0.0012 m^{-1}), the input final volume should be increased by a factor of five (E = 0.0014 m^{-1}). Meaning that a higher entrainment rate than expected is necessary to obtain desired volume increase. The difference between the modelled and expected final volumes increases with increasing expected final volume. More analyses and back-calculations are needed to state the relation between expected and modelled final volume. Thus, the problem emphasize the disadvantages of the difficult parametrization of the entrainment rate.

Why is not the calculated final volume obtained when the entrainment rate is specified and set to reach the desired volume? The explanation might be found in the entrainment algorithm and the mathematics behind the model. Entrainment of material in DAN3D occurs when a particle is centered within a fixed grid cell containing erodible material (McDougall and Hungr, 2005). This could mean that material can only be entrained from a pixel once. When the masses are

propagating downslope, entrainment will only occur from a cell when the first particle reaches the particular cell. However, there might be other explanations. The shallow erosion depths definitely may be one of them.

Modelled volume entrained compared to estimated volume available for entrainment

As the volume of deposits at Børa is estimated, it is possible to compare the volume of deposits available for entrainment to the volume actually entrained. The difference between the estimated volume of deposits in the path (18 Mm^3) and the modelled volume of entrained material (0.20 Mm^3) is significant (Table 7.4). The difference between the estimated volumes in the area were entrainment actually occurs and the volume entrained (from the same area) is noticeable as well. Perhaps, this indicates that the entrainment potential at Børa are of a greater extent than expected. The expected volume increase is based on the study of the Loen and Tafjord events known to have entrained significant volumes. In this case, the entrainment rate, *E* should have been higher.

Table 7.4: Volume entrained (DAN3D) compared to volume available for entrainment (based on SLBL analysis). The areas used for calculation can be seen in Figure 6.21.

	Volume [Mm^3]
Path, (E=0.0012 m^{-1}, r_u= 0.75)	18
Path, (E=0.0012 m^{-1}, r_u= 0)	14
Area were entrainment occur, SLBL thickness	11
Area were entrainment occur, erosion depth DAN3D	0.17
Modelled volume increase, (final volume – initial volume)	0.20

The estimated volume based on the erosion depth in DAN3D (0.17 Mm^3) and the calculated volume increase based on initial and modelled finale volume (0.20 Mm^3) are in the same order of size. Indicating that the method applied for volume estimation provides reliable results.

The volume of material available for entrainment are much larger than the modelled volume of entrained material. It should be kept in mind that the volume of the scenario used for analyses of the entrainment potential at Børa is quite small (76 000 m^3). Thus, one could not expect

enormous volumes to be entrained. However, the estimated volume available for entrainment is based on the run-out and path of the particular scenario. Yet, the volumes are not corresponding. This is probably because of the shallow erosion depths modelled by DAN3D. Erosion depths of maximum 2 m are found for the simulation with $E = 0.0012$ m^{-1} and $r_u = 0.75$ (Figure 7.2). Otherwise, there might be limitations in the DAN3D entrainment algorithm.

Entrainment and presence of water at different elevations

The effect of entrainment from different elevations, i.e. parts of the slope, is assessed by allowing entrainment from one of the two scree deposit zones at the time. The run-out is slightly sensitive to where on the slope the material is entrained (Table 6.21, Table 6.23). Entrainment of unsaturated material from the upper part leads to longer run-outs compared to entrainment from the lower part. This indicates that entrainment from the lower part of the slope will decelerate the moving rock mass. However, the difference between the run-out distances is small, approximately 15 m. Thus, one could not emphasize the effect of the elevation at which entrainment of unsaturated material occur. In addition, entrainment of unsaturated material is not considered realistic at Børa (Hermanns, 2017).

The opposite is observed when saturated material ($r_u = 0.75$) is entrained. Entrainment of saturated material from the lower part of the slope leads to longer run-outs compared to entrainment from the upper part. When entrainment is allowed from both scree deposits zones, i.e. the entire slope, most material is entrained from the lower part of the slope (Figure 7.2). Comparing the final volumes obtained with modelling of entrainment from separated zones, one can see that more material is entrained when entrainment occurs in the lower part (Table 6.23). More saturated material entrained will decrease the friction component and enhance the mobility.

The results from simulations of an entrainment event at Børa indicate that entrainment of saturated material from the lower part of the slope will lead to longer run-out distances compared to entrainment from the upper part. However, it is difficult to determine if the run-out is longer because of physical processes or the fact that more material is entrained from the lower part.

7.2.3 Possible explanations to unrealistic output values

There are two main problems regarding the output values from the modelling of the scenarios at Børa. The output maximum velocities from the analyses of scenario Børa C Large and Børa B are high. Especially the results from Børa B reveal unrealistically high values of the maximum velocity (up to 2000 m/s). The second problem appeared when entrainment was included to the model. The output travel angles were observed to drop to extremely low values (0.003 – 0.016) making no sense. The developers of DAN and DAN3D, Oldrich Hungr and Scott McDougall were contacted in order to explain the problems.

The explanations to the problems are by Hungr (2017) and McDougall (2017) proposed to be found in the input grid files. The extremely high velocities may be caused by particles getting "lost in space" meaning that they are leaving the grid. This may be solved by expanding the grid and thereby avoid losing particles. As the answers were received close to the deadline of the thesis, this is not tested at Børa. However, the explanations may be useful for future users of DAN3D.

Problems (not similar to what is experienced here) have been seen when users do not zero the grid files, meaning that the lower left-hand corner is set to (0, 0) or some small number. To make optimum use of the available memory that DAN3D uses for calculations, this should be done (McDougall, 2017). The input files used in this analysis have UTM-coordinates, not local coordinates. DAN3D does not like the large real numbers on the coordinates, which may explain the problems (Hungr, 2017). However, only the results showing unrealistic values are considered being affected by this. The rest of the results are assumed reliable.

The input files are considered one of the main sources to errors, as they are complicated to produce. This is also emphasized in the master thesis by Frekhaug (2015).

7.2.4 Including results from fieldwork and laboratory work

Results from fieldwork are included in terms of the geomorphological map. Mapping of the geomorphological features at Børa was necessary to create the DAN3D input file dividing the slope in different materials. The file is required when entrainment are included in the modelling, which is one of the aims of the thesis. The extent of the scree deposits at Børa was also necessary to map in order to estimate the debris thickness and volume by the SLBL technique.

Including block size and block-form data from field and laboratory work carried out in the project was one of the proposed objectives of the study. It has been challenging to do this, and no systematic method is found. The idea was to divide the slope in sections based on the results, but as the modelling did not succeed with too complicated input files, this methods was rejected. The friction angle required when running the model with a frictional rheology is not the friction angle of the material. It is therefore difficult to include the measured block size and - form in the input parameters directly. By studying and analyzing the relation between the grainsize and –form and the friction angle of the moving masses, this could possibly be implemented in the modelling.

8 Conclusion

The debris entrainment potential of Norwegian rock avalanches is studied by numerical run-out modelling in DAN3D in combination with field observations. The study area is the unstable rock slope Børa, Romsdal Valley, western Norway.

The thickness and the volume of the scree deposits at Børa are estimated using the Sloping Local Base Level (SLBL) technique.

- The estimated total volume of scree deposits at Børa is 56 Mm^3. The volume is estimated by multiplying the summed thickness of deposits by the grid cell size. The thickness is found by dividing the slope in different polygons based on the chosen curvature. This leads to sudden jumps in curvature and thickness along the slope, affecting the estimate of the total volume. However, the volume is not required as direct input in the numerical modelling at any stage. Comparing the estimated volume to nearby similar slopes, the estimate is found to be in a sufficient order of size.
- The volume of debris in the extent of the landslide is estimated by using the debris thickness found from the SLBL analysis, in combination with DAN3D outputs showing the path. Thus, the same error is affecting these estimates. The estimated volume is 18 Mm^3 for the simulation with entrainment rate, E = 0.0012 m^{-1} and pore pressure ratio, r_u = 0.75.

Sensitivity analyses are carried out in order to determine reasonable input parameters and to assess the sensitivity of the run-out and maximum velocity to the different parameters. Sensitivity analyses are carried out on three scenarios at Børa: Børa C (76 000 m^3), Børa C Large (476 000 m^3) and Børa B (2.4 Mm^3).

- The input parameters applied by Schleier et al. (2015) are found to be sufficient for the studies at Børa. The assumed rheology is Voellmy, with μ = 0.15 and ξ =500 m/s^2. The simulations with these parameters are used as reference when assessing the sensitivity.
- The run-out is found to be sensitive to the Voellmy friction coefficient, μ and the friction angle, φ_b (frictional model). The run-out distance increases with decreasing values of the parameters. The run-out of the larger scenarios are slightly affected by changes in the Voellmy turbulence coefficient, ξ. None of the remaining input parameters in DAN3D are found to affect the modelled run-out distance. For the two smallest events, friction angles of 17°-20° replicate the run-outs obtained by the Voellmy rheology. Larger events probably require even smaller friction angles.

- The maximum velocity is sensitive to more parameters than the run-out. For scenario Børa C the velocity decreases with increasing values of μ, decreasing values of ξ and increasing friction angles, φ_b. When increasing the internal friction angle, the modelled maximum velocity significantly increases. The impact of the program parameters tested are small compared to the above-mentioned parameters. The modelled maximum velocities of the larger scenarios (Børa C Large and Børa B) are not considered reliable. Thus, no conclusion regarding the sensitivity is stated.

Further numerical run-out modelling in DAN3D is carried out to assess the effect of entrainment to the run-out distance and to study the factors influencing the entrainment potential. Scenario Børa C is used for this purpose.

- The run-out distance is found to decrease when unsaturated material is entrained. However, entrainment of completely unsaturated material is not considered realistic at Børa. On the other hand, Entrainment of saturated material enhance the mobility. Increasing the pore pressure leads to increased run-outs. When the pore pressure ratio is exceeding a value between 0.25 – 0.5 the run-out distance is longer compared to events of no entrainment.
- The effect of the elevation of the entrainment process is assessed. When entraining unsaturated material, entrainment from the upper part of the slope provides longer run-out distances. The opposite is observed for saturated material, meaning that entrainment from the lower part of the slope leads to longer run-outs. In addition, more material is entrained when material is entrained from the lower part. When entraining from the entire slope, one could see that most material is entrained from the lower part, even though the deposits are thicker in the upper part.
- The entrainment potential is highly affected by the friction angle, φ_b, in terms of both run-out distance and volume of debris entrained. Thus, the parameter should be carefully considered when parameters are determined. The run-out is also found to be sensitive to the pore pressure in the scree deposits. However, the volume of entrained material is not significantly affected by this parameter. The results implicates that the properties of the entrained material are of great importance to the entrainment potential and entrainments impact to the run-out.
- The maximum erosion depth was set based on estimation of debris thickness by the SLBL technique. The run-out and final volume are found to be insensitive to changes in this parameter. This is probably because the modelled erosion depths (2 m) are much

shallower than the estimated debris thickness (20 - 40 m). The expected final volumes of an event at Børa are not obtained with modelling in DAN3D. This may be caused by the above-mentioned problem.

- The difference between the estimated volume available for entrainment at Børa (18 Mm^3) and the modelled volumes of material entrained (0.17 Mm^3) are significant.

Entrainment in DAN3D is controlled by the user defined entrainment rate, *E*. The run-out distance is found to be insensitive to the parameter, but the lateral spread of the material increases with increasing *E*, because of the increased final volume. It is extremely difficult to assess the entrainment rate, as the expected final volume is required to calculate *E*. Knowledge about final volume is often limited in terms of a forward analysis. Thus, DAN3D will perhaps not constitute the most suitable tool for a forward analysis of an entrainment event.

9 Further work

Further work and analyses are needed in order to assess the debris entrainment potential of Norwegian events and the factors influencing the entrainment processes.

- First, a back-calculation of Norwegian event/events known to have entrained significant volumes of debris should be done. This is important in order to calibrate the model and to verify the results. In addition, a back calculation will reveal DAN3Ds ability to model entrained volumes of sufficient size, and what values of the entrainment rates that are needed to do so.
- Assess a range of pore pressure ratios suitable for modelling. As the run-out is sensitive to the pore pressure ratio in the material entrained, this is important in order to model realistic run-outs in the future. A warmer climate with more precipitation will result in more water in the scree slopes in the future, highlighting this problem.
- Study the influence of entrainment to run-out of the larger scenarios. An analysis similar to what is done for scenario Børa C should be carried out on Børa C Large and Børa B as well. This, to emphasize the effect of entrainment to larger volumes and detect if there are differences related to volume.
- Include results from laboratory tests and field work, in terms of block size and – form and their distribution on the slope. Possibly find a method to implement this in the input parameters in DAN3D. This will lead to modelled results taking the site specific debris conditions into account.
- Further sensitivity analysis. In the sensitivity analysis carried out in this thesis, one parameter is altered while the others are kept constant. Additionally, one may alter more than one parameter in each simulation to check how modelled run-out distance is affected. The Voellmy coefficients are well suited for the purpose. Altering the turbulence coefficient and friction coefficient simultaneously, may be useful to check the models sensitivity to this.

10 References

ABELE, G. 1974. Bergstürze in den Alpen. Wissenschaftliche Alpenvereinshefte, Number 25, Munich.

ABELE, G. 1997. Rockslide movement supported by the mobilization of groundwater-saturated valley floor sediments. *Zeitschrift fur geomorphologie,* 41**,** 1-20.

ALLABY, M. 2013. A Dictionary of Geology and Earth Sciences, 4th edition. *Dictionary of Geology and Earth Sciences.* Oxford University Press.

ANDA, E. & BLIKRA, L. H. 1998. Rock-avalanche hazard in Møre & Romsdal, western Norway. *Publication 203.* Norwegian Geotechnical Institute

ANDRESEN, M. L. 2015. *Mapping and characterization of debris material at the unstable rock slope Børa (Romsdal Valley, western Norway).* Project, The Norwegian University of Science and Technology (NTNU).

ARCGIS RESOURCE CENTER. 2016. *ArcGIS - Zonal Statistics* [Online]. Esri. Available: http://help.arcgis.com/EN/ArcGISDesktop/10.0/Help/index.html#//009z000000w8000000.htm [Accessed 06.04 2016].

BLIKRA, L. H., ANDA, E. & LONGVA, O. 1999. Fjellskredprosjektet i Møre og Romsdal: Status og planer. *NGU Report 99.120.* Trondheim, Norway: The Geological Survey of Norway.

BLIKRA, L. H., BRAATHEN, A., ANDA, E., STALSBERG, K. & LONGVA, O. 2002. Rock avalanches, gravitational fractures and neotectonic faults onshore northern West Norway: Examples, regional distribution and triggering mechanisms. *NGU Report 2002.016.* Geological Survey of Norway.

BLIKRA, L. H., BRAATHEN, A. & SKURTVEIT, E. 2001. Hazard evaluation of rock avalanches : the Baraldsnes - Oterøya area. *NGU Report 2001.108.* Trondheim: Geological Survey of Norway.

BOWMAN, E. T., TAKE, W. A., RAIT, K. L. & HANN, C. 2012. Physical models of rock avalanche spreading behaviour with dynamic fragmentation. *Canadian Geotechnical Journal,* 49**,** 460-476.

BRAATHEN, A., BLIKRA, L. H., BERG, S. S. & KARLSEN, F. 2004. Rock-slope failures in Norway; type, geometry, deformation mechanisms and stability. *Norsk Geologisk Tidsskrift,* 84**,** 67-88.

BRATTLI, B. 2015. *Ingeniørgeologi Løsmasser,* Trondheim, NTNU, Institutt for geologi og bergteknikk.

BUSS, E. & HEIM, A. 1881. Der Bergsturz von Elm: Zurich. *Worster, 133p*.

CAMPBELL, C. S. 1989. Self-lubrication for long runout landslides. *The Journal of Geology,* 97**,** 653-665.

CHEN, H. & LEE, C. F. 2000. Numerical simulation of debris flows. 37**,** 146-160.

CHRISTEN, M., KOWALSKI, J. & BARTELT, P. 2010. RAMMS: Numerical simulation of dense snow avalanches in three-dimensional terrain. *Cold Regions Science and Technology,* 63**,** 1-14.

COROMINAS, J. 1996. The angle of reach as a mobility index for small and large landslides. *Canadian Geotechnical Journal,* 33**,** 260-271.

CROSTA, G. B., IMPOSIMATO, S. & RODDEMAN, D. 2009. Numerical modelling of entrainment/deposition in rock and debris-avalanches. *Engineering Geology,* 109**,** 135-145.

CROSTA, G. B., IMPOSIMATO, S. & RODDEMAN, D. G. 2003. Numerical modelling of large landslides stability and runout. *Nat. Hazards Earth Syst. Sci.,* 3**,** 523-538.

CRUDEN, D. M. & VARNES, D. J. 1996. Landslide types and processes. *In:* A.K., T. & SCHUSTER, R. L. (eds.) *Landslides: Investigation and mitigation. (Special Report).* Washington, DC, USA: National Research Council, Transportation and Research Board.

DAHLE, H., ANDA, E., SAINTOT, A. & SÆTRE, S. 2008. Faren for fjellskred fra fjellet Mannen i Romsdalen. *NGU Report 2008.087.* Trondheim: Geological Survey of Norway.

DALSEGG, E. & TØNNESEN, J. F. 2004. Geofysiske målinger Breitind og Børa, Rauma kommune Møre og Romsdal. *NGU Report 2004.008.* Norges geologiske undersøkelse.

DAVIES, T. & MCSAVENEY, M. 1999. Runout of dry granular avalanches. *Canadian Geotechnical Journal,* 36**,** 313-320.

DAVIES, T. R. & MCSAVENEY, M. J. 2002. Dynamic simulation of the motion of fragmenting rock avalanches. *Canadian Geotechnical Journal,* 39**,** 789-798.

DAVIES, T. R. & MCSAVENEY, M. J. 2012. Mobility of long-runout rock avalanches. *In:* CLAGUE, J. J. & STEAD, D. (eds.) *Landslides: Types, Mechanisms and Modeling.* Cambridge: Cambridge Univeristy Press.

DAVIES, T. R., MCSAVENEY, M. J. & HODGSON, K. A. 1999. A fragmentation-spreading model for long-runout rock avalanches. *Canadian Geotechnical Journal,* 36**,** 1096-1110.

DERRON, M. H., JABOYEDOFF, M. & BLIKRA, L. 2005. Preliminary assessment of rockslide and rockfall hazards using a DEM (Oppstadhornet, Norway). *Natural Hazards and Earth System Sciences,* 5**,** 285-292.

DOMAAS, U. & GRIMSTAD, E. 2014. Fjell- og steinskred. *In:* HØEG, K., KARLSRUD, K. & LIED, K. (eds.) *Skred, skredfare og sikringstiltak.* Oslo, Norway: NGI, Universitetsforlaget.

DSB 2013. Nasjonalt risikobilde - Katastrofer som kan ramme det norske samfunnet Direktoratet for samfunnssikkerhet og beredskap.

DUNNING, S. A. & ARMITAGE, P. J. 2011. Chapter 19: The Grain-Size Distribution of Rock-Avalanche Deposits: Implications for Natural Dam Stability. *In:* EVANS, S. G., HERMANNS, R. L., STROM, A. & SCARASCIA-MUGNOZZA, G. (eds.) *Natural and Artificial Rockslide Dams.* Berlin, Heidelberg: Springer Berlin Heidelberg.

EBERHARDT, E. 2006. From cause to effect: Using numerical modelling to understand rock slop instability nechanisms. *In:* EVANS, S. G., MUGNOZZA, G. S., STROM, A. & HERMANNS, R. L. (eds.) *Landslides from Massive Rock Slope Failure.* Dordrecht, The Netherlands: Springer.

ERISMANN, T. 1979. Mechanisms of large landslides. *Rock Mechanics,* 12**,** 15-46.

EVANS, G. S., MUGNOZZA, G. S., STROM, G. S., HERMANNS, G. S., ISCHUK, G. S. & VINNICHENKOS, G. S. 2006. Landslides from massive rock slope failure and associated phenomena. *Landslides,* 49**,** 3-52.

EVANS, S. G., BISHOP, N. F., FIDEL SMOLL, L., VALDERRAMA MURILLO, P., DELANEY, K. B. & OLIVER-SMITH, A. 2009. A re-examination of the mechanism and human impact of catastrophic mass flows originating on Nevado Huascarán, Cordillera Blanca, Peru in 1962 and 1970. *Engineering Geology,* 108**,** 96-118.

FARSUND, T. O. 2010. *Geology, DEM analysis and geohazard assessment of the Romsdalen valley. .* Project, NTNU.

FLO-2D SOFTWARE INC. 2007. FLO-2D User's Manual. Version 2007.06.

FREKHAUG, M. H. 2015. *An assessment of prediction tools to Norwegian debris flows.* Master, Norwegian University of Science and Technology.

FURSETH, A. 1995. *Dommedagsfjellet : Tafjord 1934,* Valldal, A. Furseth.

GOGUEL, J. & PACHOUD, A. 1972. Geology and dynamics of the rockfall of the Granier Range which occurred in November 1248. *Bulletin, Bureau de Récherches Geologiques et Miniéres, Hydrogeologie, Lyon,* 1**,** 29-38.

GRIMSTAD, E. & NESDAL, S. 1990. *The Loen rockslides : a historical review,* Oslo, Norges geotekniske institutt.

HEIM, A. 1932. *Bergsturz und menschenleben,* Zurich, Switzerland, Fretz & Wasmuth.

HELLER, V., HAGER, W. H. & MINOR, H.-E. 2009. Landslide generated impulse waves in reservoirs; basics and computation. *Mitteilungen der Versuchsanstalt fuer Wasserbau, Hydrologie und Glaziologie der Eidgenoessischen Technischen Hochschule Zuerich,* 211.

HERMANNS, R. L. 23.03.2017 2017. *RE: Water content in scree deposits.*

HERMANNS, R. L., BLIKRA, L. H., NAUMANN, M., NILSEN, B., PANTHI, K. K., STROMEYER, D. & LONGVA, O. 2006. Examples of multiple rock-slope collapses from Köfels (Ötz valley, Austria) and western Norway. *Engineering Geology,* 83**,** 94-108.

HERMANNS, R. L. & LONGVA, O. 2012. Rapid rock-slope failures. *In:* CLAGUE, J. J. & STEAD, D. (eds.) *Landslides: types, mechanisms and modeling.* Cambridge University Press. .

HERMANNS, R. L., OPPIKOFER, T., BLIKRA, L. H., BÖHME, M., BUNKHOLT, H., FISCHER, L., MOLINA, F. X. Y., ANDA, E., CROSTA, G. B., DAHLE, H., DEVOLI, G., JABOYEDOFF, M., LOEW, S. I. & SÆTRE, S. 2013. Hazard and risk classification for large unstable rock slopes in Norway. *Italian Journal of Engineering Geology and Environment,* 2013**,** 245-254.

HERMANNS, R. L., OPPIKOFER, T., MOLINA, F. X. Y., DEHLS, J. F. & BÖHME, M. 2014. Approach for systematic rockslide mapping of unstable rock slopes in Norway. *Landslide Science for a Safer Geoenvironment.* Springer.

HSÜ, K. 1975. Catastrophic debris streams (sturzstorms) generated by rockfalls. *Geological Society of America Bulletin,* 86**,** 123-140.

HUNGR, O. 1995. A model for the runout analysis of rapid flow slides, debris flows and avalanches. *Can. Geotech. J.,* 32**,** 610-623.

HUNGR, O. 2010. DAN3D - Dynamic Analysis of Landslides in Three Dimensions. User Manual. . Vancouver, Canada: O. Hungr Geotechinical Engineering.

HUNGR, O. 2017. *RE: Personal communication: DAN3D - Possible explanations to unrealistic output values.*

HUNGR, O. & EVANS, S. G. 2004. Entrainment of debris in rock avalanches; an analysis of a long run-out mechanism. *Geological Society of America Bulletin,* 116**,** 1240-1252.

HUNGR, O., LEROUEIL, S. & PICARELLI, L. 2014. The Varnes classification of landslide types, an update. *Journal of the International Consortium on Landslides,* 11**,** 167-194.

HUNGR, O. & MCDOUGALL, S. 2009. Two numerical models for landslide dynamic analysis. *Comput. Geosci.,* 35**,** 978-992.

HUTCHINSON, J. N. 1983. Methods of locating slip surfaces in landslides. *Bulletin of the Association of Engineering Geologists.,* 20**,** 35-252.

JABOYEDOFF, M., BAILLIFARD, F., COUTURE, R., LOCAT, J. & LOCAT, P. 2004. Toward preliminary hazard assessment using DEM topographic analysis and simple mechanical modeling by means of sloping local base level. *In:* LACERDA, W. A., EHRLICH, M., FONTOURA, A. B. & SAYAO, A. (eds.) *Landslides: Evaluation and Stabilization.* Proceedings of the Ninth International Symposium on Landslides, June 28 -July 2, 2004 Rio de Janeiro, Brazil ed. London: Taylor & Francis Group.

JABOYEDOFF, M., COUTURE, R. & LOCAT, P. 2009. Structural analysis of Turtle Mountain (Alberta) using digital elevation model: Toward a progressive failure. *Geomorphology,* 103**,** 5-16.

JABOYEDOFF, M. & DERRON, M.-H. 2005. A new method to estimate the infilling of alluvial sediment of glacial valleys using a sloping local base level. *Geografice Fisica e Dinamika Quaternaria,* 28**,** 37-46.

JABOYEDOFF, M., DERRON, M. H., RUDAZ, B., OPPIKOFER, T., PENNA, I. & DAICZ, S. 2015. A review of geometrical methods for determination of landslide volume and failure surface geometry. *GEOQuébec 2015: Challenges from North to South.* Québec, Canada.

KWAN, J. & SUN, H. W. 2007. Benchmarking exercise on landslide mobility modelling: runout analyses uding 3dDMM. *In:* HO, K. & V., L. (eds.) *Proceedings of the 2007 International Forum on Landslide Disaster Management.* Hong Kong Geotechnical Engineering Office.

LIED, K. 2014. Innledning og historikk. *In:* LIED, K., KARLSRUD, K. & HØEG, K. (eds.) *Skred, skredfare og sikringstiltak.* Oslo, Norway: NGI. Universitetsforlaget.

MANGENEY-CASTELNAU, A., VILOTTE, J. P., BRISTEAU, M. O., PERTHAME, B., BOUCHUT, F., SIMEONI, C. & YERNENI, S. 2003. Numerical modeling of avalanches based on Saint Venant equations using a kinetic scheme. *Journal of Geophysical Research: Solid Earth,* 108**,** n/a-n/a.

MCDOUGALL, S. 2006. *A new continuum dynamic model for the analysis of extremely rapid landslide motion across complex 3D terrain.* Ph.D: Doctor of Philosophy, The University of British Columbia.

MCDOUGALL, S. 2017. *RE: Peronal communication: DAN3D - Possible explanations to unrealistic output values.*

MCDOUGALL, S. & HUNGR, O. 2004. A model for the analysis of rapid landslide motion across three-dimensional terrain. *Canadian Geotechnical Journal,* 41**,** 1084-1097.

MCDOUGALL, S. & HUNGR, O. 2005. Dynamic modelling of entrainment in rapid landslides. *Canadian Geotechnical Journal,* 42**,** 1437-1448.

MCDOUGALL, S., MCKINNON, M. & HUNGR, O. 2012. Developments in landslide runout prediction. *In:* CLAGUE, J. J. & STEAD, D. (eds.) *Landslides: Types, Mechanisms and Modeling.* Cambridge: Cambridge University Press.

MCKINNON, M., HUNGR, O. & MCDOUGALL, S. 2008. Dynamic Analyses of Canadian Landslides. *In:* LOCAT, J., PERRET, D., TURMEL, D., DEMERS, D. & LEROUEIL, S. (eds.) *The 4th Canadian Conference on Geohazards: From Causes to Management.* Québec: Presse de l'Université.

MEDINA, V., HÜRLIMANN, M. & BATEMAN, A. 2008. Application of FLATModel, a 2D finite volume code, to debris flows in the northeastern part of the Iberian Peninsula. *Journal of the International Consortium on Landslides,* 5**,** 127-142.

MELOSH, H. J. 1979. Acoustic fluidization: A new geologic process? *Journal of Geophysical Research: Solid Earth,* 84**,** 7513-7520.

MOLINA, F. X. Y., BUNKHOLT, H. S., KRISTENSEN, L., DEHLS, J. & HERMANNS, R. L. 2015. The Use of Remote Sensing Techniques and Runout Analysis for Hazard Assessment of an Unstable Rock Slope at Storhaugen, Manndalen, Norway. *Engineering Geology for Society and Territory-Volume 2.* Springer.

MYRVANG, A. 2001. *Bergmekanikk,* Trondheim, Institutt for geologi og bergteknikk, NTNU.

NGU. 2015a. *Quaternary geology* [Online]. Geological Survey of Norway. Available: http://geo.ngu.no/kart/losmasse/ [Accessed 15.11 2015].

NGU. 01.06.2015 2015b. *RE: Ustabile fjellparti - Hovedpunkt Børa.*

NICOLETTI, P. G. & SORRISO-VALVO, M. 1991. Geomorphic controls of the shape and mobility of rock avalanches. *Geological Society of America Bulletin,* 103**,** 1365-1373.

NIGUSSIE, D. G. 2013. Numerical modelling of run-out of sensitive clay slide debris.

NILSEN, G. 2016. *Paraglasiale prosesser på Gråhøa, Sunndal, Norge - En studie i geomorfologiske prosesser på ustabile fjellparti.* Masteroppgave, Norges teknisk-naturvitenskapelige universitet.

NORDGULEN, Ø. & ANDRESEN, A. 2006. Kap. 3: Jordas Urtid - De eldste bergarter dannes. *In:* RAMBERG, I. B., BRYHNI, I. & NØTTVEDT, A. (eds.) *Landet blir til - Norges geologi.* Trondheim: Norsk Geologisk Forening.

NVE 2009. Fjellskredfare ved Mannen i Romsdalen. *In:* HALLGEIR DAHLE, M. O. R. F. (ed.) *Dokumentserien 2009.* Norwegian Water Resources and Energy Directorate (NVE).

OPPIKOFER, T. 2008. Åknes/Tafjord Project: Analysis of ancient rockslide scars and potential instabilities in the Tafjord area & Laser scanner monitoring of

instabilities at Hegguraksla. . *Faculty of Geosciences and Environment, Institute of Geomatics and Risk Analysis.* University of Lausanne.

OPPIKOFER, T. 02.03 2016a. *RE: Volume estimation of debris - SLBL*

OPPIKOFER, T. 28.01 2016b. *RE: Volume estimation of scenarios at Børa.*

OPPIKOFER, T., BÖHME, M., NICOLET, P., PENNA, I. & HERMANNS, R. L. 2016a. Metodikk for konsekvensanalyse av fjellskred. *NGU Report 2016.047.* Trondheim: Geological Survey of Norway.

OPPIKOFER, T., HERMANNS, R., L, REDFIELD, T., F. , SEPÚLVEDA, S., A. , DUHART, P. & BASCUÑÁN, I. 2012. Morphologic description of the Punta Cola rock avalanche and associated minor rockslides caused by the 21 April 2007 Aysén earthquake (Patagonia, southern Chile) Descripción morfológica de la avalancha de rocas de Punta Cola y deslizamientos de rocas asociados causados por el terremoto de Aysén del 21 de abril de 2007 (Patagonia, sur de Chile). *Revista de la Asociación Geológica Argentina,* 69**,** 339.

OPPIKOFER, T., HERMANNS, R. L., SANDØY, G., BÖHME, M., JABOYEDOFF, M., HORTON, P., ROBERTS, N. J. & FUCHS, H. 2016b. Quantification of casualties from potential rock-slope failures in Norway. *Paper presented at the 12th International Symposium on Landslides, Napoli, Italy*.

OPPIKOFER, T., NORDAHL, B., BUNKHOLT, H., NICOLAISEN, M., JARNA, A., IVERSEN, S., HERMANNS, R. L., BÖHME, M. & YUGSI MOLINA, F. X. 2015. Database and online map service on unstable rock slopes in Norway — From data perpetuation to public information. *Geomorphology,* 249**,** 69-81.

OPPIKOFER, T., SAINTOT, A., OTTERÅ, S., HERMANNS, R. L., ANDA, E., DAHLE, H. & EIKEN, T. 2013. Investigations on unstable rock slopes in Møre og Romsdal - status and plans after field surveys in 2012. *NGU Report 2013.014.* Geological Survey of Norway.

PASTOR, M., HADDAD, B., SORBINO, G., CUOMO, S. & DREMPETIC, V. 2009. A depth-integrated, coupled SPH model for flow-like landslides and related phenomena. *International Journal for Numerical and Analytical Methods in Geomechanics,* 33**,** 143-172.

PEDRAZZINI, A., FROESE, C. R., JABOYEDOFF, M., HUNGR, O. & HUMAIR, F. 2012. Combining digital elevation model analysis and run-out modeling to characterize hazard posed by a potentially unstable rock slope at Turtle Mountain, Alberta, Canada. *Engineering Geology,* 128**,** 76-94.

PEDRAZZINI, A., JABOYEDOFF, M., LOYE, A. & DERRON, M.-H. 2013. From deep seated slope deformation to rock avalanche: Destabilization and transportation models of the Sierre landslide (Switzerland). *Tectonophysics,* 605**,** 149-168.

PENNA, I. 28.01 2016. *RE: Rheology in DAN3D.*

PIRULLI, M. 2005. *Numerical modelling of landslide runout: A continuum mechanics approach.* Ph. D., Politechnico di Torino, Italy.

PIRULLI, M. & MANGENEY, A. 2008. Results of Back-Analysis of the Propagation of Rock Avalanches as a Function of the Assumed Rheology. *Rock Mechanics and Rock Engineering,* 41**,** 59-84.

PITMAN, E. B., NICHITA, C. C., PATRA, A., BAUER, A., SHERIDAN, M. & BURSIK, M. 2003. Computing granular avalanches and landslides. *Physics of Fluids,* 15**,** 3638-3646.

POISEL, R. & PREH, A. 2008. 3D landslide runout modelling using the particle flow code PFC3D. *In:* CHEN, Z., ZHANG, J., LI, Z., WU, F. & HO, K. (eds.) *Proceeding of the 10th International Symposium on Landslides and Engineered Slopes.* London: Taylor and Francis.

POWERS, M. C. 1953. A new roundness scale for sedimentary particles. *Journal of Sedimentary Petrology,* 23**,** 117-119.

RODDEMAN, D. G. 2002. *TOCHNOG User Manual: A Free Explicit/Implicit FE Program* [Online]. FEAT. Available: http://www.feat.nl/manuals/ [Accessed 21.03.2017].

SAINTOT, A., OPPIKOFER, T., DERRON, M.-H. & HENDERSON, I. 2012. Large gravitational rock slope deformation in Romsdalen Valley (Western Norway) Deformación gravitacional de las vertientes rocosas del valle de Romsdalen (Noruega occidental). *Revista de la Asociación Geológica Argentina,* 69**,** 354.

SASSA, K. 1985. The mechanism of debris flows. *XI International Conference on Soil Mechanics and Foundation Engineering.* San Francisco, California.

SCHEIDEGGER, A. 1973. On the prediction of the reach and velocity of catastrophic landslides. . *Rock Mechanics,* 5**,** 231-236.

SCHEIDEGGER, A. E. 1975. Physical aspects of natural catastrophes. *Elsevier Science Publishing Co.* New York.

SCHLEIER, M., HERMANNS, R. L., ROHN, J. & GOSSE, J. C. 2015. Diagnostic characteristics and paleodynamics of supraglacial rock avalanches, Innerdalen, Western Norway. *Geomorphology,* 245**,** 23-39.

SHREVE, R. L. 1968. The blackhawk landslide. *Geological Society of America Special Papers,* 108**,** 1-48.

SINTEF. 2015. *Typiske materialdata for naturstein - tetthet gneis* [Online]. Available: https://sintef.no/globalassets/upload/teknologi_og_samfunn/berg-og-geoteknikk/lister/typiske-materialdata-for-naturstein.pdf [Accessed 29.11 2015].

SOLLID, J. L. & KRISTIANSEN, K. 1984. *Raumavassdraget, Kvartærgeologi og geomorfologi 1 : 80 000*. Geografisk Institutt, Universitetet i Oslo.

SOSIO, R., CROSTA, G. B. & HUNGR, O. 2008. Complete dynamic modeling calibration for the Thurwieser rock avalanche (Italian Central Alps). *Engineering Geology,* 100**,** 11-26.

TRAVELLETTI, J., DEMAND, J., JABOYEDOFF, M. & MARILLIER, F. 2010. Mass movement characterization using a reflexion and refraction seismic survey with the sloping local base level concept. *Geomorphology,* 116**,** 1-10.

TVETEN, E., LUTRO, O. & THORSNES, T. 1998. *Berggrunnsgeologisk kart M 1:250 000 Ålesund*. Trondheim: NGU.

VOELLMY, A. 1955. Über die Zerstörungskraft von Lawinen. *Schweizerische Bauzeitung***,** 159.

WANG, F. W. & SASSA, K. 2002. A modified geotechnical simulation model for the areal prediction of landslide motion *Proceedings of the First European Conference on Landslides.*

WANG, X. 2008. Geotechnical analysis of flow slides, debris flows, and related phenomena. University of Alberta Libraries.

11 Appendix

Appendix I: Estimation of debris thickness and volume – SLBL profiles

Appendix II: Estimation of debris thickness and volume – Curvature, Δz

Appendix III: Sensitivity analysis – complete results

Appendix IV: Analyses of entrainment – complete results

Appendix V: Analyses of entrainment – maps with results from small entrainment rates

11.1 Appendix I

Estimation of debris thickness and volume – SLBL profiles.

Computed profiles from the SLBL analysis. The profiles are used to assess curvature, Δz for each scree deposit zone along the profile lines. Curvature is needed when estimating the debris thickness. Profile 1 to 6 are presented below. The location of each profile can be seen in Figure 5.2.

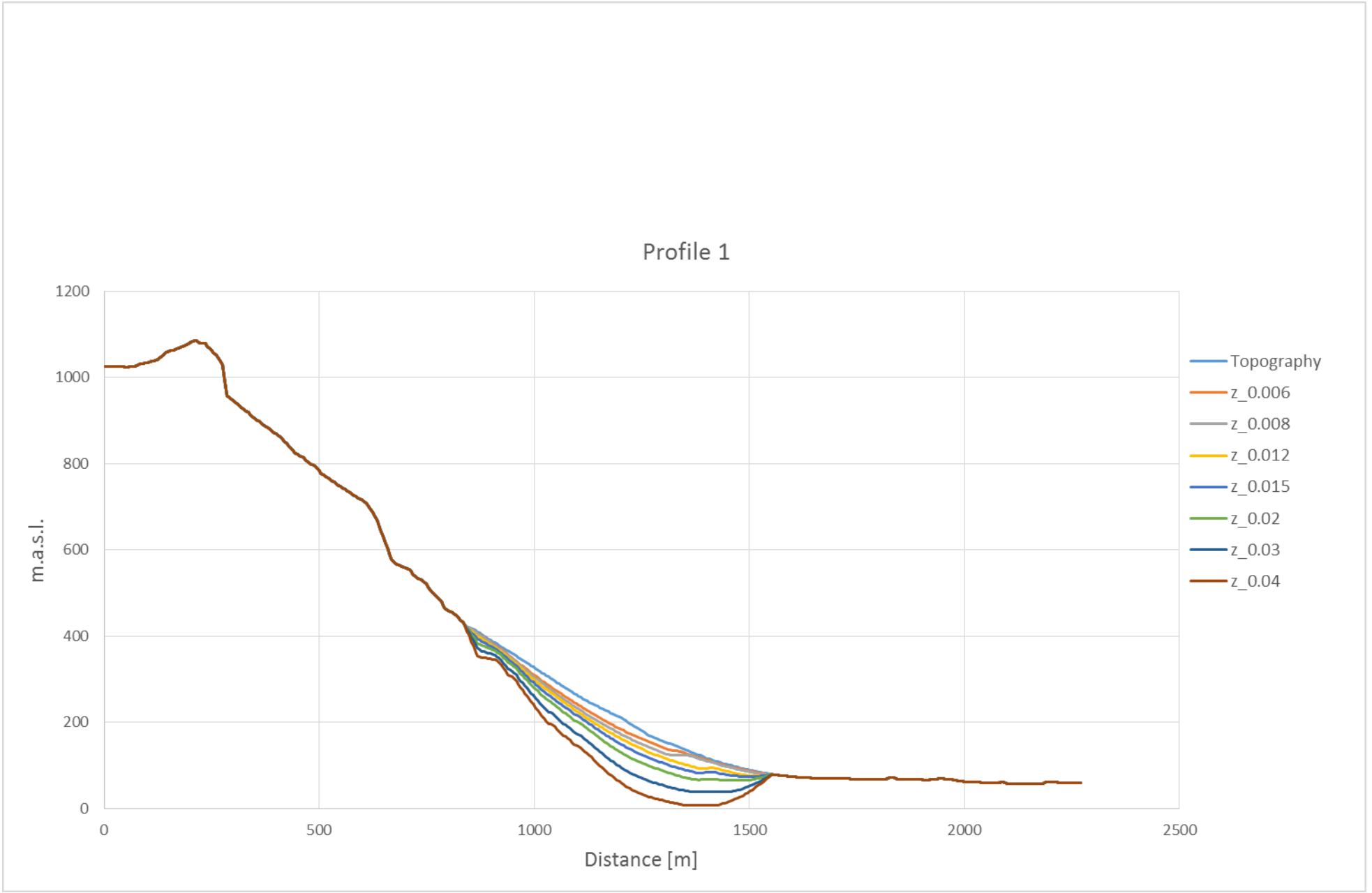
Profile 1
1200
1000
800
600
400
200
0
m.a.s.l.
0
500
1000
1500
2000
2500
Distance [m]
Topography
z_0.006
z_0.008
z_0.012
z_0.015
z_0.02
z_0.03
z_0.04

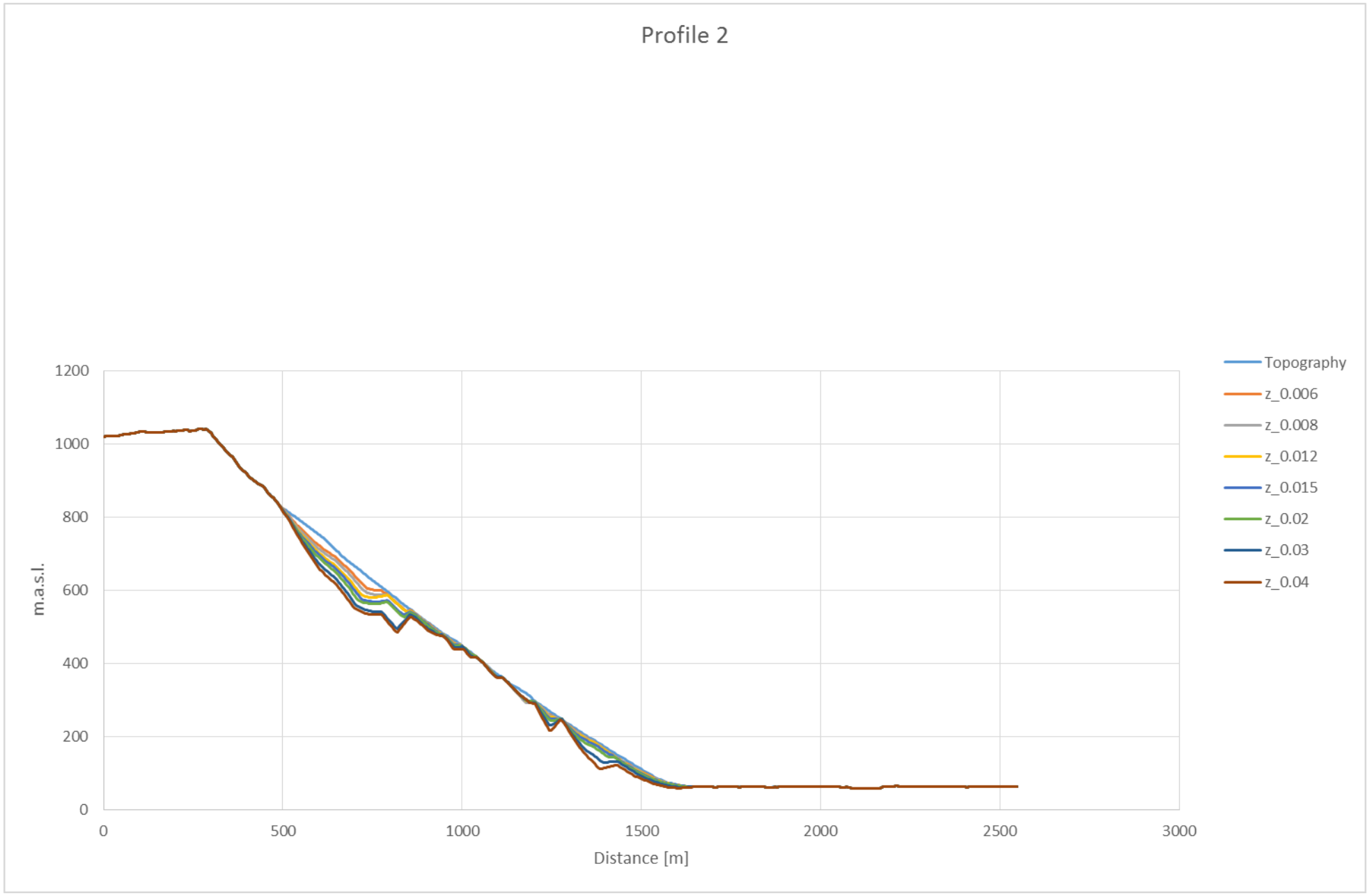
Profile 2
1200
1000
800
600
400
200
0
m.a.s.l.
0
500
1000
1500
2000
2500
3000
Distance [m]
Topography
z_0.006
z_0.008
z_0.012
z_0.015
z_0.02
z_0.03
z_0.04

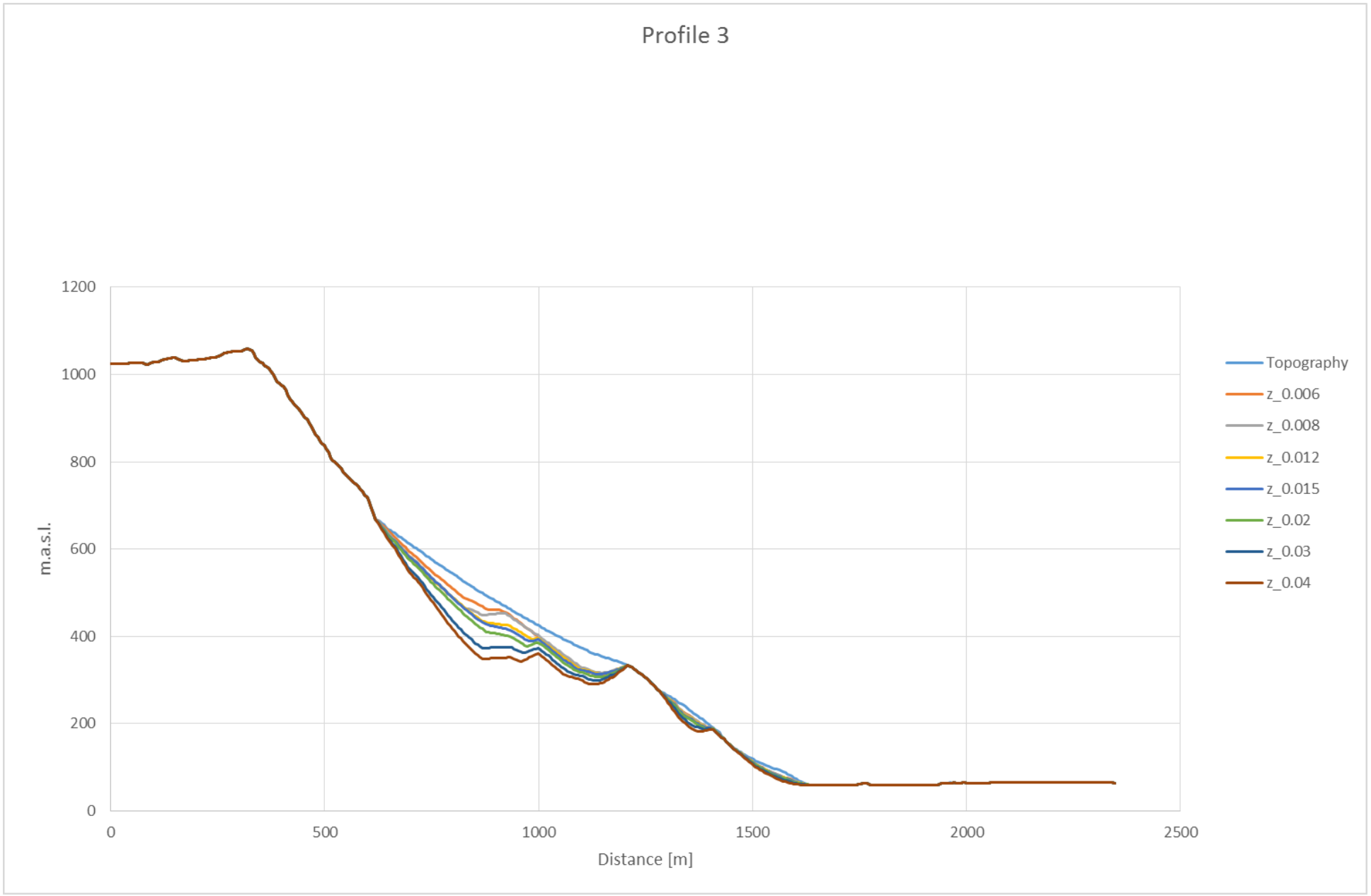
Profile 3
1200
1000
800
600
400
200
0
m.a.s.l.
0
500
1000
1500
2000
2500
Distance [m]
Topography
z_0.006
z_0.008
z_0.012
z_0.015
z_0.02
z_0.03
z_0.04

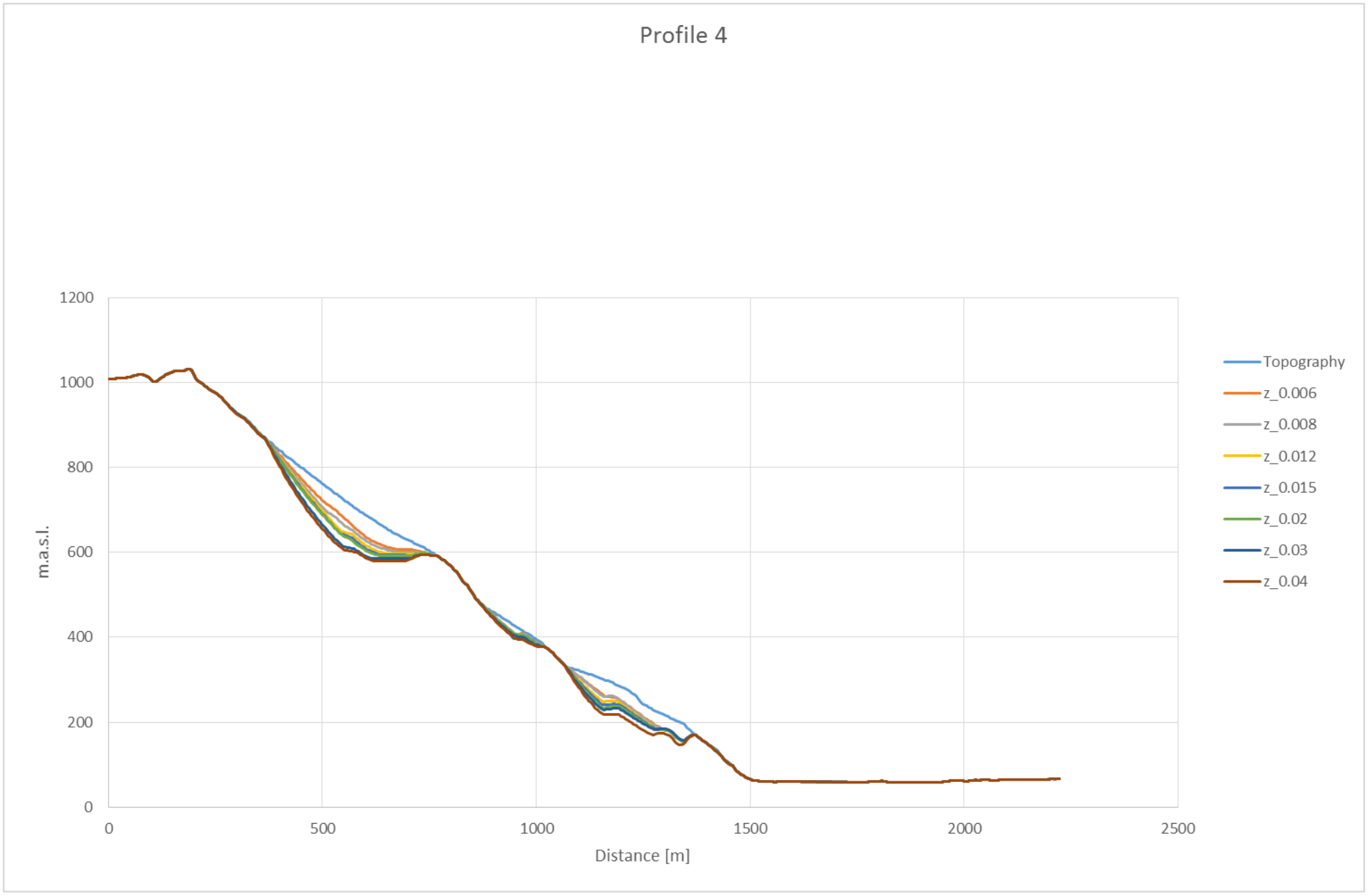
Profile 4
1200
1000
800
600
400
200
0
m.a.s.l.
0
500
1000
1500
2000
2500
Distance [m]
Topography
z_0.006
z_0.008
z_0.012
z_0.015
z_0.02
z_0.03
z_0.04

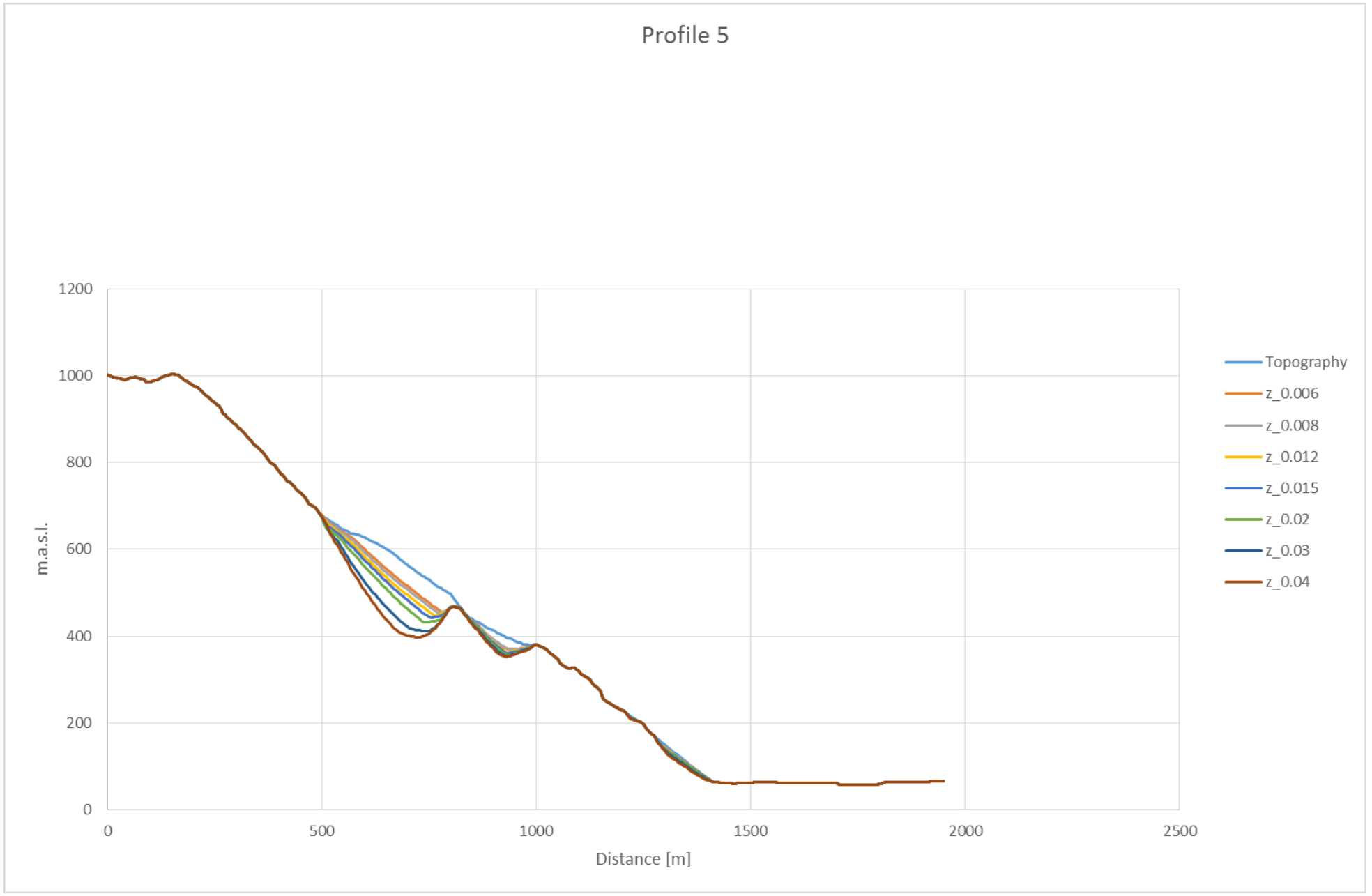
Profile 5
1200
1000
800
600
400
200
0
m.a.s.l.
0
500
1000
1500
2000
2500
Distance [m]
Topography
z_0.006
z_0.008
z_0.012
z_0.015
z_0.02
z_0.03
z_0.04

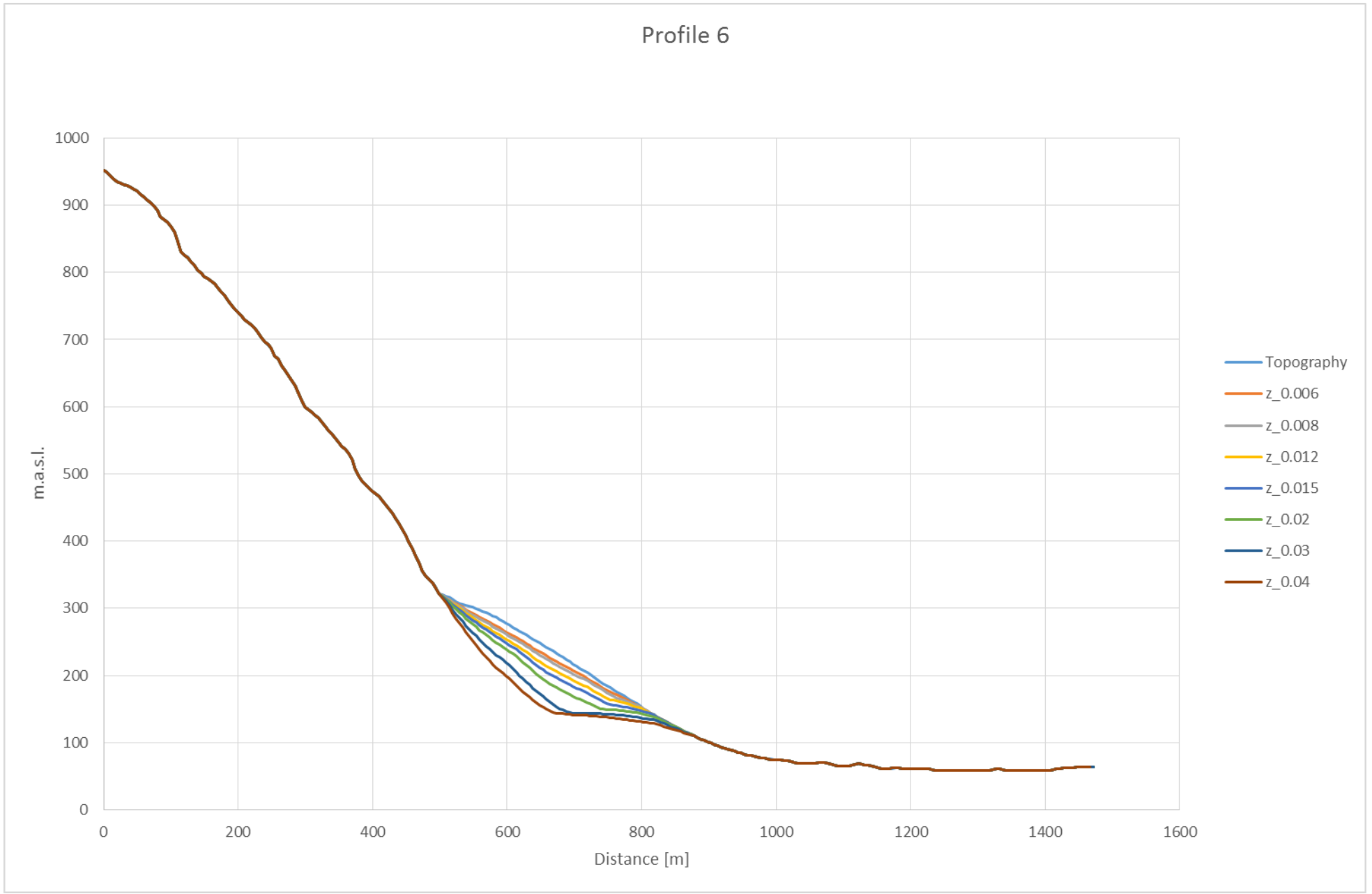
Profile 6
m.a.s.l.
1000
900
800
700
600
500
400
300
200
100
0
0
200
400
600
800
1000
1200
1400
1600
Distance [m]
Topography
z_0.006
z_0.008
z_0.012
z_0.015
z_0.02
z_0.03
z_0.04

11.2 Appendix II

Estimation of debris thickness and volume – Curvature, *Δz*.

Table showing max, min and mean curvature for the scree deposit zones. For location of profiles see Figure 5.2.

Profile	Scree deposit zone	Length of zone [m]	Δz_min	Δz_average	Δz_max
1	1	710	0.006	0.012	0.017
2	1	774	0.015	0.02	0.03
	2	370	0.03	0.04	0.05
3	1	605	0.012	0.02	0.03
	2	134	0.008	0.02	0.025
	3	184	0.02	0.03	0.04
4	1	387	0.005	0.006	0.008
	2	162	0.006	0.02	0.03
	3	430	0.015	0.03	0.04
5	1	481	0.006	0.006	0.008
	2	84	0.006	0.008	0.012
	3	149	0.03	0.04	0.05
6	1	391	0.012	0.015	0.02

11.3 Appendix III

Results from analysis of the sensitivity of input parameters to the modelled run-out distance.

Scenario Børa C, V = 76000 m^3

Børa C																	
Volume [m^3]	75567.5																
Elevation crown, [m.a.s.l.]	1035																
														Deviation %		Deviation	
Parameter	Value	Runout [m]	Elevation toe, [m.a.s.l]	Height difference, [m]	H/L	Fahrböschung, [deg]	Max velocity [m/s]	Velocity, 10 s [m/s]	Travel angle [deg]	Runout	Max velocity	Runout [m]	Max velocity [m/s]				
Reference simulation	Schleier	1448	70	965	0.666436464	33.68	37.2889		33.5401								
Material parameters																	
Friction coefficient, μ	0.1	1491	70	965	0.647216633	32.91	38.6845	22	32.9728	2.97	3.74	43	1.40				
	0.15	1448	70	965	0.666436464	33.68	37.2889	22.3	33.5401	0.00	0.00	0	0.00				
	0.17	1428	71	964	0.675070028	34.02	37.0613	22.2	33.5401	-1.38	-0.61	-20	-0.23				
	0.2	1409	73	962	0.682753726	34.32	35.6849	22.2	33.8192	-2.69	-4.30	-39	-1.60				
	0.25	1369	76	959	0.700511322	35.01	31.9291	22.5	34.2218	-5.46	-14.37	-79	-5.36				
Turbulence coefficient, ξ [m/s^2]	450	1434	70	965	0.672942817	33.94	35.345	22	33.4124	-0.97	-5.21	-14	-1.94				
	500	1448	70	965	0.666436464	33.68	37.2889	22.3	33.5401	0.00	0.00	0	0.00				
	600	1456	70	965	0.662774725	33.54	39.9425	23	33.5047	0.55	7.12	8	2.65				
	800	1442	71	964	0.66851595	33.76	39.6078	24.5	33.6064	-0.41	6.22	-6	2.32				
	1000	1452	71	964	0.663911846	33.58	42.9563	26.7	33.6516	0.28	15.20	4	5.67				
Internal friction angle [deg]	30	1449	70	965	0.665976536	33.66	35.5771		33.4167	0.07	-4.59	1	-1.71				
	35	1448	70	965	0.666436464	33.68	37.2889		33.5401	0.00	0.00	0	0.00				
	38	1449	70	965	0.665976536	33.66	39.914		33.3665	0.07	7.04	1	2.63				
	40	1445	70	965	0.667820069	33.74	43.1679		33.3621	-0.21	15.77	-3	5.88				
	45	1459	70	965	0.661411926	33.48	50.4421		33.3092	0.76	35.27	11	13.15				
	50	1446	70	965	0.66735823	33.72	46.6722		33.4568	-0.14	25.16	-2	9.38				
Unit weight [kN/m^3]	26	1449	70	965	0.665976536	33.66	37.2835		33.3965	0.07	-0.01	1	-0.01				
	28	1448	70	965	0.666436464	33.68	37.2889		33.5401	0.00	0.00	0	0.00				
	30	1449	70	965	0.665976536	33.66	37.3392		33.5422	0.07	0.13	1	0.05				
Program parameters																	
Number of particles	1000	1452	70	965	0.664600551	33.61	35.6667		33.1891	0.28	-4.35	4	-1.62				
	2000	1448	70	965	0.666436464	33.68	37.2889		33.5401	0.00	0.00	0	0.00				
	4000	1440	70	965	0.670138889	33.83	39.9536		33.5337	-0.55	7.15	-8	2.66				
Velocity smoothing coefficient	0	1436	71	964	0.671309192	33.87	38.5298		33.5141	-0.83	3.33	-12	1.24				
	0.01	1448	70	965	0.666436464	33.68	37.2889		33.5401	0.00	0.00	0	0.00				
	0.05	1437	71	964	0.670842032	33.86	34.4434		33.5849	-0.76	-7.63	-11	-2.85				
	0.1	1441	71	964	0.668979875	33.78	34.5168		33.4201	-0.48	-7.43	-7	-2.77				
Smoothing length constant	1	1443	70	965	0.668745669	33.77	2936.78		33.8774	-0.35	7775.75	-5	2899.49				
	3	1445	70	965	0.667820069	33.74	39.6962		33.5415	-0.21	6.46	-3	2.41				
	4	1448	70	965	0.666436464	33.68	37.2889		33.5401	0.00	0.00	0	0.00				
	5	1456	70	965	0.662774725	33.54	36.6381		33.4724	0.55	-1.75	8	-0.65				
	7	1448	71	964	0.665745856	33.65	34.7653		33.7288	0.00	-6.77	0	-2.52				
Frictional rheology																	
Friction angle	15	1624	68	967	0.59544335	30.77	54.4527	50.8	32.0333	12.15	46.03	176	17.16				
	17	1552	70	965	0.621778351	31.87	53.3099	48.2	33.0566	7.18	42.96	104	16.02				
	20	1467	70	965	0.657805044	33.34	50.1196	40	34.1729	1.31	34.41	19	12.83				
	25	1350	77	958	0.70962963	35.36	44.7542	36.6	36.5078	-6.77	20.02	-98	7.47				
	30	1199	115	920	0.767306088	37.50	40.8939	31.3	38.9219	-17.20	9.67	-249	3.61				
	35	892	270	765	0.857623318	40.62	36.2394	28.8	42.4935	-38.40	-2.81	-556	-1.05				

Results from sensitivity analysis, Børa C Large, $V = 476000\ m^3$

BøraC_Large													
Volume [m^3]	475647												
Elevation crown, [m.a.s.l.]	1035												
										Deviation %		Deviation	
Parameter	Value	Runout [m]	Elevation toe, [m.a.s.l]	Height difference, [m]	H/L	Fahrböschung, [deg]	Max velocity [m/s]	Velocity, 10 s [m/s]	Travel angle [deg]	Runout	Max velocity	Runout [m]	Max velocity [m/s]
Reference simulation	Schleier	1598	70	965	0.60387985	31.13	140.607		33.0674				
Material parameters													
Friction coefficient, μ	0.1	1655	68	967	0.58429003	30.30	96.6178	32	32.4581	3.57	-31.29	57	-43.99
	0.15	1598	70	965	0.60387985	31.13	140.607	31	33.0674	0.00	0.00	0	0.00
	0.17	1576	70	965	0.61230964	31.48	106.98	30.8	33.3486	-1.38	-23.92	-22	-33.63
	0.2	1552	69	966	0.62242268	31.90	80.6739	30.4	33.6141	-2.88	-42.62	-46	-59.93
	0.25	1512	69	966	0.63888889	32.57	82.9714	29.2	33.9902	-5.38	-40.99	-86	-57.64
Turbulence coefficient, ξ [m/s^2]	450	1597	70	965	0.60425798	31.14	88.7656	36.9	33.0986	-0.06	-36.87	-1	-51.84
	500	1598	70	965	0.60387985	31.13	140.607	31	33.0674	0.00	0.00	0	0.00
	600	1627	70	965	0.59311616	30.67	84.2322	46.1	32.9268	1.81	-40.09	29	-56.37
	800	1654	68	967	0.58464329	30.31	89.3649	41.7	32.7515	3.50	-36.44	56	-51.24
	1000	1691	68	967	0.57185098	29.76	120.855	51	32.4642	5.82	-14.05	93	-19.75
Frictional rheology													
Friction angle, [deg]	17	1615	69	966	0.59814241	30.89	76.2531	53.6	32.8187	1.06	-45.77	17	-64.35
	20	1541	70	965	0.62621674	32.06	57.9837	52.7	33.6093	-3.57	-58.76	-57	-82.62

Results from sensitivity analysis, Børa B, $V = 2.4$ Mm^3

Børa B															
Volume [m^3]	2 400 000														
Height crown [m.a.s.l.]	985														
												Deviation %		Deviation	
Parameter	Value	Runout [m]	Height toe, [m.a.s.l]	Height difference, [m]	H/L	Fahrböschung, [deg]	Max velocity [m/s]	Velocity, 10 s [m/s]	Travel angle [deg]	Runout	Max velocity	Runout [m]	Max velocity [m/s]
Reference simulation	Schleier	1767	69	916	0.518392756	27.40	791.434		33.4872				
Material parameters													
Friction coefficient, μ	0.1	1861	69	916	0.49220849	26.21	1259.63	55.2	32.2601	5.32	59.16	94	468.20
	0.15	1767	69	916	0.518392756	27.40	791.434	62.6	33.4872	0.00	0.00	0	0.00
	0.17	1740	69	916	0.526436782	27.76	633.984	76.2	33.8542	-1.53	-19.89	-27	-157.45
	0.2	1675	62	923	0.551044776	28.86	856.079	48.5	34.3004	-5.21	8.17	-92	64.65
	0.25	1610	58	927	0.575776398	29.93	1186.96	41.9	34.8574	-8.89	49.98	-157	395.53
Turbulence coefficient, ξ [m/s^2]	450	1767	69	916	0.518392756	27.40	1243.14	52.6	33.3452	0.00	57.07	0	451.71
	500	1767	69	916	0.518392756	27.40	791.434	62.6	33.4872	0.00	0.00	0	0.00
	600	1776	69	916	0.515765766	27.28	1057.04	49.8	33.2552	0.51	33.56	9	265.61
	800	1805	69	916	0.507479224	26.91	2263.15	55.3	32.8577	2.15	185.96	38	1471.72
	1000	1821	69	916	0.503020319	26.70	1790.69	72.6	32.4653	3.06	126.26	54	999.26
Frictional rheology													
Friction angle, [deg]	17	1592	59	926	0.581658291	30.18	833.293	315	34.0768	-9.90	5.29	-175	41.86
	20	1473	58	927	0.629327902	32.18	212.217	79.7	34.9838	-16.64	-73.19	-294	-579.22

11.4 Appendix IV

Results from modelling with different entrainment rates.

Børa C																	
Volume [m^3]	75567.5																
Height crown [m.a.s.l.]	1035																
Entrainment rate																	
V0	75567.5	75567.5	75567.5	75567.5	75567.5	75567.5	75567.5	75567.5	75567.5	75567.5	75567.5	75567.5	75567.5	75567.5	75567.5	75567.5	75567.5
Volume increase, %	20	25	32	35	37	40	43	50	100	200	300	400	600	900			
Factor of expected volume increase	1.2	1.25	1.32	1.35	1.37	1.4	1.43	1.5	2	3	4	5	7	10			
Vf	90681.0	94459.4	99749.1	102016.1	103527.5	105794.5	108061.5	113351.25	151135	226702.5	302270	377837.5	528972.5	755675			
S	1144	1144	1144	1144	1144	1144	1144	1144	1144	1144	1144	1144	1144	1144			
E	0.000159	0.000195	0.000243	0.000262	0.000275	0.000294	0.000313	0.000354	0.000606	0.000960	0.001212	0.001407	0.001701	0.002013			
Final volume	88379	91019	95627	96712	98649	100483	102450	106658	138391	197526	251935	307499	411329	553742			
Factor of modelled volume increase	1.17	1.20	1.27	1.28	1.31	1.33	1.36	1.41	1.83	2.61	3.33	4.07	5.44	7.33			
Travel angle [deg]	0.0066	0.0067	0.0067	0.0067	0.0055	0.016	0.0068	0.00683222	0.00698538	0.00717174	0.00726021	0.00731849	0.00734067	0.00734207			
Max. Velocity [m/s]	41.534	41.6957	41.221	56.1532	54.9726	41.2602	41.245	41.0162	39.0237	38.2031	38.2031	38.2031	38.2031	38.2031			
Run-out [m]	1403	1403	1403	1403	1403	1403	1403	1400	1400	1400	1400	1403	1408	1413			
Height toe, [m.a.s.l.]	74	74	74	74	74	74	74	74	74	74	74	74	74	74			
Height difference, [m]	961	961	961	961	961	961	961	961	961	961	961	961	961	961			
H/L	0.6849608	0.6849608	0.6849608	0.6849608	0.6849608	0.6849608	0.6849608	0.68642857	0.68642857	0.68642857	0.68642857	0.6849608	0.68252841	0.68011323			
Fahrböschung. [deg.]	34.41	34.41	34.41	34.41	34.41	34.41	34.41	34.47	34.47	34.47	34.47	34.41	34.31	34.22			
Deviation final volumes [%]	-2.53856927	-3.64217422	-4.13246836	-5.1993006	-4.71225151	-5.02058236	-5.19289821	-5.90487533	-8.43219638	-12.8699507	-16.6523307	-18.6160717	-22.240003	-26.722202			

Results from sensitivity analysis of parameters influencing the processes of entrainment. Dry conditions, $r_u = 0$. Entrainment rates $E = 0.00028$ m^{-1} and $E = 0.0012$ m^{-1}

Børa C										
Volume [m^3]	75567.5									
Height crown [m.a.s.l.]	1035									
Parameter	Value	Final volume, [m^3]	Travel angle, [deg.]	Max. Velocity, [m/s]	Run-out, [m]	Height toe [ma.s.l.]	Heigh difference, H [m]	H/L	Fahrböschung, [deg.]	
Friction angle deposits, [°]										
E=0.00028	15	100716	0.0052	49.2211	1454	71	964	0.662998624	33.54432341	
	20	98649	0.0055	54.9726	1404	74	961	0.684472934	34.39058421	
	25	94779.5	0.0067	38.2031	1334	77	958	0.71814093	35.68367465	
E=0.0012	15	266193	0.0067469	40.7352	1439	71	964	0.669909659	33.81851261	
	20	251935	0.0073	38.2031	1400	74	961	0.686428571	34.46681669	
	25	197903	0.00684563	38.2031	1331	77	958	0.719759579	35.74481411	
Max. Erosion depth [m]										
E=0.00028	mean	98649	0.0055	54.9726	1404	74	961	0.684472934	34.39058421	
	mean + std	99597	0.013	43.4468	1401	74	961	0.685938615	34.44773081	
	mean + 2std	99472.2	0.0056	41.0981	1404	74	961	0.684472934	34.39058421	
E=0.0012	mean	251935	0.0073	38.2031	1400	74	961	0.686428571	34.46681669	
	mean + std	251933	0.00726026	38.2031	1400	74	961	0.686428571	34.46681669	
	mean + 2std	251932	0.00726027	38.2031	1400	74	961	0.686428571	34.46681669	
Upper zone, erosion rate										
	0.00026	85076	0.0066	41.6585	1407	74	961	0.683013504	34.33360367	
	0.00028	85876	0.0056	41.0981	1407	74	961	0.683013504	34.33360367	
	0.0012	133486	0.00688327	39.0434	1414	73	962	0.680339463	34.22899993	
	0.002	200776	0.00706619	38.2031	1410	73	962	0.682269504	34.30452584	
Lower zone, erosion rate										
	0.00026	86479	0.0067	43.6094	1400	75	960	0.685714286	34.43898931	
	0.00028	87396	0.0067	43.6094	1400	75	960	0.685714286	34.43898931	
	0.0012	139302	0.00704008	43.6094	1397	75	960	0.687186829	34.49633684	
	0.002	205103	0.0072533	43.6094	1395	75	960	0.688172043	34.53466157	

Results from analysis of the impact of pore pressure in the entrained material.

Børa C									
Volume [m^3]	75567.5								
Height crown, [m.a.s.l.]	1035								
Parameter	Value	Final volume, [m^3]	Travel angle, [deg.]	Max. Velocity, [m/s]	Run-out, [m]	Height toe [ma.s.l.]	Heigh difference, H [m]	H/L	Fahrböschung, [deg.]
Pore-pressure coeff. Ru									
E=0.00028	0	98649	0.0055	54.9726	1404	74	961	0.68447293	34.39058421
	0.1	100078	0.00554606	43.3996	1418	73	962	0.67842031	34.15376556
	0.25	100630	0.00519004	48.5702	1440	71	964	0.66944444	33.8001105
	0.5	100932	0.00512084	59.4596	1507	70	965	0.64034506	32.63326632
	0.75	100444	0.00308142	72.62	1589	68	967	0.60855884	31.32297301
	0.9	99767.6	0.00392762	84.0735	1640	68	967	0.58963415	30.52505316
E=0.0012	0	251935	0.0073	38.2031	1400	75	960	0.68571429	34.43898931
	0.25	265467	0.00677891	40.087	1437	71	964	0.67084203	33.85536985
	0.5	272688	0.00523825	46.3373	1477	70	965	0.65335139	33.15864887
	0.75	272029	0.00518996	53.6288	1522	70	965	0.63403417	32.37609363
	0.9	267285	0.00312995	60.2834	1550	69	966	0.62322581	31.93222555
Erosion from different elevations									
E = 0.00028, Ru = 0.5	Upper				1426	72	963	0.67531557	34.03176945
	Lower				1488	69	966	0.64919355	32.99137314
E = 0.0012, Ru = 0.75	Upper	135472	0.0067788	54.5943	1435	71	964	0.671777	33.8922979
	Lower	150815	0.00505089	47.2864	1498	70	965	0.64419226	32.7893208
Erosion from both, pore-pressure in one									
E = 0.00028, Ru = 0.5	Upper				1420	72	963	0.67816901	34.14390433
	Lower				1489	69	966	0.64875756	32.97379567
E = 0.0012, Ru = 0.75	Upper	244043	0.00704638	56.1532	1415	73	962	0.67985866	34.21016406
	Lower	275249	0.00509411	45.4303	1511	69	966	0.63931171	32.59125768

11.5 Appendix V

Figures not included in the text showing results from numerical run-out modelling. The study of the effects and processes of entrainment were first carried out based on small final volumes, meaning low entrainment rates, *E* and little material allowed to be entrained. Most of the results from the study are not included in the text, but presented here, as the values of *E* were found to be too low for the scenario at Børa. A figure showing the effect of the location of pore-pressure is also presented here.

Entrainment rates *E* based on bulk slide porosity *n* from the VAW-model (Heller et al., 2009) . Low values.

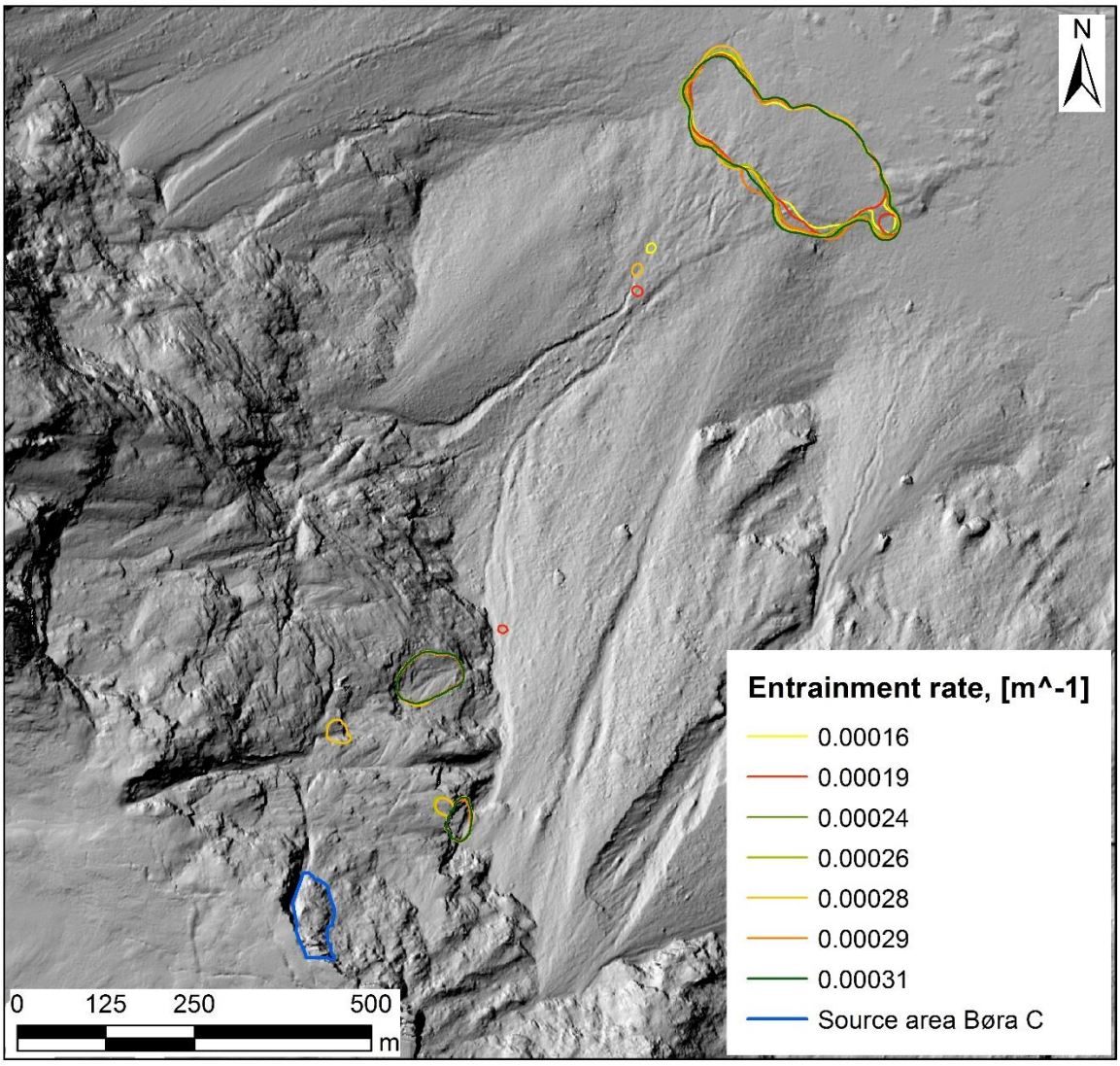

Erosion, friction angle, E = 0.00028 m^{-1}

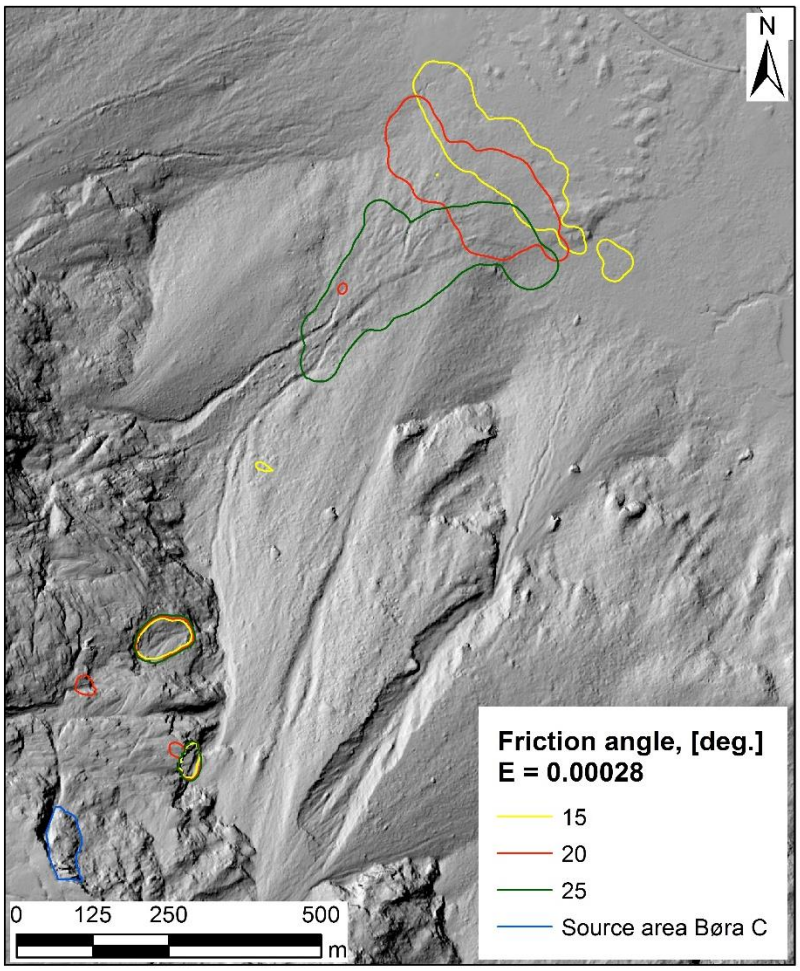

Entrainment from the entire slope (both scree deposit zones), pore-pressure in one scree deposit zone.